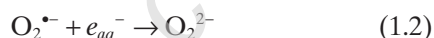


CHEMISTRY OF REACTIVE SPECIES

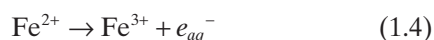
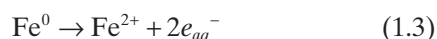
FREDERICK A. VILLAMENA

1.1 REDOX CHEMISTRY

Electron is an elementary subatomic particle that carries a negative charge. The ease of electron flow to and from atoms, ions or molecules defines the reactivity of a species. As a consequence, an atom, or in the case of molecules, a particular atom of a reactive species undergoes a change in its oxidation state or oxidation number. During reaction, oxidation and reduction can be broadly defined as decrease or increase in electron density on a particular atom, respectively. A more direct form of oxidation and reduction processes is the loss or gain of electrons on a particular atom, respectively, which is often referred to as electron transfer. Electron transfer can be a one- or two-electron process. One common example of a one-electron reduction process is the transfer of one electron to a molecule of oxygen (O_2) resulting in the formation of a superoxide radical anion ($O_2^{\bullet-}$) (Eq. 1.1). Further one-electron reduction of $O_2^{\bullet-}$ yields the peroxide anion (O_2^{2-}) (Eq. 1.2):



Conversely, two-electron oxidation of metallic iron (Fe^0) leads to the formation of Fe^{2+} (Eq. 1.3) and further one-electron oxidation of Fe^{2+} leads to the formation of Fe^{3+} (Eq. 1.4). Electrons in this case can be introduced electrochemically or through reaction with reducing or oxidizing agents:



Another method by which oxidation state on a particular atom can be altered is through change in bond polarity. Electronegative atoms have the capability of attracting electrons (or electron density) toward itself. Listed below are the biologically relevant atoms according to their decreasing electronegativities (revised Pauling): F (3.98) > O (3.44) > Cl (3.16) > N (3.04) > Br (2.96) > S > (2.58) > C = Se (2.55) > H (2.20) > P (2.19). Therefore, changing the electronegativity (or electropositivity) of an atom attached to an atomic center of interest can result in the reversal of the polarization of the bond. By applying the “whose-got-the-electron-rule” will be beneficial in identifying atomic centers that underwent changes in their oxidation states. For example, based on the electronegativity listed above, one can examine the relative oxidation states of a carbon atom in a molecule (Fig. 1.1). Since carbon belongs to group 14 of the periodic table, the carbon atom has 4 valence electrons. When carbon is bonded to an atom that is less electronegative to it (e.g., hydrogen atom), the carbon atom tends to pull the electron density toward itself, making it electron-rich. The two electrons that it shares with each hydrogen atom are counted toward the number of electrons the carbon atom can claim. In the first example, methane has four hydrogen atoms attached to it. Since hydrogen is less electronegative than carbon, all eight shared electrons can be claimed by carbon, but since carbon is only entitled to four electrons by virtue of its valence electron, it has an excess of four electrons, making its oxidation state -4 . However, when a carbon atom is covalently bound to a more electronegative atom (e.g., oxygen and chlorine), the spin density distribution around the

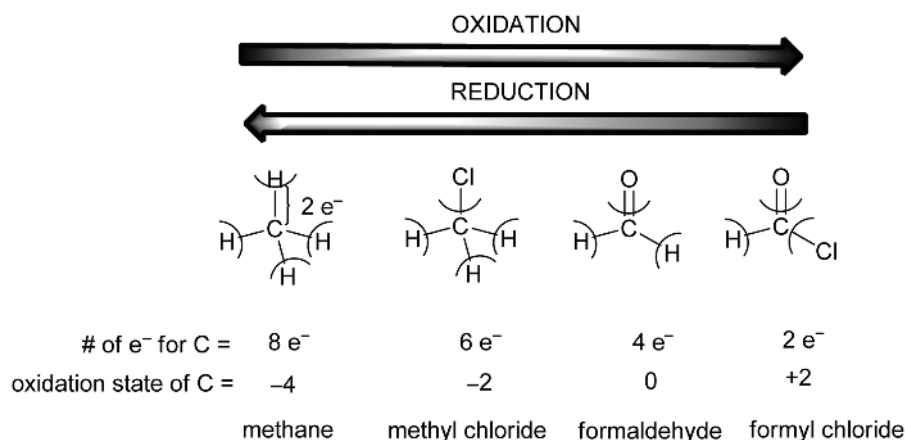


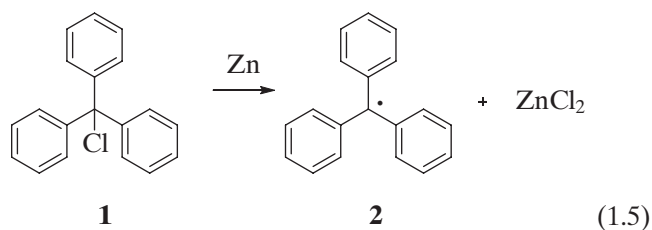
Figure 1.1 Oxidation states of the carbon atom calculated as number of valence electrons for the carbon atom (i.e., 4 e⁻) minus the number of electrons that carbon can claim in a molecule. Order of increasing electronegativity: H < C < O < Cl.

carbon atom decreases and are polarized toward the more electronegative atoms. In this case, the electrons shared by carbon with a more electronegative atom are counted toward the more electronegative atom. In the case of formyl chloride, only the two electrons it shares with hydrogen can be counted toward the total number electrons the carbon atom can claim since the four electrons it shares with oxygen and the two electrons it shares with chlorine cannot be counted toward the carbon because these electrons are polarized toward the more electronegative atoms. Hence, the carbon becomes deficient in electron density, and by virtue of its four valence electrons, it can only claim two electrons from the hydrogen atom, therefore, the net oxidation state can be calculated to be +2. The increasing positivity of the carbon from methane to formyl chloride indicates oxidation of carbon and therefore, oxidation can now be broadly defined as (1) loss of electron; (2) loss of hydrogen atom; and (3) gain of oxygen or halogen atoms, while reduction can be defined as (1) gain of electron; (2) gain of hydrogen atom; and (3) loss of oxygen or halogen atoms.

1.2 CLASSIFICATION OF REACTIVE SPECIES

Definition. Free radicals are integral part of many chemical and biological processes. They play a major role in determining the lifetime of air pollution in our atmosphere¹ and are widely exploited in the design of polymeric, conductive, or magnetic materials.² In biological systems, free radicals have been implicated in the development of various diseases.³ So what are free radicals? The word “radical” came from the Latin word *radix* meaning “root. In the mid-1800s, chemists began to use the word radical to refer to a group of atoms. How

the word “radical” had become a chemical terminology is not clear, but one could only speculate that these groups of atoms that make up a molecule was figuratively referred to as “roots” or basic foundation of an entity. In the early 1900s, early literature referred to metallic atoms as basic radicals and nonmetallic ones as acid radicals, for example, in Mg(OH)₂ or H₂S, respectively. During this time, radicals are still referred to as group entities that are part of a compound but not until Gomberg had demonstrated during this same time that radicals can indeed exist by themselves as exemplified by his synthesis of the stable triphenylmethyl radical **2** from the reduction of triphenylchloromethane **1** by Zn (Eq. 1.5):⁴



In the late 1950s, the electron paramagnetic resonance spectrum of **2** had been obtained, further confirming the radical nature of trityl which can indeed be stable enough to exist by itself and be spectroscopically detected.⁵ Radical is defined in modern times as a finite chemical entity by its own that is capable of undergoing chemical reaction. Radicals carry an odd number of electrons in the form of an atom, neutral or ionic molecule. By virtue of Pauli’s exclusion principle, the number of electrons occupying an atomic or molecular orbital is limited to two provided that they have different spin quantum number. This pairing of electron results in the formation of a chemical bond between atoms, existence of lone pair of electron or completion

of the inner core nonbonding electrons. For radicals, electrons are typically on an open shell configuration in which the atomic or molecular orbitals are not completely filled with electrons, making them thermodynamically more energetic species than atoms or molecules with closed shell configuration or with filled orbitals. For example, the noble gases He, Ne, or Ar, with filled atomic orbitals, $1s^2$ (He), $1s^2 2s^2 2p_x^2 2p_y^2 2p_z^2$ (Ne), $1s^2 2s^2 2p^6 3s^2 3p_x^2 3p_y^2 3p_z^2$ (Ar), are known to be inert, while the atomic H, N, or Cl with electron configurations of $1s^1$ (H), $1s^2 2s^2 2p_x^2 2p_y^1 2p_z^0$ (N), and $1s^2 2s^2 2p^6 3s^2 3p_x^2 3p_y^2 3p_z^1$ (Cl) are known to be highly reactive and hence exist as diatomic molecules. Similarly, molecules with open shell molecular orbital configurations are more reactive than molecules with closed shell configuration. For example, hydroxyl radical has an open shell configuration of $\sigma_{pz}^2 p_x^2 p_y^1$ while the hydroxide anion has a closed shell configuration of $\sigma_{pz}^2 p_x^2 p_y^2$, making the former more reactive than the latter.

1.2.1 Type of Orbitals

Radicals can be classified according to the type of orbital (SOMO) that bears the unpaired electron as σ - or π -radicals. Radical stability is governed by the extent of electron delocalization within the atomic orbitals. In general, due to the restricted spin delocalization in the σ -radicals, these radicals are more reactive than the π -radicals. Examples of σ -radicals are H^\bullet , formyl-, vinyl-, or phenyl-radicals (Fig. 1.2).

Almost all of the radical-based reactive oxygen species (ROS) that will be discussed in this chapter fall under the π -type category but each will differ only on the extent of spin delocalization within the molecule. Examples of π -radicals with restricted spin delocalization are $^\bullet CH_3$, $^\bullet SH$, and HO^\bullet and are relatively less stable than π -radicals with extended spin delocalization (e.g., HOO^\bullet , $O_2^{\bullet -}$, and NO) (Fig. 1.3).

1.2.2 Stability of Radicals

Radicals can also be categorized according to their stability as stable, persistent, and unstable (or transient). Although the terms stable and persistent are often used interchangeably, free radical chemists agree that persistent radicals refer to the thermodynamic favorability of being monomeric as opposed to being dimeric as formed via radical-radical reaction in solution. Radical-based ROS are not persistent (or stable) making their detec-

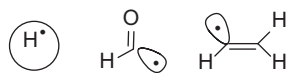


Figure 1.2 Hydrogen, formyl, and vinyl σ -radicals.

tion in solution very difficult. ROS detection is commonly accomplished by detecting secondary products arising from their redox or addition reaction with a reagent as will be discussed in Section 1.5. Figure 1.4 shows examples of dimer formation from HO^\bullet , HO_2^\bullet , TEMPO, and trityl, and their respective approximate dissociation enthalpies. Rates of ROS decomposition in solution, of course, depend on the type of substrates that are present in solution but lifetimes of these radicals vary in solution since even one of the most stable radicals such as the trityl radical for example is not stable in the presence of some oxido-reductants.

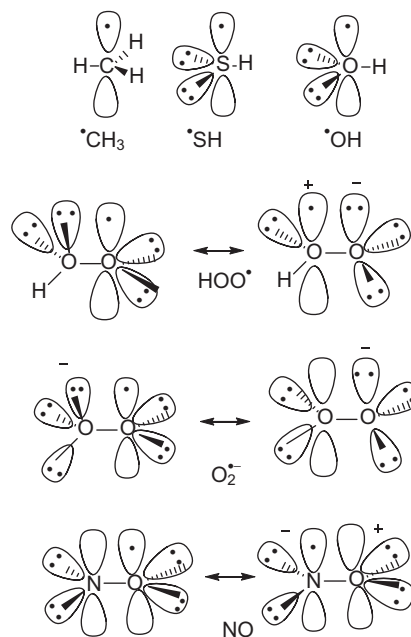


Figure 1.3 Methyl, thiyl, hydroxyl, hydroperoxyl, superoxide, and nitric oxide as examples of π -radicals.

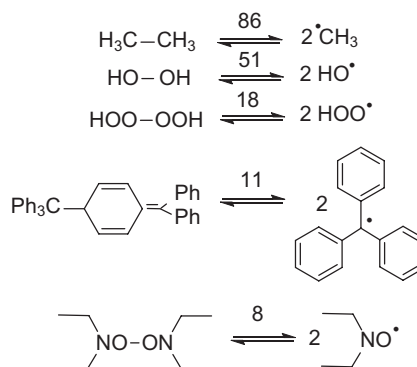


Figure 1.4 Dissociation enthalpies (ΔH° in kcal/mol) of various dimers showing nitroxide to be the most stable radical and the methyl radical being the least stable.

Classification of reactive species is sometimes cumbersome since, for example, a number of molecules contain more than one atom whose oxidation states are altered during reaction. Nitric oxide (NO), for example, can react with hydroxyl radical (HO^\bullet) to form nitrous acid (HNO_2), but in order to classify whether NO is a reactive nitrogen or oxygen species, one has to carefully examine the oxidation states of the relevant atoms of the reactants and the product (Fig. 1.5).

Using the “whose-got-the-electron-rule” mentioned earlier, one can assign the oxidation states for each of the species involved in the transformation. The nitrogen atom of NO underwent an oxidation since its oxidation state has increased from +2 to +3 in HNO_2 , while the oxygen of HO^\bullet (not of NO) underwent reduction (from -1 to -2). We can therefore classify NO as reactive nitrogen species (RNS) while HO^\bullet as ROS since it was the nitrogen atom of NO and the oxygen atom of HO^\bullet that underwent oxidation state modification after reaction. Figure 1.6 shows the various reactive oxygen, nitrogen, and sulfur species with their respective oxidation states.

1.2.3 ROS

1.2.3.1 Oxygen Molecule (O_2 , Triplet Oxygen, Dioxygen)

The electronic ground state of molecular

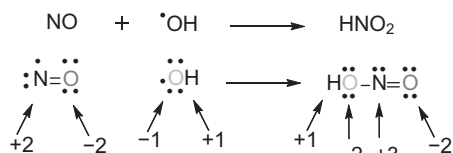


Figure 1.5 Reaction of nitric oxide with hydroxyl radical to produce nitrous acid showing pertinent oxidation states of the atoms undergoing redox transformation.

oxygen is the triplet state, $\text{O}_2(\text{X}^3\Sigma_g^-)$. Dioxygen's molecular orbital $\text{O}_2(\text{X}^3\Sigma_g^-)$ has the two unpaired electrons occupying each of the two degenerate antibonding π_g -orbitals and whose spin states are the same or are parallel with each other (Fig. 1.7).

Owing to dioxygen's biradical (open-shell) property, it exhibits a radical-type behavior in many chemical reactions. Elevated physiological concentrations of O_2 (hyperoxia) have been shown to be toxic to cultured epithelial cells due to necrosis, while lethal concentrations of H_2O_2 and $\text{O}_2^{\bullet-}$ cause apoptosis, suggesting that the mechanism of O_2 toxicity is distinct from other oxidants. However, in *in vivo* systems, apoptosis is predominantly the main mechanism of cell death in the lung upon breathing 99.9% O_2 .⁶

Chlorinated aromatics have been widely used as biocides and as industrial raw materials, and they are ubiquitous as environmental pollutants. The toxicology of polychlorinated biphenyls (PCBs) have been shown to be due to the formation H_2O_2 and $\text{O}_2^{\bullet-}$ from one-electron oxidation or reduction by molecular oxygen of reactive hydroquinone and quinone products, respectively, via formation of semiquinone radicals (Eq. 1.6).⁷ Oxygenation of pentachlorophenol⁸ (PCP) also leads to the formation of superoxide via the same mechanisms (Eq. 1.7):

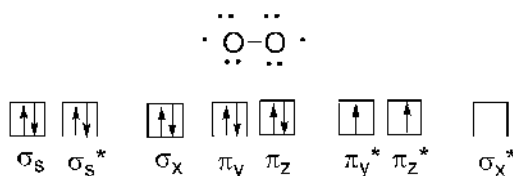


Figure 1.7 Molecular orbital diagram of dioxygen showing its biradical nature.

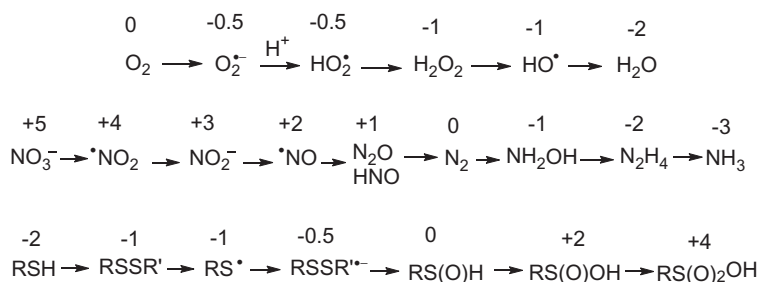
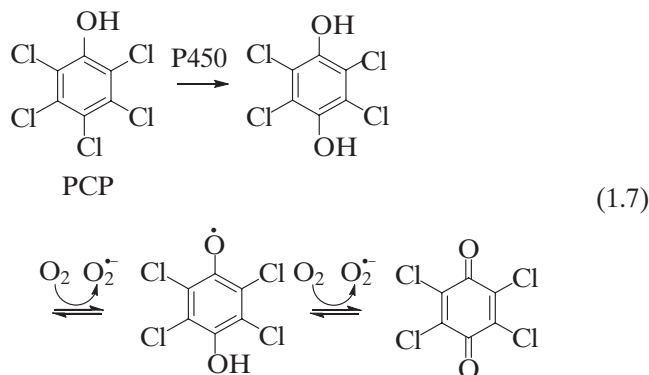
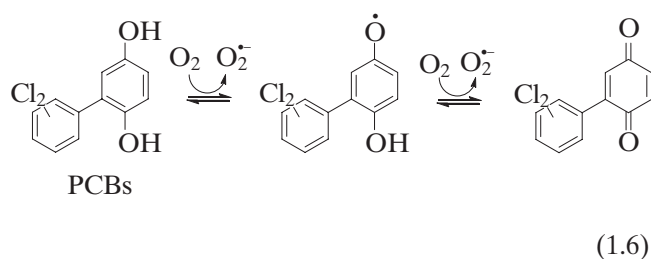
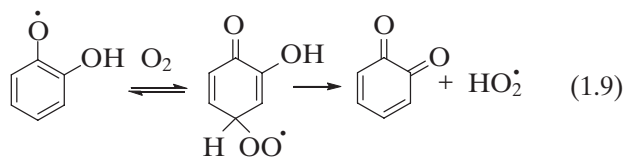
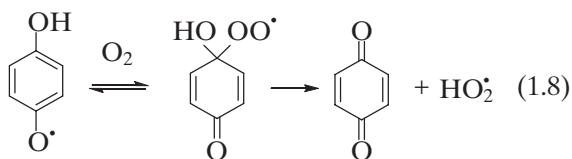


Figure 1.6 Reaction of nitric oxide with hydroxyl radical to produce nitrous acid showing pertinent oxidation states of the atoms undergoing redox transformation.



Oxygen addition to 1,4-semiquinone radicals was observed to be more facile than their addition to 1,2-semiquinones with free energies of reaction of 7.4 and 10.3 kcal/mol, respectively (Eq. 1.8 and Eq. 1.9).⁹ The experimental rate constants for the reaction of O_2 with 2,5-di-*tert*-butyl-1,4-semiquinone radicals were $2.4 \times 10^5 M^{-1} s^{-1}$ and $2.0 \times 10^6 M^{-1} s^{-1}$ in acetonitrile and chlorobenzene, respectively, similar to that observed in aqueous media at pH 7. The formation of quinones was suggested to occur via a two-step mechanism in which O_2 adds to the aromatic ring followed by an intramolecular H-atom transfer to the peroxy moiety and concomitant release of HO_2^\bullet . This reactivity of O_2 to semiquinone to yield HO_2^\bullet underlies the pro-oxidant activity of hydroquinones:¹⁰



Perhaps one of the most important reactions of O_2 , although reversible in most cases, is its addition to carbon- or sulfur-centered radicals which is relevant in the propagation steps in lipid peroxidation processes or thiol oxidation, respectively. The reaction of dioxygen

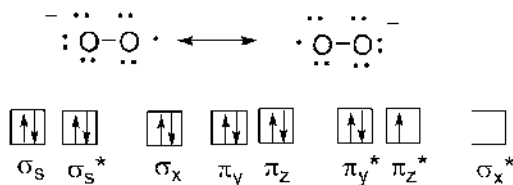


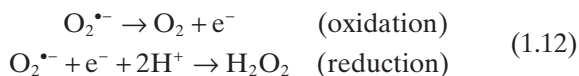
Figure 1.8 Molecular orbital diagram of $O_2^{\bullet-}$.

with lipid and thiol radicals form peroxy (LOO^\bullet) and thiol peroxy ($RSOO^\bullet$) radicals, respectively, (Eq. 1.10 and Eq. 1.11):

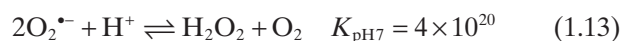


1.2.3.2 Superoxide Radical Anion ($O_2^{\bullet-}$) Superoxide is the main precursor of the most highly oxidizing or reducing species in biological system. The one-electron reduction of triplet dioxygen forms $O_2^{\bullet-}$ and initiates oxidative cascade. The molecular orbital of $O_2^{\bullet-}$ shows one unpaired electron in the antibonding π_g^* -orbital (Fig. 1.8) and is delocalized between the π^* orbitals of the two oxygen atoms.

Dismutation Reaction By virtue of superoxide's oxidation state, $O_2^{\bullet-}$ can either undergo oxidation or reduction to form dioxygen or hydrogen peroxide, respectively (Eq. 1.12),



thereby allowing $O_2^{\bullet-}$ to dismutate to H_2O_2 and O_2 according to Equation 1.13:



The dismutation of two $O_2^{\bullet-}$ in the absence of proton is slow with $k < 0.3 M^{-1} s^{-1}$ due to repulsive effects between the negative charges. However, in acidic medium, the rate $O_2^{\bullet-}$ dismutation significantly increases due to the formation of the neutral HO_2^\bullet (Eq. 1.14 and Eq. 1.15) in which electron transfer between the radicals becomes more facile:



The pK_a of the conjugate acid of $O_2^{\bullet-}$ was determined to be 4.69, which indicates that $O_2^{\bullet-}$ is a poor base but $O_2^{\bullet-}$ has strong propensity to abstract proton from protic substrates. For example, $O_2^{\bullet-}$ addition to water results in the formation of HO_2^- and HO^- , with an equilibrium constant equivalent to 0.9×10^9 .¹⁰ This indicates that $O_2^{\bullet-}$ can undergo proton abstraction from substrates to an extent equivalent to a conjugate base of an acid with a pK_a of 24 (Eq. 1.16):¹⁰



This ability of $O_2^{\bullet-}$ to act as “strong base” is due to its slow initial self-dismutation to O_2 and peroxide (O_2^{2-}) that can drive the equilibrium further right to form the hydroperoxide, HO_2^- . Since the pK_a of H_2O_2 is ~ 11.75 ,¹¹ the basicity of HO_2^- can approach those of RS^- .

Dismutation has also been reported to be catalyzed by SOD mimetics, fullerene derivatives, nitroxides, and metal complexes. Superoxide dismutation should meet the following criteria: (1) no structural or chemical modification of the mimetic upon reaction with $O_2^{\bullet-}$; (2) regeneration of O_2 ; (3) production of H_2O_2 ; and (4) absence of paramagnetic primary by-products. *Tris-*

malonyl-derivatives of fullerene (C_{60}) have been shown to exhibit SOD mimetic properties with rate constants in the order of $10^6 M^{-1} s^{-1}$ compared to dismutation rates imparted by SODs (i.e., $\sim 10^9 M^{-1} s^{-1}$).¹² *In vivo* studies using SOD2-/- knockout mice indicate increased life span by 300% and show localization in the mitochondria functioning as MnSOD.¹³ Computational studies show that electron density around the malonyl groups is low, thereby making this region more susceptible to nucleophilic attack by $O_2^{\bullet-}$ via electrostatic effects.¹³ Osuna et al.¹⁴ suggested a dismutation mechanism by which $O_2^{\bullet-}$ interacts with the fullerene surface and is stabilized by a counter-cation and water molecules. An electron is transferred from $O_2^{\bullet-}$ to the fullerene-producing O_2 and fullerene radical anion. Subsequent electron transfer from fullerene radical anion to another molecule of $O_2^{\bullet-}$ gives the fullerene- O_2^{2-} complex, and protonation of the peroxide by the malonic acid groups gives fullerene- H_2O_2 , where H_2O_2 is released along with the regenerated fullerene (Fig. 1.9).

SOD exists in two major forms: as a Cu,ZnSOD that is primarily present in cytosol while MnSOD is located in the mitochondria. There is also an FeSOD that has chemical similarities with MnSOD such as being suscep-

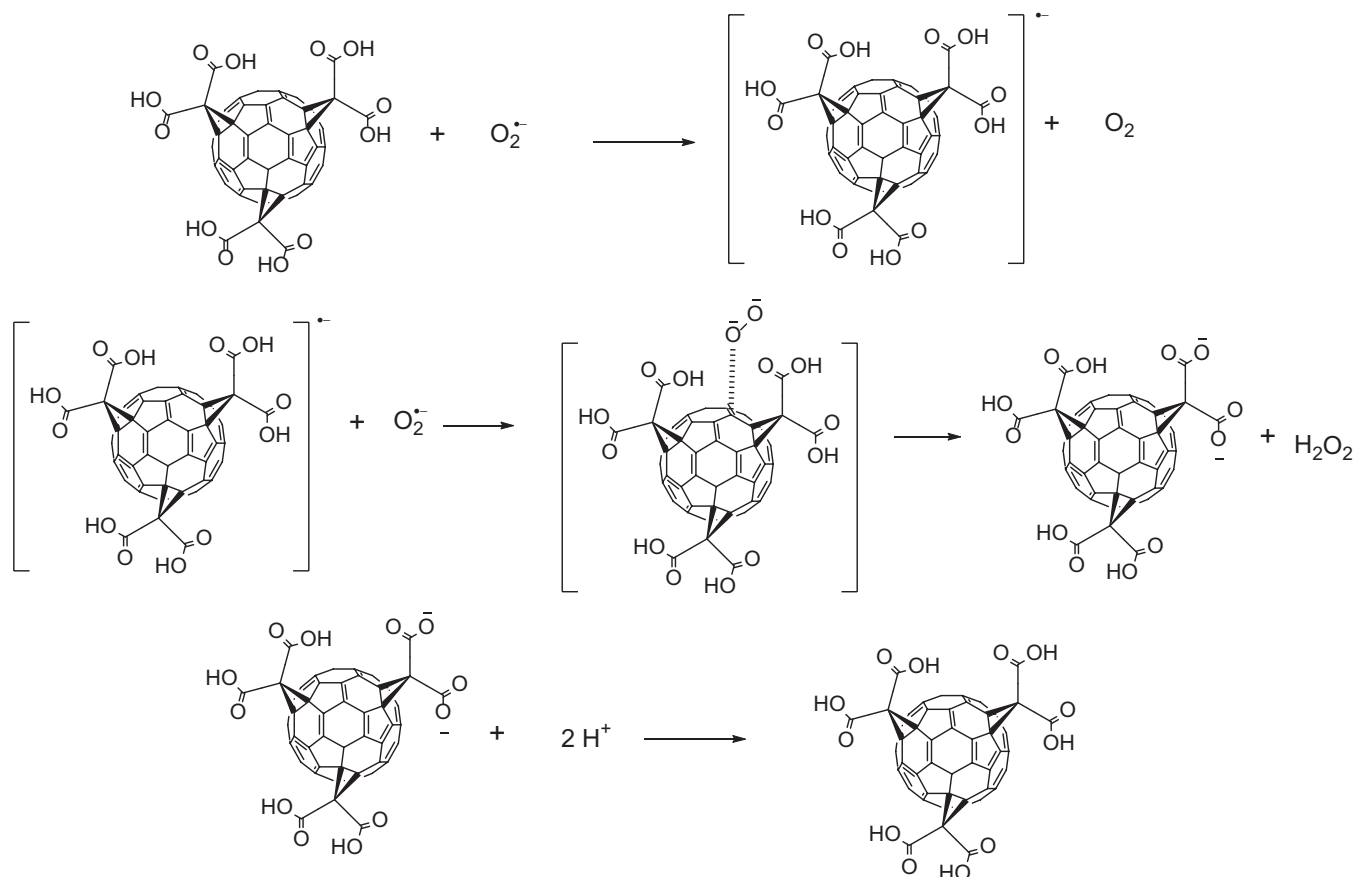
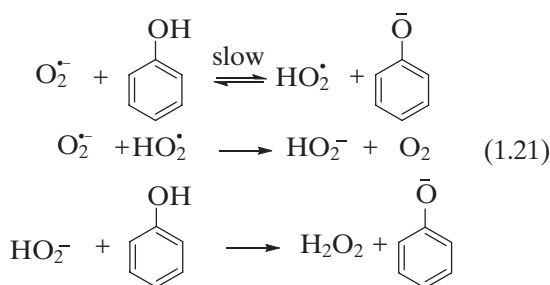
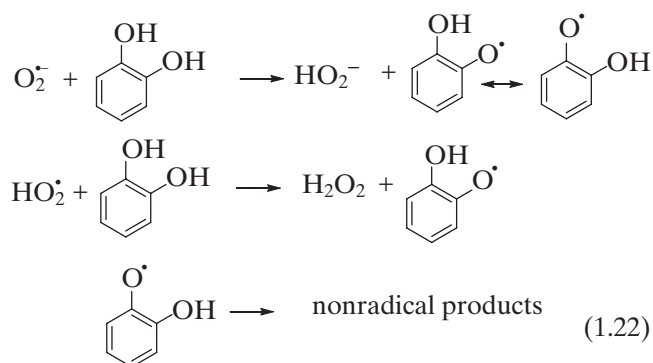


Figure 1.9 SOD mimetic property of tris-malonyl-derivative of fullerene (C_{60}).

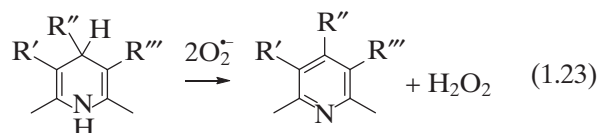
For monophenols, electrogenerated $O_2^{\bullet-}$ acts as weak base and the phenolic compound (PhOH) acting as Bronsted acid according to Equation 1.21 in which the formation of phenoxide PhO^- and HO_2^{\bullet} though thermodynamically unfavorable, can be driven to completion by the subsequent electron transfer reaction between HO_2^{\bullet} and $O_2^{\bullet-}$ to form HO_2^- (a very strong base) and O_2 in which the former can further abstract proton from phenol to form the phenoxide (PhO^-) according to Equation 1.21:



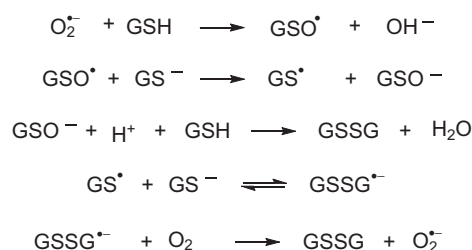
Polyphenols, however, undergo radical (or H-atom) transfer reaction with $O_2^{\bullet-}$ to form the phenoxyl radical (PhO^{\bullet}) and HO_2^- ; similarly with monophenols, HO_2^- can also abstract proton from PhOH to form phenoxide (PhO^-). The fate of PhO^{\bullet} was shown to form nonradical products via dimerization or oligomerization, or semiquinone formation. This difference in the pathway between monophenols and polyphenol decomposition with $O_2^{\bullet-}$ can be due to the stabilization of the radical in polyphenols via resonance as evidenced by the higher reactivity of polyphenols containing o-diphenol rings with $O_2^{\bullet-}$ according to Equation 1.22:



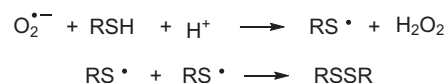
Reactivity of $O_2^{\bullet-}$ was also reported with cardiovascular drugs such as 1,4-dihydropyridine analogues of nifedipine to form pyridine (Eq. 1.23).³⁰ The proposed mechanism involves a two-electron oxidation of DHP to form the pyridine and hydrogen peroxide:



Pathway 1



Pathway 2



Net Reactions

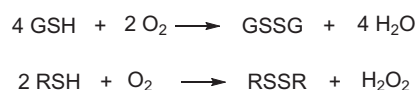


Figure 1.12 Various pathways for the reaction of $O_2^{\bullet-}$ with thiols.

Reaction of $O_2^{\bullet-}$ with thiols were found to be highest for acidic thiols with approximated rate constants in the orders of $10\text{--}10^3 M^{-1} s^{-1}$.³¹ Oxygen uptake shows concomitant formation of H_2O_2 in some thiols such as penicillamine and cysteine via a complex radical chain reaction with the formation of oxidized thiols (Fig. 1.12), but this mechanism was not observed for GSH, DTT, cysteamine, and *N*-acetylcysteine. This difference in mechanisms among thiols for H_2O_2 formation is not clear but was proposed to be due to the nature of the thiol oxidation products formed during the propagation step and of the termination products; thus, stoichiometry could play an important factor in product formation.

Computational studies show that reaction of $O_2^{\bullet-}$ with MeSH to give $MeSO^{\bullet}$ and HO^- (Pathway 1) as the most favorable mechanism with ΔG_{aq} of -170.5 kcal/mol compared to the formation of MeS^{\bullet} and HO_2^- (Pathway 2) with endoergic ΔG_{aq} of 68.2 kcal/mol.³² However, the free energies for the formation of $MeSO^- + HO^{\bullet}$ and $MeS^- + HO_2^{\bullet}$ are $\Delta G_{aq} = -52.5$ and 32.2 kcal/mol, respectively. Therefore, the proposed Pathway 2 is unfavorable unless the reacting species is HO_2^{\bullet} to give MeS^{\bullet} and H_2O_2 with $\Delta G_{aq} = -11.3$ kcal/mol but formation of $MeSO^{\bullet}$ and H_2O from HO_2^- and MeSH is far more favorable with $\Delta G_{aq} = -278.7$ kcal/mol. As previously suggested,³² the reactivity of other oxidants such as H_2O_2 and HO^{\bullet} to thiols should also be considered and may involve a more complex mechanistic pathway.

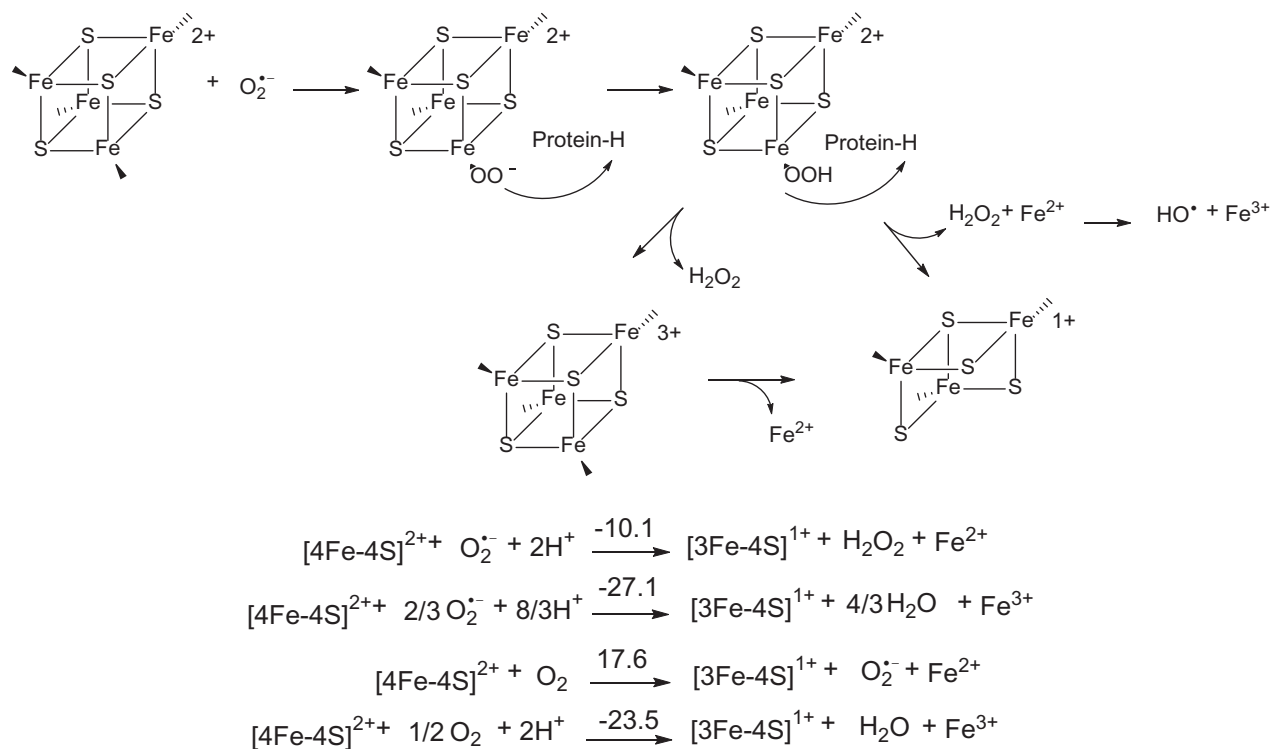


Figure 1.13 Free energies (in kcal/mol) of the reaction of $\text{O}_2^{\bullet-}$ and O_2 with $[\text{4Fe-4S}]^{2+}$ cluster.

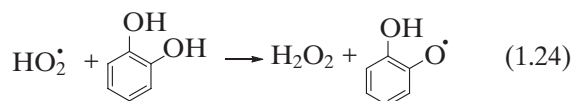
Reaction with Iron–Sulfur [Fe–S] Cluster Iron–sulfur clusters are important cofactors in biological system. They serve as active sites in various metalloproteins catalyzing electron-transfer reactions and plays a role in other biological functions such as O_2 sensing ability (e.g., by the transcription factor FNR).³³ The ubiquitousness of [Fe–S] clusters in enzymatic systems such as in Complex II and III of the mitochondrial electron transport chain, ferredoxins, NADH dehydrogenase, nitrogenase, or hydro-lyases underlies their susceptibility for inactivation by ROS specifically by $\text{O}_2^{\bullet-}$ through formation of unstable oxidation state of the [Fe–S] cluster and their subsequent degradation (Fig. 1.13). For example, hydro-lyase enzymes such as dihydroxy-acid dehydratase, fumarase A and B and aconitase can be inactivated by $\text{O}_2^{\bullet-}$ with a second-order rate constant of 10^6 – $10^7 \text{ M}^{-1} \text{ s}^{-1}$ while the rate of their inactivation by O_2 is orders of magnitude lower ($10^2 \text{ M}^{-1} \text{ s}^{-1}$).³⁴ This difference in the rates of inactivation of $\text{O}_2^{\bullet-}$ versus O_2 can be accounted to the favorability of the initial steps in the oxidation of a $[\text{4Fe-4S}]^{2+}$ by $\text{O}_2^{\bullet-}$ and O_2 with ΔG of -10.1 kcal/mol and 17.6 kcal/mol, respectively.³⁴ However, these initial steps only represent formation of Fe^{2+} , H_2O_2 , or $\text{O}_2^{\bullet-}$ and can further undergo redox reactions to form H_2O as end product. The overall free energies of oxidation of $[\text{4Fe-4S}]^{2+}$ by $\text{O}_2^{\bullet-}$ and O_2 leading to the formation of the most

stable product (H_2O) and Fe^{3+} are comparable with ΔG of -27.1 kcal/mol and -23.5 kcal/mol, respectively.

1.2.3.3 Hydroperoxyl Radical (HO_2^{\bullet}) Protonation of $\text{O}_2^{\bullet-}$ leads to the formation of HO_2^{\bullet} whose concentration in biological pH exists a hundred times smaller than that of $\text{O}_2^{\bullet-}$; however, the presence of small equilibrium concentration of HO_2^{\bullet} ($\text{pK}_a = 4.8$) can contribute to the $\text{O}_2^{\bullet-}$ instability in neutral pH due to dismutation reaction shown in Equation 1.14. In acidosis condition, the reactivity of HO_2^{\bullet} is expected to be more relevant than $\text{O}_2^{\bullet-}$. Electrochemical reduction of O_2 in the presence of strong or weak acids such as HClO_4 or phenol, respectively, generates HO_2^{\bullet} .³⁵ Hydroperoxyl radical is a stronger oxidizer than $\text{O}_2^{\bullet-}$ with $E^{\circ'} = 1.06$ and 0.94 V , respectively, and due to its neutral charge, it is capable of penetrating the lipid bilayer and hence, it has been suggested that HO_2^{\bullet} is capable of H-atom abstraction from PUFAs or from the lipids present in low-density lipoproteins. Cheng and Li³⁶ argued against the role of HO_2^{\bullet} in LPO initiation since the concentration of HO_2^{\bullet} at physiological pH is less than 1% of the generated $\text{O}_2^{\bullet-}$ and that SOD have little effect on peroxidation in liposomal or microsomal systems. However, it has been demonstrated that LOOH is more likely the preferred species for HO_2^{\bullet} attack and not the LPO initiation

process. H-atom abstraction from peroxy-OOH and not from the alkyl C–H backbone is the preferred mechanism of HO_2^\bullet reactivity, and therefore, HO_2^\bullet is more important than $\text{O}_2^{\bullet-}$ in initiating LOOH-dependent LPO, but not as the H-abstraction initiator in LPO.³⁶

Relevant to the antioxidant activity of catechols or hydroquinones (QH_2), the reactivity of HO_2^\bullet with QH_2 involves H-atom transfer reaction to form semiquinone radical and H_2O_2 with a rate constant of $4.7 \times 10^4 \text{ M}^{-1} \text{ s}^{-1}$ for 1,2-dihydroquinone (Eq. 1.24):³⁷



1.2.3.4 Hydrogen Peroxide (H_2O_2) Hydrogen peroxide is perhaps one of the most ubiquitous ROS present in biological systems due to its relative stability with an oxidation potential of 1.8 V compared to other ROS such as $\text{O}_2^{\bullet-}$, HO_2^\bullet , or HO^\bullet . Hydrogen peroxide is the protonated form of the two-electron reduction product of molecular oxygen and is a nonradical ROS with all the antibonding orbitals occupied by paired electrons (Fig. 1.14). Hydrogen peroxide undergoes highly exoergic disproportionation reaction to form two equivalents of water and one equivalent of oxygen where the rate of disproportionation is temperature dependent.

Perhaps the most common reaction of H_2O_2 is its metal-catalyzed reaction to produce HO^\bullet and HO_2^\bullet (the Fenton chemistry) as proposed by Haber and Weiss (Eq. 1.25, Eq. 1.26, Eq. 1.27, Eq. 1.28, Eq. 1.29, Eq. 1.30, Eq. 1.31, and 1.32).³⁸ Perez-Benito³⁹ proposed that this reaction can undergo propagation in which the HO^\bullet can further react with H_2O_2 to produce HO_2^\bullet according to

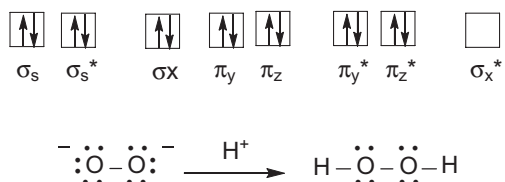


Figure 1.14 Molecular orbital diagram of H_2O_2 .

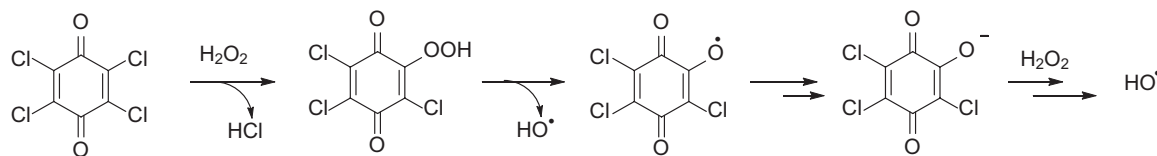
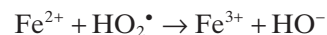
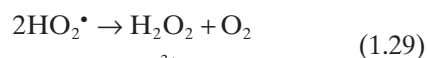
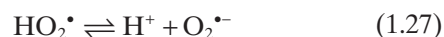
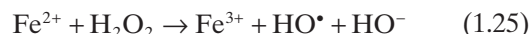


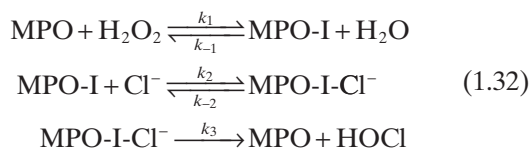
Figure 1.15 Metal-independent generation of HO^\bullet from H_2O_2 .

Equation 1.26. Depending on the pH, the equilibrium concentrations of HO_2^\bullet and $\text{O}_2^{\bullet-}$ can vary (Eq. 1.27), and it has been suggested³⁹ that HO_2^\bullet and $\text{O}_2^{\bullet-}$ are involved in the reduction and oxidation of Fe^{3+} (Eq. 1.28) and Fe^{2+} (Eq. 1.29), respectively. Iron (III) reaction with H_2O_2 can also lead to HO^\bullet production in acidic pH via formation of FeOOH^{2+} complex and its subsequent decomposition to Fe^{2+} and HO_2^\bullet (Eq. 1.30 and Eq. 1.31) in which the formed Fe^{2+} can propagate the cycle to produce HO^\bullet as shown in Equation 1.25, Equation 1.26, Equation 1.27, Equation 1.28, and Equation 1.29:



Shown in Figure 1.15 is the metal-independent generation of HO^\bullet from H_2O_2 , which was proposed to be formed from tetrachloro-1,4-benzoquinones (TCBQ)⁸ through nucleophilic substitution reaction forming the hydroperoxyl-TCNQ and O–O homolytic cleavage to yield HO^\bullet and TCBQ-O^\bullet . Subsequent disproportionation TCBQ-O^\bullet yields TCBQ-O^- , which can further react with excess H_2O_2 to produce HO^\bullet .

Hydrogen peroxide oxidation of anions is not favorable. For example, oxidation of Cl^- to HOCl by H_2O_2 is highly endoergic with $\sim 30 \text{ kcal/mol}$. However, myeloperoxidase-mediated oxidation of Cl^- in the presence of H_2O_2 gave rate constants that are dependent on the Cl^- concentration. It was proposed that Cl^- reacts with MPO-I (an active intermediate formed from the reaction of MPO with excess H_2O_2) to form the chlorinating intermediate MPO-I-Cl^- . The rate-limiting step is $[\text{Cl}^-]$ dependent; that is, at low $[\text{Cl}^-]$, k_2 is the rate-limiting step with $k_2 = 2.2 \times 10^6 \text{ M}^{-1} \text{ s}^{-1}$ and $k_3 = 5.2 \times 10^4 \text{ s}^{-1}$ (Eq. 1.32):⁴⁰



In the absence of ionic substrates, myeloperoxidase has been reported to degrade H_2O_2 to oxygen and water thereby imparting a catalase activity.⁴¹ Kinetic analysis show that there is 1 mol of oxygen produced per 2 mol of H_2O_2 consumed with a rate constant of $\sim 2 \times 10^6 \text{ M}^{-1} \text{ s}^{-1}$ which is an order of magnitude slower than the rate constant observed for catalase of $3.5 \times 10^7 \text{ M}^{-1} \text{ s}^{-1}$. Oxidation of nitrite to nitrate by H_2O_2 in the presence of catalase has been reported.⁴² In the absence of catalase, nitrite reacts with H_2O_2 to form peroxynitrite.⁴³ Hydroxylation and nitration of tyrosine and salicylic acid by H_2O_2 in the presence of nitrite occur between the pHs of 2–4 and 5–6, respectively, as mediated by peroxynitrite formation.⁴⁴

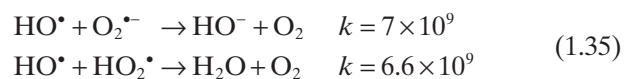
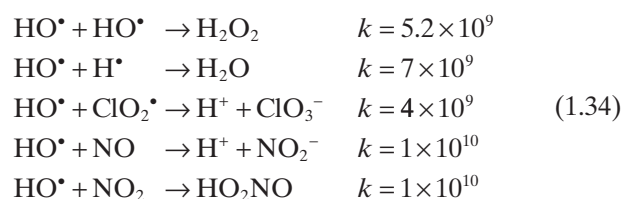
Four major detoxification pathways for H_2O_2 operate intracellularly: (1) catalase; (2) glutathione peroxidase; (3) peroxiredoxin enzymes; and (4) nonenzymatic mean via oxidation of protein thiol residues.⁴⁵ These pathways will be discussed in detail in the succeeding chapters. Probably one of the most important reactions in biological systems is the reaction of H_2O_2 with thiols. The cellular signaling property H_2O_2 is mainly dependent on the oxidation of intracellular protein thiols in which majority of these reactions form protein disulfides as opposed to *S*-glutathiolation.⁴⁵ The H_2O_2 reaction with thiols is free radical mediated and the rate is dependent on the pK_a of the thiol in which the thiolate (RS^-) is the reacting species to form the sulfenic acid (RSOH) intermediate according to Equation 1.33.³¹ The reported rate constant for the reaction of H_2O_2 with thiolates range from $18\text{--}26 \text{ M}^{-1} \text{ s}^{-1}$ which is relatively slow compared to the reaction of $\text{O}_2^{\bullet-}$ with thiols ($>10^5 \text{ M}^{-1} \text{ s}^{-1}$).³¹ Catalysis of RSSR formation with Cu(II) from peroxides has also been reported.⁴⁶



1.2.3.5 Hydroxyl Radical (HO^\bullet) Hydroxyl radical originates from the three-electron reduction of oxygen. Among all the ROS, HO^\bullet perhaps is the most reactive and short-lived. Aside from the HO^\bullet 's significant role in controlling atmospheric chemistry, it plays a direct role in the initiation of oxidative damage to macromolecules in biological systems. Unlike $\text{O}_2^{\bullet-}$ and H_2O_2 whose reactions are limited due to their lower oxidizing ability, HO^\bullet can practically react with almost every organic molecules via H-atom abstraction, electrophilic addi-

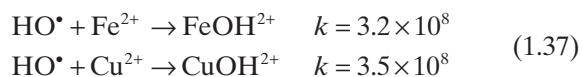
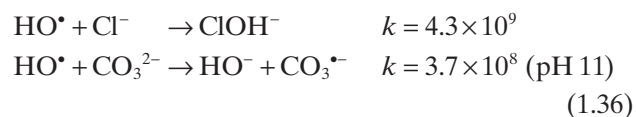
tion, or radical–radical reactions, to name a few. The standard reduction potential for $\text{HO}^\bullet_{\text{aq}}/\text{HO}^-_{\text{aq}}$ couple was determined to be 1.77 V in neutral solution.⁴⁷ The half-life of HO^\bullet is $\sim 10^{-9}$ s compared to $\sim 10^{-5}$ s and ~ 60 s for $\text{O}_2^{\bullet-}$ and H_2O_2 , respectively.

Reactivity with ROS/RNS. Radical–radical reaction of HO^\bullet proceeds at diffusion-controlled rate. For example, at neutral pH, reaction of HO^\bullet with various ROS and non-ROS radicals ranges between $\sim 10^9$ and $10^{10} \text{ M}^{-1} \text{ s}^{-1}$ (Eq. 1.34). The reactions are characteristic of addition of the hydroxyl-O to the heteroatoms. In the case of HO^\bullet reaction to $\text{O}_2^{\bullet-}$ and HO_2^\bullet , their oxidation via electron transfer reactions to form O_2 was observed (Eq. 1.35):



Theoretical studies show that hydrogen bonding between HO^\bullet and H_2O_2 forms a five-membered ring structure with two distorted hydrogen bonds with a binding energy of $\sim 4 \text{ kcal/mol}$.⁴⁸ This $\text{HO}^\bullet\text{--H}_2\text{O}_2$ interaction leads to H-atom abstraction to yield $\text{O}_2^{\bullet-}$. In pyridine, H_2O_2 reaction with HO^\bullet has a relatively slower rate of $3 \times 10^7 \text{ M}^{-1} \text{ s}^{-1}$ compared to most of HO^\bullet reactions.⁴⁹

Reactivity with ions. Reaction of HO^\bullet to anions leads to a one-electron oxidation of the anion. It has been suggested that simple electron transfer mechanism from the anion to the HO^\bullet is not likely the mechanism due to the large energy associated with the formation of the hydrated hydroxide ion.⁵⁰ Instead, an intermediate $\text{HOX}^{\bullet-}$ adduct is initially formed (Eq. 1.36). Reaction of HO^\bullet to cations can also result in an increase in the oxidation state of the ion, but unlike its reaction with anions, the reaction occurs at a much slower rate constants that is no more than $\sim 3 \times 10^8 \text{ M}^{-1} \text{ s}^{-1}$ via H-atom abstraction from the metal-coordinated water (Eq. 1.37)⁵⁰:



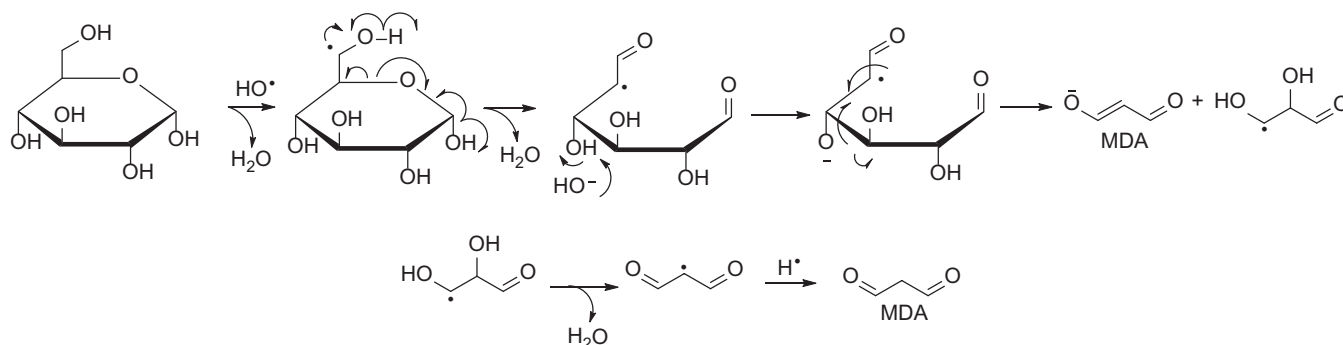


Figure 1.16 Malonaldehyde (MDA) formation from the reaction of hydroxyl radical to deoxyribose.

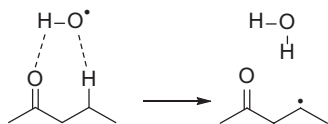
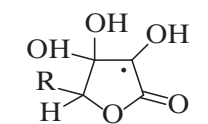


Figure 1.17 Transition state H-bonding interaction of hydroxyl radical to carbonyl leading to H-atom abstraction at the beta position.

Modes of reaction with organic molecules. There are two main mechanisms of HO^\bullet reaction with organic compounds, that is, H-atom abstraction and addition reaction. With protic compounds such as alcohols, reaction of HO^\bullet proceeds via H-atom abstraction from C–H bond and not from the O–H to form water and the radical species. The general reaction for HO^\bullet with alcohol is $\text{HO}^\bullet + \text{RH} \rightarrow \text{R}^\bullet + \text{H}_2\text{O}$, and not $\text{HO}^\bullet + \text{ROH} \rightarrow \text{RO}^\bullet + \text{H}_2\text{O}$. For example, ascorbate/ascorbic acid (AH^-/AH_2) react with HO^\bullet to form ascorbate radical anion ($\text{A}^{\bullet-}$) and ascorbyl radical (HA^\bullet) with rate constants of $1.1 \times 10^{10} \text{ M}^{-1} \text{ s}^{-1}$ (pH = 7) and $1.2 \times 10^{10} \text{ M}^{-1} \text{ s}^{-1}$ (pH = 1), respectively.⁵⁰ EPR studies revealed formation of a C-centered radical.⁵¹ Reaction of HO^\bullet with aliphatic alcohols such as methanol and ethanol gave rate constants of $9.0 \times 10^8 \text{ M}^{-1} \text{ s}^{-1}$ and $2.2 \times 10^9 \text{ M}^{-1} \text{ s}^{-1}$, respectively, using pulse radiolysis.⁵² Preference to abstract H atom at the alpha position (i.e., the H attached to the C atom that is also attached to the OH group) was theoretically demonstrated and was found to be both kinetically and thermodynamically favorable. For example, the relative energies of H-atom abstraction as calculated at the CCSD(T) level of theory are as follows: $\alpha\text{-H} = -25.79 \text{ kcal/mol} > \beta\text{-H} = -16.26 \text{ kcal/mol} > \text{OH} = -15.67 \text{ kcal/mol}$.⁵³

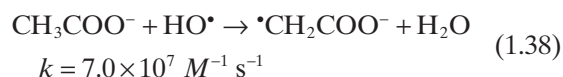


Ascorbyl Radical

Reaction of HO^\bullet with deoxyribose forms a C-centered radical which further decomposes to form malonaldehyde (MDA) (Fig. 1.16).⁵⁴ MDA is a toxic by-product of polyunsaturated lipid degradation.^{55,56} Increase dose of HO^\bullet results in increase MDA-like products,⁵⁴ therefore, production of MDA in biological systems has become a popular biomarker of oxidative stress using thiobarbituric acid (TBARS) via MDA electrophilic addition reaction to form an UV detectable adduct, TBARS-MDA. Radiolysis of D-glucose undergoes H-atom abstraction at the C-6 position and rearrangement leads to the initial elimination of two water molecules. Fragmentation yields MDA upon protonation and a dihydroxyaldehyde radical species which can further undergo dehydration to form another molecule of MDA.⁵⁷

Reaction of HO^\bullet to ketones and aldehydes also gave preference to H-atom abstraction. Rate constants for H-atom abstraction in aqueous phase were faster $2.4\text{--}2.8 \times 10^9 \text{ M}^{-1} \text{ s}^{-1}$ for acetaldehyde and propionaldehyde, compared to acetone with $k = 3.5 \times 10^7 \text{ M}^{-1} \text{ s}^{-1}$.⁵⁸ Computational studies show that for ketones with at least an ethyl group attached to the carbonyl carbon, the preference for H-atom abstraction is at the beta-position rather than the alpha position due to the presence of strong H-bond interaction forming 7-member ring transition state structure (Fig. 1.17).⁵⁹ In aldehydes, abstraction of the aldehydic-H was shown to be the most favored according to the equation, $\text{RHC}=\text{O} + \text{HO}^\bullet \rightarrow [\text{RC}=\text{O}]^\bullet + \text{H}_2\text{O}$.⁶⁰

Reaction of HO^\bullet to carboxylic acids is also that of H-atom abstraction of the acidic-H and alpha-H. There are two possible reactions in acetic acid/acetate system. One that involves H-atom abstraction from C–H and the other from OH according to Equation 1.38 and Equation 1.39, respectively:



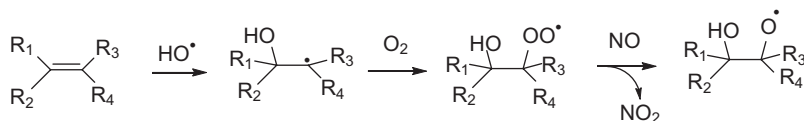


Figure 1.18 Addition reaction of hydroxyl radical to alkenes and subsequent reaction of O_2 and NO with the formed HO-alkene adduct.



Rate constants for these reactions show that H-atom abstraction from C–H bond is $4\times$ faster than abstraction from O–H in aqueous solution.⁶¹ The same trend in the relative reactivities of HO^\bullet with various acids and their respective conjugate base had been observed.⁶¹

The reaction of HO^\bullet with alkenes is relevant in the initiation of lipid peroxidation processes and will be discussed in detail in the succeeding chapter. It has been demonstrated that increasing alkyl substitution on the C=C bond enhances its reaction rate with HO^\bullet by two orders of magnitude.⁶² In the gas phase, initial reaction of HO^\bullet to alkenes forms the HO-alkene adduct which in the presence of O_2 gives the (β -hydroxylalkyl)peroxy radical. Further reaction with NO yields the β -hydroxyalkoxy radical and NO_2 according to Fig. 1.18.⁶³

Reaction of HO^\bullet with aromatic hydrocarbons mainly proceeds via addition reaction. Laser flash photolytic study in acetonitrile gave rate constants ranging from $1.2\text{--}7.9 \times 10^8 \text{ M}^{-1} \text{ s}^{-1}$ for one-ringed aromatic hydrocarbons compared to $1.8\text{--}5.2 \times 10^9 \text{ M}^{-1} \text{ s}^{-1}$ for naphthalenic systems.⁶⁴ Experimental and computational studies indicate that the electrophilic nature of HO^\bullet addition was supported by the higher rate of HO^\bullet addition reaction in aqueous solution compare to acetonitrile by a factor of 65. The stabilized aromatic ring-OH complex in the transition state has the aromatic unit and assumes a radical cation-like form and that the HO^\bullet like a hydroxide anion. This can have implication in the HO^\bullet reactivity with DNA bases in which the stabilization of the radical cation form can increase HO^\bullet reactivity to bases.⁶⁵ The same addition mechanism was proposed for benzaldehyde and its methoxy-, chloro- and nitro-analogues.⁶⁶

Thiols, such as GSH or thiol-based synthetic antioxidants such as *N*-acetyl cysteine, are important biological species. H-atom abstraction is the main mechanism of HO^\bullet reaction with thiols ($\text{RSH} + \text{HO}^\bullet \rightarrow \text{RS}^\bullet + \text{H}_2\text{O}$) with rate constants that range from $8.8 \times 10^9 \text{ M}^{-1} \text{ s}^{-1}$ to $2 \times 10^{10} \text{ M}^{-1} \text{ s}^{-1}$.⁵⁰ Computational studies also show that H-atom abstraction of the thiol-H is the main reaction channel⁶⁷ via formation of a short-lived, weakly bonded

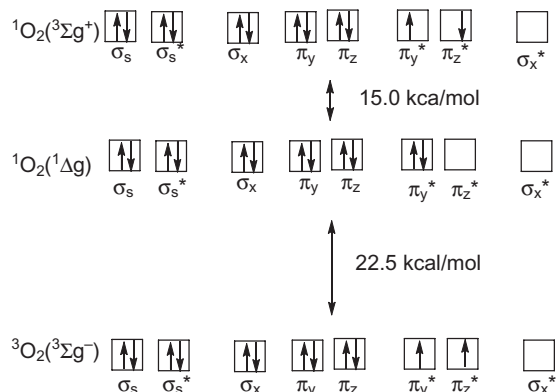


Figure 1.19 Bonding orbitals of singlet oxygens, $^1\Delta_g$ and $^3\Sigma_g^-$, in comparison to the triplet ground state, $^3\Sigma_g^-$.

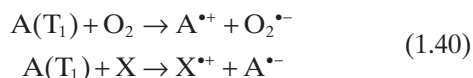
adduct prior to the abstraction process.⁶⁸ Using peroxynitrite, formation of RS^\bullet species as source of HO^\bullet was demonstrated by spin trapping.⁶⁹

1.2.3.6 Singlet Oxygen ($^1O_2(^1\Delta_g)$ or $^1O_2^*$) Singlet oxygen is the diamagnetic and less stable form of molecular oxygen. The energy separation between $^1O_2(^1\Delta_g)$ and the triplet ground state oxygen $^3O_2(^3\Sigma_g^-)$ was estimated to be 22.5 kcal/mol (94.3 kJ/mol), corresponding to a near-infrared transition of 1270 nm, while the energy separation between the $^1O_2(^1\Delta_g)$ and the singlet $^1O_2(^3\Sigma_g^+)$ is 15.0 kcal/mol.⁷⁰ Electronic configuration of the various spin states of oxygen show only variations in the electronic distribution at the pi-antibonding (π^*) orbitals. As shown in Figure 1.19, unlike the ground state oxygen ($^3\Sigma_g^-$), the electron distribution in $^1\Delta_g$ and $^3\Sigma_g^+$ have antiparallel spins where in the former, the two electrons occupy the same orbital while in the latter, each electron occupies two separate orbitals. Spin-forbidden transition from $^1\Delta_g$ and $^3\Sigma_g^-$ makes $^1O_2^*$ a relatively longer-lived species compared to the short-lived $^3\Sigma_g^+$ due to the spin-allowed transition. In solution, lifetimes of $^1O_2^*$ is solvent dependent and range from 10^{-3} to 10^{-6} s, with the shortest lifetime observed in water.⁷¹

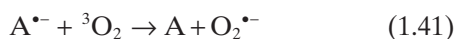
Due to the high energy state of $^1O_2^*$, its generation in biological system usually involves photo-excitation

via direct absorption through vibrationally excited water at 600 nm, or indirectly through photosensitization. Certain organic molecules absorb photons of a particular wavelength causing transition from singlet ground state (S_0) to one of the higher energy 1st or 2nd excited states, that is, S_1 and S_2 , respectively. Through vibrational relaxation (VR) or internal conversion (IC) (a nonradiative transition), $S_2 \rightarrow S_1$ ($\tau_{S1} = 10^{-8}$ s) transition occurs which can further undergo conversion to $S_1 \rightarrow S_0$ via IC, or through emission of fluorescence which is a radiative transition between spin states of the same multiplicity. One has to note that these processes do not involve change in multiplicity ($S = 1$) where the lowest energy orbitals still have the two electrons of opposite spins and are usually referred to as “spin allowed” transitions. Transition from S_0 to excited triplet states (T_1), whereby two electrons with the same spins occupy different orbitals is “spin forbidden”. However, the energy difference between S_1 and the lower lying T_1 is about ~12 kcal which can facilitate $S_1 \rightarrow T_1$ transition via intersystem crossing (ISC), another nonradiative process, for molecules with large spin-orbit coupling. Higher excited states transition ($S_2 \rightarrow T_2$) can also occur and through VR and IC, $T_2 \rightarrow T_1$ is possible. Photosensitizers typically have longer T_1 half-life than S_1 with $\tau_{S1} = 10^{-4}$ – 10^{-3} s and has a quantum yield of 0.7–0.9. Conversion of $T_1 \rightarrow S_0$ emits phosphorescence as a spin forbidden radiative transition.

The high quantum yield and longer half-life for T_1 state of photosensitizers have significant ramification in the initiation of a variety of chemical reactions. There are two major types of reaction resulting from T_1 quenching (i.e., Type I and II). Type I processes are typically characterized by H-atom abstraction or electron transfer between the excited sensitizer (A) to a substrate (X) (triplet oxygen for example to yield $O_2^{\bullet-}$) and sensitizer (A)^{•+} according to Equation 1.40:

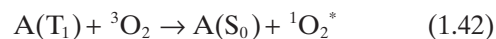


where $O_2^{\bullet-}$ can further dismutate to H_2O_2 and to form HO^{\bullet} . Alternatively, $O_2^{\bullet-}$ can also be produced from $A^{\bullet-}$ as a secondary product depending on the direction of the electron transfer reaction (Eq. 1.41).



Formation of ROS from $O_2^{\bullet-}$ can have implications in the initiation of oxidative damage to key biomolecular systems. Type II processes involve photosensitization of biological or synthetic compounds through energy-transfer mechanism (in contrast to electron-transfer mechanism for Type I) from a sensitizer triplet state

molecule T_1 to the ground state triplet O_2 , a spin-allowed process (Eq. 1.42).⁷¹



Oxidative modification via Type I or Type II processes may depend on the O_2 concentration in which the former is more likely to occur at low O_2 concentration.

The generation of singlet oxygen through photosensitization has been widely exploited in photodynamic therapy, environmental remediation and synthesis.⁷⁰ In general, the reactivity of ${}^1O_2^*$ was found to be lower than that of HO^{\bullet} but higher than $O_2^{\bullet-}$, and is ca. 1 V more oxidizing than 3O_2 .⁷⁰ There are two major quenching mechanisms for singlet ${}^1O_2^*$, that is, through physical means where interaction of ${}^1O_2^*$ with substance A forms 3O_2 ; or chemical where ${}^1O_2^*$ reacts with A to form product B or a combination of both. Physical quenching of ${}^1O_2^*$ occurs mainly through its interaction with solvents, or other substrates such as, azide, carotene, or lycopene, but its most common reaction is chemical which accounts for its main mode of action in photodynamic therapy. For example, reaction of ${}^1O_2^*$ with double bonds results in the formation hydroperoxides via “ene”-reactions, or endoperoxides through Diels-Alder-type addition to unsaturated lipids (PUFA or cholesterol), amino acids (e.g., His, Trp, and Met), or nucleic acids (e.g., guanosine).⁷² Singlet oxygen has also been shown to be chemically produced from H_2O_2 and hypochlorite, KO_2 reaction with water, and thermal decomposition of aryl peroxides.⁷¹ In biological systems, ${}^1O_2^*$ can be endogenously produced from the decomposition of alpha-linolenic acid hydroperoxide by cytochrome c and lactoperoxidase,⁷³ metabolism of indole-3-acetic acid by horseradish peroxidase and neutrophils,⁷⁴ oxidation of NADPH by liver microsomes,⁷⁵ from myeloperoxidase- H_2O_2 -chloride system,⁷⁶ or from horseradish peroxidase- H_2O_2 -GSH system.⁷⁷

1.2.4 Reactive Nitrogen Species

1.2.4.1 Nitric Oxide (NO or $\cdot NO$) Nitric oxide is a paramagnetic molecule with a bond order of 2.5 where the unpaired electron occupies an antibonding orbital (Fig. 1.20). Nitric oxide is nonpolar and with solubility in aqueous solution of 1.94×10^{-6} mol/cm/atm at 298K.⁷⁸ The diffusivity (D) at 298 K of NO is similar to that O_2 with D_{NO} in water of 2.21×10^{-5} cm²/s and 2.13×10^{-5} cm²/s for O_2 .⁷⁸

Nitric oxide functions as an intracellular signaling molecule and is the main precursor of highly oxidizing RNS's in biological system. Nitric oxide's toxicity is generally limited to its reaction or oxidation to form the more highly reactive species such as $ONOO^-$ and $\cdot NO_2$.⁴³

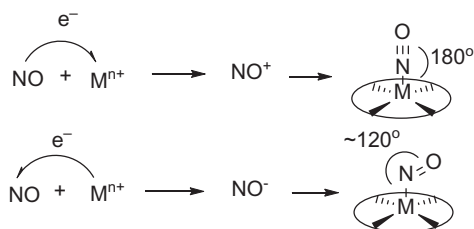


Figure 1.21 Binding modes of nitric oxide to metal ions.

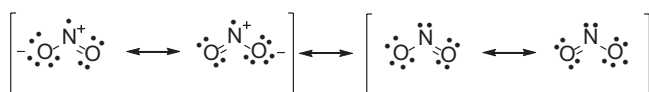


Figure 1.22 Mesomeric structures of nitrogen dioxide.

the direction of the charge transfer between the metal and NO: (1) NO assumed the NO^+ upon complexation and is characterized by a 180° M–N–O angle; and (2) NO assumed the NO^- upon complexation and is characterized by a 120° M–N–O angle (Fig. 1.21).

The direction of charge transfer is dependent on several factors such as the oxidation state and type of the metal ion, as well as, the coordination number and type of co-ligands bound to the metal other than the NO. The nature of the M–NO bonding mode determines protein conformation and NO–M reactivity (e.g., in the activation of O_2 to yield nitrate). For example, M–N–O bond angles for $\text{Fe}^{\text{II}}(\text{OEP})(\text{NO})$ and $[\text{Fe}^{\text{III}}(\text{OEP})(\text{NO})]^+$ (OEP = octaethylporphyrinato) are 143.6° and 176.9° , respectively.⁸⁶ Dependence of NO binding mode on the type of metal ions can also be seen with tetraphenylporphyrin complexes of Mn^{II} , Fe^{II} and Co^{II} , where the M–N–O bond angles are as follows, 176.1° , 142.1° , and 128.5° , respectively.⁸⁵

1.2.4.2 Nitrogen Dioxide (NO_2) Nitrogen dioxide is one of the nitrogen oxides (NO_x) and is a paramagnetic π molecule where the unpaired electron is delocalized between the three atoms (Fig. 1.22). The polar property of NO_2 is due to its bent structure with an O–N–O bond angle of 136° having negative charges on the O atoms and a positive charge on the N.

Nitrogen dioxide is sparingly soluble in water. Surface chemistry of adsorbed NO_2 in aqueous system leads to its decomposition to H^+ , nitrate and nitrous acid (HONO), and the presence of antioxidants such as ascorbate, urate and glutathione catalyzes this hydrolytic disproportionation.⁸⁷ In the gas and aqueous phases, NO_2 dimerizes with a rate constant of $\sim 5 \times 10^8 \text{ M}^{-1} \text{ s}^{-1}$ where

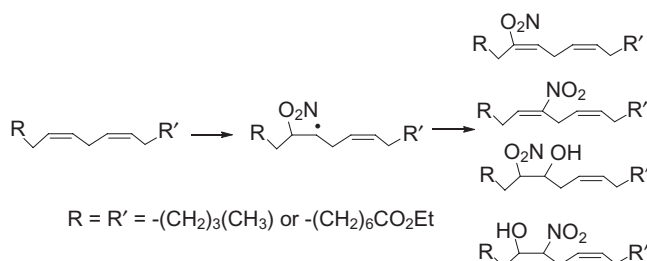


Figure 1.23 Nitration and hydroxylation of PUFA by NO_2 .

it reacts rapidly with water to form nitrites and nitrates.⁸⁸ Nitrogen dioxide is a powerful oxidizer with a $E^0(\text{NO}_2/\text{NO}_2^-) = 0.89\text{--}1.13 \text{ V}$.⁸⁹ Among the most important reactions of NO_2 are: (1) H-atom abstraction from C–H bond; (2) addition reaction to C=C bonds; (3) O-transfer reactions; (4) radical–radical addition; (5) electron transfer. The H-atom abstraction involving NO_2 is a slow process due to the weak H–O bond in HONO with a dissociation energy of $\sim 79 \text{ kcal/mol}$ compared to C–H bond of $\sim 100 \text{ kcal/mol}$.⁸⁷

Addition to Double Bonds Nitration of PUFA occurs via NO_2 addition to C=C bond (Fig. 1.23). Nitrated PUFA are important biomarker of nitrosative stress due to their abundance in biological systems. Reaction of NO_2 with 1,4-pentadiene moiety of ethyl linoleate⁹⁰ for example proceed via competition between H-atom abstraction and free radical combination. The formation of vicinal –OH along with – NO_2 results from the O-centered addition of another NO_2 to the alkyl radical and the subsequent hydrolysis of the nitrite to form the hydroxyl group. Addition of NO_2 to double bonds have also been observed in xenobiotics, food additives, retinoic acid, 17β -estradiol, or cinnamic acids.⁹¹

Radical–Radical Addition The major product in the reaction of NO_2 with MeO^\bullet is methyl nitrate (MeONO_2) through O–N bond formation.⁸³ However, reaction of NO_2 with tyrosyl radical (Tyr^\bullet) forms the 3-nitrotyrosine via C–N bond formation which is one of the most studied biomarker of oxidative damage to protein systems due to their abundance in biological systems. One could initial assume that HO^\bullet can abstract H-atom from tyrosine but its preferred mode of reaction is the ortho-directed addition to the aromatic ring to form the ortho-dihydroxytyrosine with $k = 7.0 \times 10^9 \text{ M}^{-1} \text{ s}^{-1}$.⁹² While NO_2 is able to abstract H-atom from Tyr^\bullet to form Tyr^\bullet , this reaction is relatively slower ($k = 3.2 \times 10^5 \text{ M}^{-1} \text{ s}^{-1}$)⁹³ than the H-atom abstraction by $\text{CO}_3^{\bullet-}$ with $k = 4.5 \times 10^7 \text{ M}^{-1} \text{ s}^{-1}$ (Fig. 1.24) Resonance structure of Tyr^\bullet shows localization of the unpaired electron on the

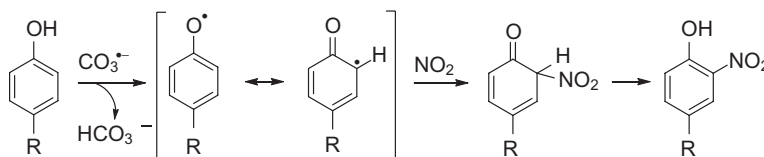
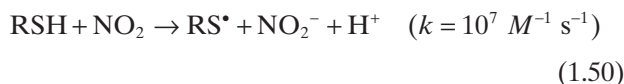


Figure 1.24 Radical–radical addition of $\cdot\text{NO}_2$ to tyrosyl radical.

phenoxyl-O and the carbon atom ortho to the phenoxyl-O. Subsequent addition of $\cdot\text{NO}_2$ to Tyr \cdot yields the 3-nitrotyrosine with $k = 3 \times 10^9 \text{ M}^{-1} \text{ s}^{-1}$.⁹³ Lost of enzyme function has been correlated with the degree of tyrosyl nitration and has been observed in prostaglandin H2 synthase (PGSH-1),⁹⁴ MnSOD⁹⁵ and mitochondrial cytochrome c.⁹⁶

Reaction with Thiols Nitrosation of thiol-containing biomolecules is one of the most important processes in posttranslational protein modification. Production of nitrosothiols (RSNO) is an important regulatory function of NO in cell signaling and pathology. Examination of RSNO formation at low micromolar concentrations of NO indicate N_2O_3 and $\cdot\text{NO}_2$ as the nitrosating agents via a one-electron oxidation of thiols to RS \cdot (Eq. 1.50) and its subsequent radical–radical addition to NO to form S-nitrosothiols (RSNO).⁹⁷ Using laser flash photolysis, the rate of glutathyl radical (GS \cdot) reaction with NO to form GSNO was reported to be $2.8 \times 10^7 \text{ M}^{-1} \text{ s}^{-1}$, which is lower than that expected for GSSG formation through radical–radical reaction further demonstrating that GS \cdot does react slowly with NO to form GSNO.⁹⁸



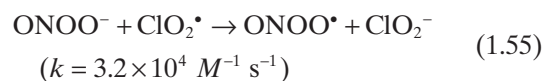
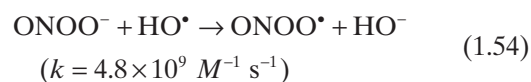
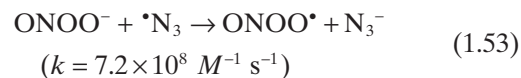
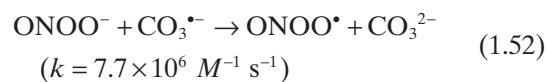
1.2.4.3 Peroxynitrite (ONOO^-) Peroxynitrite is formed from the addition reaction of NO with superoxide ($\text{O}_2^{\cdot-}$) at a diffusion-controlled rate.^{43,81} Peroxynitrite is known to exist in the relatively stable cis-conformation, or gain a proton to form peroxynitrous acid (ONOOH , pK_a 6.8). One relevant mechanism for $\text{ONOO}^-/\text{ONOOH}$ decay is its homolytic cleavage through $\cdot\text{ONO}$ · $\text{O}^{\cdot-}$ and $\cdot\text{ONO}$ · $\cdot\text{OH}$ intermediates.⁹⁹ The higher membrane permeability of ONOOH compared to its unprotonated form can result in its homolysis to form HO \cdot and $\cdot\text{NO}_2$ leading to the initiation of oxidation of key biomolecular systems. For ONOO^- , the rate of radical cleavage has been reported at $\approx 10^{-6}/\text{s}$, with negligible $\cdot\text{NO}_2$ and $\text{O}^{\cdot-}$ release,¹⁰⁰ while for ONOOH , the rate of radical cleavage has been reported to be $0.35 \pm 0.03/\text{s}$, with about 30% of HO \cdot and $\cdot\text{NO}_2$ being released at $\text{pH} < 5$ via escape from the solvent cage. Like $\text{O}_2^{\cdot-}$, ONOO^- is capable of reacting with

protein active sites containing Cu, Zn, sulfhydryl and Fe–S clusters to cause nitration and protein cleavage resulting in enzyme deactivation.^{59,101–103} The rate constant for ONOOH isomerization to nitric acid (HNO_3) was found to be $1.1 \pm 0.1/\text{s}$.¹⁰⁴ While the low rate of homolytic cleavage of ONOO^- makes the reaction trivial, ONOO^- is known to react with dissolved CO_2 to form nitrosoperoxycarbonate (ONOOCO_2^-) at a rate constant of $3.0 \times 10^4 \text{ M}^{-1} \text{ s}^{-1}$.¹⁰⁵ ONOOCO_2^- is a two-electron oxidant that undergoes homolytic cleavage to form 30% $\text{CO}_3^{\cdot-}$ and $\cdot\text{NO}_2$ (Eq. 1.51).^{95,106}



The modes of decay of ONOOCO_2^- and ONOOH has been shown to vary depending on the ability of the solvent to hold the intermediate species in the solvent cage, and is therefore, dependent on the viscosity of a solvent.¹⁰⁷ Peroxynitrite is a strong nucleophile, and has been shown to cause β -scission of carbonyl groups,^{108,109} where acyl- and H-spin adducts have been observed using EPR spin trapping.^{110,111} Peroxynitrite has recently been shown to form peroxynitrate (O_2NOO^-) at neutral pH through combination of ONOO^- and ONOOH to form O_2NOOH and nitrite (NO_2^-).¹¹²

Reaction of ONOO^- with inorganic radicals such as $\text{CO}_3^{\cdot-}$, $\cdot\text{N}_3$, ClO_2^{\cdot} and HO \cdot involves a one-electron transfer process. For example, ONOO^- oxidation by the inorganic radicals yields $\text{ONOO}\cdot$ and the corresponding anions with varying rate constants (Eq. 1.52–1.55).¹¹³ With NO, ONOO^- forms $\cdot\text{NO}_2$ and NO_2^- with highly exoergic free energy of -113 kJ .¹¹⁴



Peroxynitrite acts as two-electron oxidant with thiols. Thiols react with ONOOH to form sulfenic acid (RSOH). With low molecular weight thiols, the rates of thiol oxidation increases with decreasing thiol pK_a ,¹¹⁵ consistent with the mechanism of nucleophilic attack of the thiolate-O to the peroxy-O of ONOOH with nitrite as the leaving group according to the mechanism shown in Equation 1.56:



Rate constants for the reaction of ONOO⁻ with free cysteine and the single thiol of albumin was reported to be in the order of $10^3 M^{-1} s^{-1}$.¹¹⁶ The formation of RSSR' from RSOH in the presence of RS⁻ is fundamental to the regulation of protein function. With peroxidoxin thiol (PrxS⁻), the reaction with ONOO⁻ to yield NO₂⁻ and PrxSOH is faster ($10^7 M^{-1} s^{-1}$)¹¹⁷ than ONOO⁻ reaction with small molecular weight thiols. Decomposition of ONOO⁻ via one-electron or two-electron reduction processes can be catalyzed by metalloporphyrins of iron and manganese which can have protective effects against ONOO⁻ induced damage. One electron reduction leads to the formation of [•]NO₂ while its two-electron reduction forms NO₂⁻.¹⁰¹ The formation of [•]NO₂ from ONOO⁻ is shown to cause tyrosine nitration to form 3-nitrotyrosine.¹¹⁸

1.2.5 Reactive Sulfur and Chlorine Species

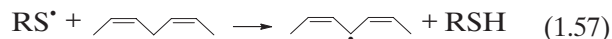
1.2.5.1 Thiyl or Sulfhydryl Radical (RS[•]) Thiyl radicals are analogous to alkoxyl radicals (RO[•]) but there are important differences between the nature of the bonds involving S and O atoms. For example, the S-H bond in thiols is weaker than the O-H bond in alcohols with experimental bond dissociation energies of 88.0 kcal/mol and 104.4 kcal/mol for CH₃S-H and CH₃O-H, respectively.¹¹⁹ The bond length for S-H is 1.33 Å compared to O-H of 0.96 Å. These differences in the structural and physical properties of thiols compared to alcohols play an important role in the reactivity of thiols compared to alcohols in which the S is more accessible. Since S is less electronegative than O, therefore, thiyls are more electrophilic than alkoxyl radicals with a longer C-S bond length of 1.81 Å compared to C-O of 1.42 Å.

Generation of RS[•] in biological systems occurs via one-electron oxidation of thiols (RSH) by metal ions such as Cu²⁺ or Fe³⁺, HO[•], peroxynitrite, DNA or protein radicals. Disulfide formation (GSSG) from GS[•] via radical-radical addition is fast with rate constant of $1.5 \times 10^9 M^{-1} s^{-1}$.¹²⁰ The susceptibility of RSH to oxidation is the basis of thiol antioxidant or repair mecha-

nisms. GSH for example is the predominant intracellular antioxidant with cytosolic concentrations of up to 10 mM. Due to the high GSH concentration, the formation of disulfide is regulated. Glutathione reacts with tyrosyl radical Tyr[•] to yield GS[•] and TyrOH ($k = 2 \times 10^6 M^{-1} s^{-1}$) as a repair mechanism but at a 220× slower rate than Tyr[•] reaction with ascorbate. Ascorbate being more abundant in tissues makes GSH a minor player in this type of repair mechanism.¹²¹

Thiyl radicals can catalyze conversion of *cis* to *trans* isomerism in unsaturated systems. In lipid systems, the conversion of the naturally occurring *cis* unsaturated fatty acids to *trans* can cause morphological changes in the lipid bi-layers.¹²² Reaction of thiyl with unsaturated compounds can also result to addition reaction where the preference for radical attack is the one with the highest electron density such as double bonds demonstrating the electrophilic nature of thiyl radicals which is due to the ability of the d-orbitals of sulfur to accommodate the negative charge. The rate constant for thiyl radical addition to monounsaturated fatty acid esters such as methyl oleate, methyl palmitoleate, methyl Z-vaccenate, and oleic acid in *tert*-butyl alcohol is in the order of k_a^Z and $k_a^E \sim 10^5 M^{-1} s^{-1}$, while the rate constant for the β-elimination to Z or E configurations are higher with k_f^Z and k_f^E of $\sim 10^7/s$ and $10^8/s$, respectively.¹²³ Thiyl radical induced isomerization for linoleic acid, linolenic acid and arachidonic acid gave k_a^Z and k_a^E of $\sim 10^6 M^{-1} s^{-1}$ and k_f^Z and k_f^E of $\sim 10^5/s$, respectively (Fig. 1.25).⁵¹

Relevant to the oxidation PUFA, thiyl can also undergo H-atom abstraction in bisallylic systems and, like HO[•] (Eq. 1.57), demonstrates their pro-oxidative role in the initiation of lipid peroxidation. The rate constant for H-atom abstraction by thiyl radicals with PUFAs was in the order of $10^7 M^{-1} s^{-1}$.¹²⁴



H-atom abstraction from aliphatic alcohols and ethers has been shown to occur at a rate constant of 10^3 – $10^4 M^{-1} s^{-1}$.¹²⁵ In peptidic systems, intramolecular H-atom transfer between cysteine thiyl radical and the αC-H bond occurs with rate constants that are in the order of 10^3 – $10^5 M^{-1} s^{-1}$.¹²⁶ The favorability of this reaction was shown to be dependent on peptide and protein sequence as well as structure and can have implications in the

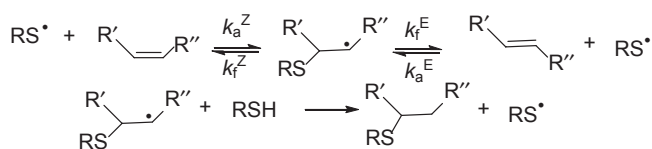
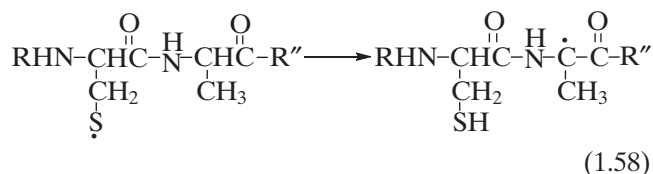


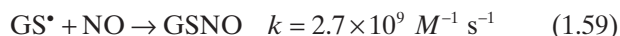
Figure 1.25 Thiyl radical mediated E and Z isomerization of monosaturated fatty acid.

catalysis of protein damage due to its potential irreversibility resulting in protein fragmentation and/or epimerization.¹²⁷ Interconversion between $^{\alpha}\text{C}^{\bullet}$, $^{\beta}\text{C}^{\bullet}$, and S-centered radicals in GS^{\bullet} (Eq. 1.58) has been shown to proceed favorably and is pH dependent with an overall rate constants of $k_{\text{forward}} = 3.0 \times 10^5/\text{s}$, $k_{\text{reverse}} = 7.0 \times 10^5/\text{s}$ and $K = 0.4$, with an equilibrium ratio at pH 7 of 8:3:1 for $\text{S}^{\bullet}:\text{C}^{\alpha}\text{C}^{\bullet}$, centered radicals.¹²⁸

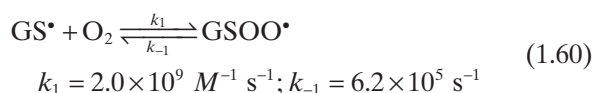


H-atom abstraction from carbohydrates by thiyl radical have been reported.¹²⁹ H-atom transfer of C^1H of 2-deoxy-D-ribose, 2-deoxy-D-glucose, α -D-glucose and inositol by cysteine-derived thiyl radical gave rate constants that are in the order of $10^4 \text{ M}^{-1} \text{ s}^{-1}$.

Quenching of thiyl radicals by ascorbate results in the formation of ascorbyl radical and RSH while thiyl reaction with radicals such as NO, O_2 , and R^{\bullet} showed varying reactivity. GSNO formation from the addition of GS^{\bullet} to NO was estimated to be much faster than the previously reported rate constant of $2.8 \times 10^9 \text{ M}^{-1} \text{ s}^{-1}$ using laser flash photolysis.⁹⁸ Using pulse radiolysis, the rate constant for the reaction of NO with thiyl radicals of glutathione (Eq. 1.59), cysteine and penicillamine were reported to be in the range of $2\text{--}3 \times 10^9 \text{ M}^{-1} \text{ s}^{-1}$.¹³⁰

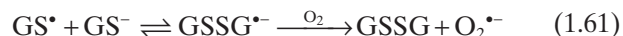


Reaction of thiyl radicals with O_2 yields RSOO^{\bullet} but the presence of excess RSH leads to the formation RSO^{\bullet} and RSOH under normal conditions.¹³¹ The reported rate constants for the reaction of GS^{\bullet} with O_2 vary from $3.0 \times 10^7 \text{ M}^{-1} \text{ s}^{-1}$ to $2.0 \times 10^9 \text{ M}^{-1} \text{ s}^{-1}$ indicating a more complex mechanism resulting from this addition reaction (Eq. 1.60).^{132, 133}



Reaction of GS^{\bullet} with GS^{\bullet} forms $\text{GSSG}^{\bullet-}$ with a rate constant of $4.5 \times 10^8 \text{ M}^{-1} \text{ s}^{-1}$ with an equilibrium constant of $2.25 \times 10^3/\text{M}$.¹³⁴ Decay of $\text{RSSR}^{\bullet-}$ forms RS^{\bullet} and RS^{\bullet} , with RS^{\bullet} further undergoing intramolecular H-atom abstraction mechanism to form the α -amino carbon-centered radical with rate constants ranging in the order of $10^4\text{--}10^5/\text{s}$ for cysteine, homocysteine and glutathione at pH 10.5.¹³⁴ Protonation of $\text{RSSR}^{\bullet-}$ leads to its decomposition to RS^{\bullet} and RSH and ultimately to RSSR with

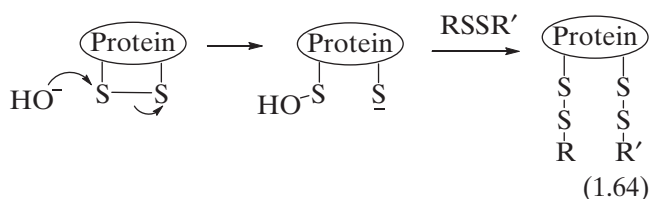
rate constants in the order of $10^5\text{--}10^6/\text{s}$.¹³⁵ Reaction of $\text{GSSG}^{\bullet-}$ with O_2 has a rate constant of $1.6 \times 10^8 \text{ M}^{-1} \text{ s}^{-1}$ (Eq. 1.61).¹³⁶



1.2.5.2 Disulfide (RSSR) Unlike the S–H bond dissociation energy being lower than the O–H, the S–S bond dissociation energy is higher compared to O–O. Reported BDE for MeS-SMe is 74 kcal/mol compared to MeO-OMe of 37.6 kcal/mol.^{119,137} Thiol-disulfide interchange as described by Equation 1.62 and Equation 1.63 shows formation of a mixed disulfide intermediate RSSR' from the oxidation of RSH and reduction of RSSR' .¹³⁸ Thiol-disulfide interchange is an important biochemical process and occurs in many metabolic reactions of thiols either endogenously or from thiol-based drugs such as penicillamine. The rate constants for the symmetrical thiol-disulfide exchange reaction have been determined for several thiols such as GSH, Cys, or homocysteine in aqueous basic medium (pH > 10) with k in the range of $12\text{--}60 \text{ M}^{-1} \text{ s}^{-1}$.¹³⁸



Disulfide bonds play a major role in protein thermal stability but through chemical means, disulfide bonds can be broken down via several mechanisms. Under basic or neutral conditions, hydroxide (HO^-) is shown to attack the sulfur atom to form sulfenic acid and thiolate anion and can ultimately result in post-translational protein modification to form complex disulfides (Eq. 1.64) or mixed sulfenic acid/disulfides with another protein/s.



Hydroxide can also abstract the α - or β -protons of the Cys residue leading to C–S or S–S bond breakage, respectively, followed by β - or α -elimination according to Figure 1.26.¹³⁹

Disulfide can be further oxidized to disulfide-S-monoxide and disulfide-S-dioxide. Oxidation of one of the sulfur atoms leads to the weakening of the S–S bond and is therefore more susceptible to reaction with RSH to form sulfenic (RSOH) and sulfenic acids (RSO_2H) to generate the mixed disulfide (Fig. 1.27).¹⁴⁰

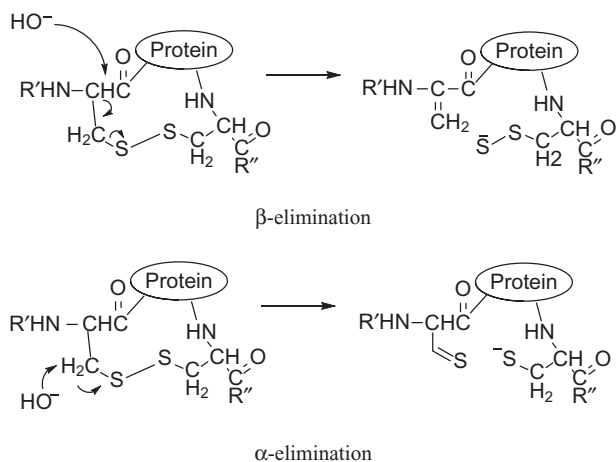


Figure 1.26 β- or α-elimination reactions of hydroxide on protein with cysteine residues.

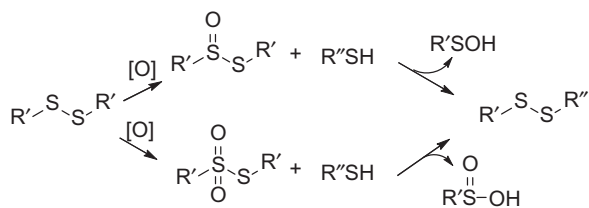


Figure 1.27 Formation of mixed disulfides through oxidation processes.

Disulfides can also be enzymatically reduced to RSH by glutathione reductase¹⁴¹ or thioredoxin reductases¹⁴² in the presence of NADPH, or chemically, by small molecules such as dithiothreitol, hydrazine or sulfones.¹⁴³

1.2.5.3 Hypochlorous Acid (HOCl) Hypochlorous acid is usually formed from the reaction of Cl_2 gas with water, however in biological systems, their formation have been mediated by a secreted heme protein, myeloperoxidase (MPO), which can convert H_2O_2 to HOCl in the presence of chloride ion (Cl^-) according to Equation 1.65.¹⁴⁴



HOCl has a pK_a of 7.5, therefore, it co-exists with the ionized hypochlorite (^-OCl) in solution at physiological pH. The HOCl produced has been shown to be a potent 2-electron oxidant capable of chlorinating electron rich substrates and oxidation of heme, tyrosine or cysteine residues in proteins, DNA and lipids.

Hypochlorous acid reacts with various ROS such as H_2O_2 to generate stoichiometric amounts of $[\text{O}_2 (^1\Delta_g)]$,¹⁴⁵

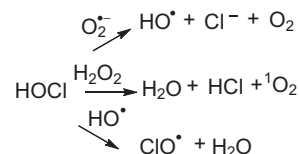
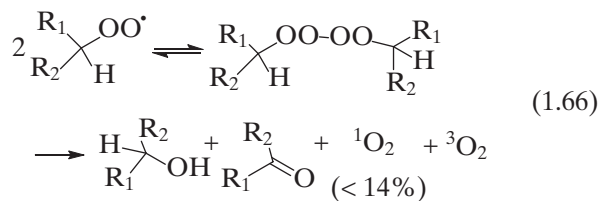


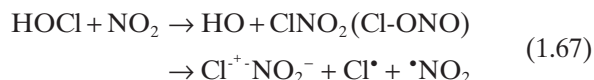
Figure 1.28 Reactions of hypochlorous acid with various reactive oxygen species.

with $\text{O}_2^{\bullet-}$ to generate HO^\bullet ,¹⁴⁶ and with HO^\bullet to form ClO^\bullet (Fig. 1.28).¹⁴⁷

Reaction of HOCl with hydroperoxide such as linoleic acid hydroperoxide (LA-OOH) mimics that of its reaction with H_2O_2 producing $[\text{O}_2 (^1\Delta_g)]$ (13% yield) at physiological pH (Eq. 1.66).¹⁴⁸



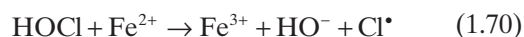
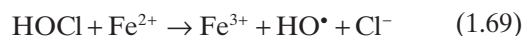
With anions such as NO_2^- , HOCl is capable of forming a reactive intermediate that can nitrate phenolic substrates such as tyrosine and 4-hydroxyphenyl acetic acid with high yield at physiological pH.^{149,150} The nitrating intermediates were identified to be $^\bullet\text{NO}_2$ and nitryl chloride ($\text{NO}_2\text{-Cl}$) based on Equation 1.67.



Sulfite reaction with HOCl gives the intermediate, Cl-SO_3^- and its subsequent hydrolysis forms Cl^- and SO_4^{2-} .¹⁵¹ Reaction rate of HOCl with low molecular weight antioxidant such as ascorbate (AH^-) is $6 \times 10^6 \text{ M}^{-1} \text{ s}^{-1}$.¹⁵²



Electron transfer reaction between Fe^{2+} and HOCl occurs with the generation of HO^\bullet and Cl^\bullet according to Equation 1.69 and Equation 1.70,



where the formation of HO^\bullet predominates due to the electron transfer reaction between Cl^\bullet and H_2O to further form HO^\bullet .¹⁵³

Reaction of HOCl with free amino acid backbone generates chloramine species at the free amino moiety.

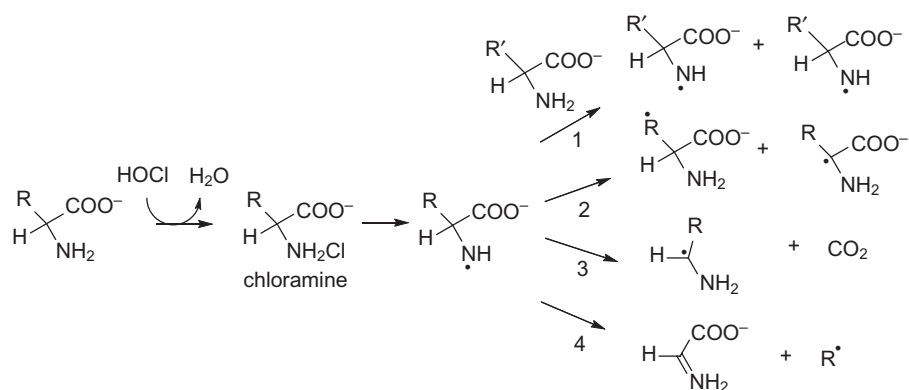


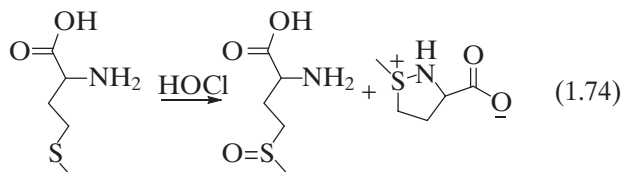
Figure 1.29 Reaction of hypochlorous acid with amino acids.

Chloramine undergoes further decomposition to nitrogen-centered radicals which subsequently undergo further decomposition pathways such as (1) intra- and intermolecular H-atom abstraction; (2) decarboxylation; (3) β -scission according to Figure 1.29.¹⁵⁴

Analogous to the reaction of amines with HOCl, GSH forms S-chloro derivative with HOCl which can hydrolyse to yield the corresponding sulfenic acid (GSOH) (via formation of thiyl radical)¹⁵⁴ with an estimated rate constant of $>10^7 \text{ M}^{-1} \text{ s}^{-1}$ (Eq. 1.71, Eq. 1.72, and Eq. 1.73).¹⁵³ With amino acids containing thiols, methionine, or cysteine, the rates were estimated to be in the order of $\sim 10^{4-5} \text{ M}^{-1} \text{ s}^{-1}$.¹⁵⁵



The formation of sulphonamide (RSO_2NHR) but not the formation of GSSG from HOCl and GSH via intramolecular cyclization reaction has also been observed.¹⁵⁶ Methionine oxidation by HOCl forms methionine sulf-oxide and dehydromethionine according to Equation 1.74¹⁵⁷:



Reaction of HOCl with tyrosine and peptidyl-tyrosyl residues yielded 3,5-dichlorotryosine (diCl-Tyr) in addition to Cl-Tyr. Further reaction of the mono- and dichlorinated tyrosines gave the corresponding mono- and dichlorinated 4-hydroxyphenylacetaldehydes, Cl-HPAA and diCl-HPAA, respectively, according to Figure 1.30.¹⁵⁸

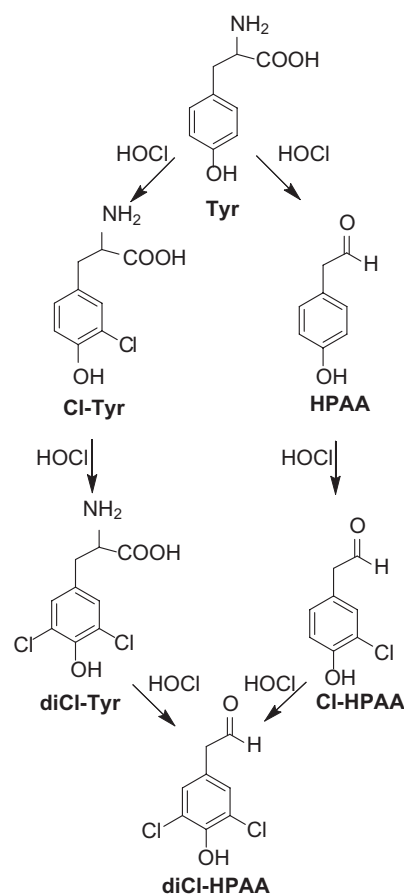
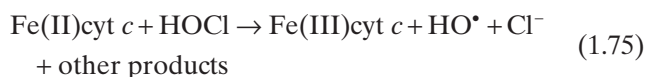
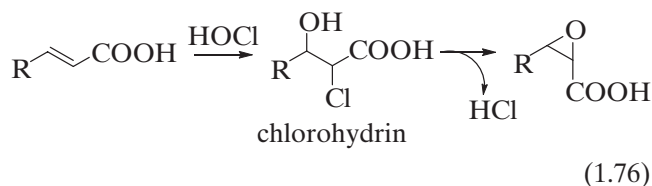


Figure 1.30 Reactions of hypochlorous acid with tyrosine.

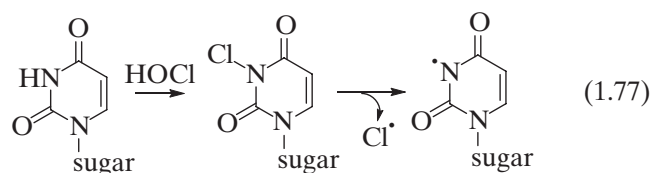
Oxidation of cytochrome *c* by HOCl has rate constant of $>3 \times 10^5 \text{ M}^{-1} \text{ s}^{-1}$. This reaction is not only selective toward the heme iron but also involves *N*-halogenation of the side chain amino groups and with concomitant generation of HO^\bullet (Eq. 1.75).¹⁵⁹



HOCl reaction with lipids occurs at either the lipid head group or the unsaturated portion of the fatty acid side-chain. For example, reaction of HOCl with phosphoryl-serine and phosphoryl-ethanolamine are rapid with $k \sim 10^5 \text{ M}^{-1} \text{ s}^{-1}$ yielding chloroamines as the major products.⁴⁴ Reaction with unsaturated fatty acid chains involves initial formation of chlorohydrins¹⁶⁰ followed by secondary dehydrohalogenation reactions to yield the epoxide (Eq. 1.76). The formed epoxide can further react with HOCl to form ROS and lipid peroxidation products.



Reaction of HOCl with nucleotide bases occur primarily on the exocyclic free amino group (e.g., of cytosine, adenosine and guanosine) or nitrogen atoms of the heterocyclic ring (e.g., of thymidine, uridine and guanosine) which contain lone pairs to form N-Cl bond. These adducts can result in miscoding and have been identified in tissues under inflammatory conditions. The rate constants for reactions within the heterocyclic ring is in the order of $10^3\text{--}10^4 \text{ M}^{-1} \text{ s}^{-1}$. With uridine for example, N-Cl formation leads to the formation of N-centered radical (Eq. 1.77).¹⁶¹



Direct chlorination on the carbon atom by HOCl of the heterocyclic ring was also observed to give chlorinated products such as 5-chloro-2'-deoxycytidine, 5-chloro-uracil, 8-chloro-2'-deoxyguanosine, and 5-chloro-2'-deoxyadenosine¹⁶² as well as hydroxylation of the pyrimidine moiety to give thymine glycol (cis/trans), 5-hydroxycytosine, 5-hydroxyuracil, 5-hydroxyhydantoin (Fig. 1.31).¹⁶³

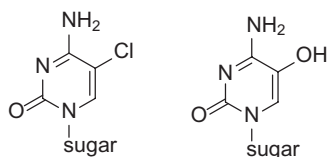


Figure 1.31 Chlorination and hydroxylation of pyrimidine by hypochlorous acid.

Reaction of related compound such as NADPH with HOCl is characterized by an initial fast reaction with $k = 4.2 \times 10^5 \text{ M}^{-1} \text{ s}^{-1}$ leading to the formation of a stable pyridine product (Py/Cl). Subsequent reaction with HOCl ($k = 3 \times 10^3 \text{ M}^{-1} \text{ s}^{-1}$) leads to the total loss of the aromatic pyridine ring absorbance.¹⁶⁴

1.3 REACTIVITY

As in all chemical reactions, reactions involving reactive species are governed thermodynamically and kinetically, and these two inter-related forces can offer insights into the favorability and rate of a reaction, respectively.

1.3.1 Thermodynamic Considerations

The favorability of redox reaction involving reactive species is governed by the overall change in the potential energy whereby the energy is released (in this case of an exothermic reaction) or addition of energy (endothermic reaction) to the system for the reaction to proceed. The thermodynamic favorability is defined by an entity called free energy (ΔG) which is either introduced or given off in a reaction. One can envision that reactants and products have stored energy in them. Calculation of ΔG can be theoretically and experimentally performed. As an example for the formation ONOO^- from $\text{O}_2^{\cdot-}$ and $\cdot\text{NO}$, one can calculate the favorability of this reaction by taking into account the potential energies of the individual species. One important theoretical consideration in determining the free energy of reaction (ΔG_{rxn}) is that the type and number of atoms in the product and reactant sides should be conserved as shown in the equation: $\text{O}_2^{\cdot-} + \cdot\text{NO} \rightarrow \text{ONOO}^-$. Each of these species carries a potential energy originating from the separation of the individual nuclei and electrons from the molecule. For example, the following are the total electronic energies (ϵ_0) (with thermal free energies, G_{corr}) for $\text{O}_2^{\cdot-}$, $\cdot\text{NO}$, and ONOO^- formed from nuclei and electrons (Fig. 1.32).

The $\Delta G_{\text{rxn}, 298\text{K}}^o$ for the reaction: $\text{O}_2^{\cdot-} + \cdot\text{NO} \rightarrow \text{ONOO}^-$ can then be calculated using the Equation 1.78:

$$\begin{aligned} \Delta G_{\text{rxn}, 298\text{K}}^o &= \sum (\epsilon_0 + G_{\text{corr}})_{\text{products}} - \sum (\epsilon_0 + G_{\text{corr}})_{\text{reactants}} \\ \Delta G_{\text{rxn}, 298\text{K}}^o &= ((-280.402251) - (-150.482170 + -129.907204)) \\ &\quad * 627.5095 \\ \Delta G_{\text{rxn}, 298\text{K}}^o &= -8.08 \text{ kcal/mol} \end{aligned} \quad (1.78)$$

The ΔG for the formation of ONOO^- from $\text{O}_2^{\cdot-}$ and $\cdot\text{NO}$ is therefore exothermic since the total energy of the reactant is greater than the reactants, and therefore,

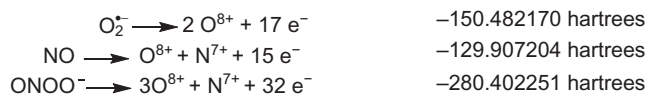


Figure 1.32 Total electronic energies for $\text{O}_2^{\bullet-}$, $\cdot\text{NO}$, and ONOO^- formed from nuclei and electrons.

excess energy is given off, hence, the reaction is said to proceed spontaneously. In contrast, the dismutation reaction of two $\text{O}_2^{\bullet-}$ to form O_2^{2-} and O_2 according to the equation: $2\text{O}_2^{\bullet-} \rightarrow \text{O}_2^{2-} + \text{O}_2$, gave $\Delta G^\circ_{\text{rxn}, 298\text{K}} = 35.7 \text{ kcal/mol}$, which is endoergic and does not proceed spontaneously due to repulsion between the two $\text{O}_2^{\bullet-}$. The two contrasting equations demonstrate the relative thermodynamic stability of the two reactions in which the formation of ONOO^- is preferred due to the less repulsion between reactants and the radical–radical nature of the reaction.

However, ΔG of formation for ROS/RNS can also be obtained experimentally. Koppenol had compiled a series free energies as shown in Table 1.1.¹¹⁴

The ΔG is defined by Equation 1.79,

$$\Delta G = \Delta H - T\Delta S \quad (1.79)$$

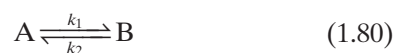
where ΔH is the change in enthalpy, T is the absolute temperature and ΔS is the change in entropy. Although the exoergicity or endoergicity of a reaction is determined by the minimization of the total enthalpy (i.e., net heat change), the minimization of the total free energy of the system at constant temperature and pressure is the driving force for all reactions. Therefore, the sign of ΔG indicates favorability of a reaction, that is,

$\Delta G < 0$ (favored or spontaneous)

$\Delta G = 0$ (equilibrium, neither forward or backward reactions are favored)

$\Delta G > 0$ (not favorable, nonspontaneous)

The concept presented above assumes that the reaction is unidirectional, meaning that the products are perfectly thermodynamically stable and does not revert back toward the formation of the reactant. However, there are reactions involving reactive species that are not unidirectional. These reactions contain significant quantities of reactants and products at equilibrium (Eq. 1.80), a state in which the composition of the reactant and products remains unchanged.



The relationship between free energy and thermodynamic equilibrium (K_{eq}) constant is described by Equation 1.81:

TABLE 1.1 Gibbs Energies of Formation for Various ROS/RNS^{114,165}

Compounds	$\Delta_f G^\circ$ (kcal/mol)
HO^\bullet	15.7 (12.7) ¹⁶⁶
H_2O	-56.7
H_2O_2	-14.1
HO_2^\bullet	10.7 (1.7) ¹⁶⁵
HO_2^-	-7.6
HO^-	-28.1
NO^\bullet	24.4
NO^+	52.3
NO^- (singlet)	32.5
NO^- (triplet)	15.3
NO_2^\bullet	15.1
NO_2^+	52.1
NO_2^-	-7.7
NO_3^\bullet	31.3
NO_3^-	-26.6
N_2	4.2
N_2O	27.2
$\text{N}_2\text{O}_2^{\bullet-}$	33.7
N_2O_3	35.1
ONOO^\bullet	20.1
ONOO^-	10.1 (16.6) ¹⁶⁷
O_2	3.9
$\text{O}_2^{\bullet-}$	7.6
ONOOH	7.5

Adapted from Reference 114.

$$\Delta G^\circ = -RT \ln K_{\text{eq}} \quad (1.81)$$

where R is the universal gas constant and T is the absolute temperature. Since K_{eq} represents the ratio of the molar concentrations of A relative to B, and of k_1 and k_2 at equilibrium, that is, $K_{\text{eq}} = [\text{B}]/[\text{A}] = k_1/k_2$, it is expected that ΔG° will obviously be dependent on temperature as temperature affect the direction of the equilibrium. Examples of temperature-dependent reversible reaction is the transnitrosation reaction between thiol and S-nitrosothiol (Eq. 1.82):



With R'SNO as S-nitroso-N-acetyl-penicillamine (SNAP), and with glutathione or L-cysteine as RSH, the K_{eq} 's were determined to be 3.69 and 3.66, at 25°C. Using Equation 1.79, ΔG° can be calculated to be -0.77 kcal/mol. With ΔG being negative, it is exoergic hence the equilibrium is shifted to the product side of the equation. At higher temperature (i.e., 33°C) for glutathione or L-cysteine, the K_{eq} is lower with 3.0 and 2.58, which correspond to ΔG° of -0.66 and -0.58 kcal/mol, respectively, indicating the equilibrium is shifted to the right.

Conversely, K_{eq} can be determined based on ΔG° of formations. For example, in the ionization of ONOOH to ONOO⁻ (Eq. 1.83),



using Table 1.1, the ΔG° for the formation of ONOOH and ONOO⁻ is 7.5 and 16.6 kcal/mol, respectively. The free energy of ionization is then equal to $\Delta G^\circ(\text{ONOO}^-) - \Delta G^\circ(\text{ONOOH}) = (16.6 \text{ kcal/mol}) - (7.5 \text{ kcal/mol}) = 9.1 \text{ kcal/mol}$ using $\Delta G^\circ = 0 \text{ kcal/mol}$ for H^+ . Using Equation 1.79 and $RT = 0.593 \text{ kcal/mol}$ at 25°C, one can calculate the pK_a to be 6.7 which is consistent to that observed experimentally of 6.5 by absorption spectroscopy measurements.¹⁶⁸

Free energy can also be described as a function of the cell potential (E°_{cell}) which is characterized by electron transfer or redox reaction. Using Equation 1.84,

$$\Delta G^\circ = -nFE^\circ_{\text{cell}} \quad (1.84)$$

where n is the number of electrons transferred in a half-reaction and F = Faraday's constant (23.06 kcal/mol/V), one can predict the spontaneity of a reaction based on the standard electrode potential of a half cell reaction. Buettner had compiled an extensive list of one electron reduction potential for a variety of half-cell reactions at pH 7.¹⁶⁹ Table 1.2 lists some of the reduction potentials of half reaction couples. Half-cell reactions are presented such that the species on the right side is the reduced form of the species in the left side. For example, the half-cell reaction, $\text{HO}^\bullet, e^-, \text{H}^+/\text{H}_2\text{O}$, can be written as $\text{HO}^\bullet + e^- + \text{H}^+ \rightarrow \text{H}_2\text{O}$ with a reduction potential of $E^\circ = 2.31 \text{ V}$ at standard conditions. Oxidation of H_2O can be written in reverse, that is, $\text{H}_2\text{O} \rightarrow \text{HO}^\bullet + e^- + \text{H}^+$ but the sign has to be reversed, that is, $E^\circ = -2.31 \text{ V}$. It should be noted that half-cell reaction potentials involving H^+ or HO^- can be pH dependent. Table 1.2 generally shows that the species with the most positive reduction potential (in this case HO^\bullet) is the most reducing and is therefore the easiest to oxidize.

To predict the spontaneity of a reaction based on reduction potentials, one can write two half-cell reactions where one is a reduction and the other is an oxidation process. For example, in Fenton chemistry, the reaction of Fe(II) with H_2O_2 is represented below. Note that the sign for the reduction potential of Fe(II) is negative (Eq. 1.85) since Fe(II) is oxidized to Fe(III) in this reaction.

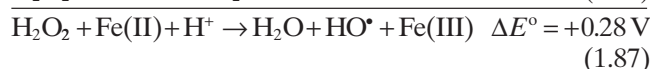
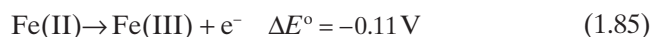


TABLE 1.2 Reduction Potentials for Various Half-Cell Reactions Showing One-Electron and Two-Electron Oxidants¹¹⁴

Half-cell reactions	ΔE° (vs NHE)
	At pH 7 in V at 25°C
$\text{HO}^\bullet, e^-, \text{H}^+/\text{H}_2\text{O}$	2.31
$\text{CO}_3^{\bullet-}, e^-, \text{H}^+/\text{HCO}_3^-$	2.10
$\text{RO}^\bullet, e^-, \text{H}^+/\text{ROH}$	1.60
$2\text{NO}, 2e^-, 2\text{H}^+/\text{N}_2\text{O}, \text{H}_2\text{O}$	1.59
$\text{H}_2\text{O}_2, 2e^-, 2\text{H}^+/\text{H}_2\text{O}$	1.35 (1.78) ⁸⁹
$\text{HOO}^\bullet, e^-, \text{H}^+/\text{H}_2\text{O}_2$	1.05
$\text{ROO}^\bullet, e^-, \text{H}^+/\text{ROOH}$	1.00
$\text{NO}_3^-, e^-, 4\text{H}^+/\text{NO}, 2\text{H}_2\text{O}$	0.96
$\text{NO}_3^-, 2e^-, 3\text{H}^+/\text{HNO}_2, \text{H}_2\text{O}$	0.93
$\text{RS}^\bullet, e^-/\text{RS}^-$	0.92
$\text{O}_2^{\bullet-}, e^-, 2\text{H}^+/\text{H}_2\text{O}_2$	0.91
$\text{N}_2\text{O}_4, 2e^-/\text{2NO}_2^-$	0.87
$\text{O}_2, 4e^-, 4\text{H}^+/\text{2H}_2\text{O}$	0.85 (1.23) ⁸⁹
$^1\text{O}_2, e^-/\text{O}_2^{\bullet-}$	0.81
$\text{PUFA}^\bullet, e^-, \text{H}^+/\text{PUFA-H}$	0.60
$^{\bullet}\text{NO}_2, e^-/\text{NO}_2^-$	0.60
$\alpha\text{-Tocopheroxyl}^\bullet, e^-, \text{H}^+/\alpha\text{-Tocopherol}$	0.50
$\text{H}_2\text{O}_2, e^-, \text{H}^+/\text{H}_2\text{O}, \text{HO}^\bullet$	0.39
$\text{O}_2, 2e^-, 2\text{H}^+/\text{H}_2\text{O}_2$	0.36
ascorbate [•] , $e^-, \text{H}^+/\text{ascorbic acid}$	0.28
$\text{Fe(III)}, e^-/\text{Fe(II)}$	0.11
$\text{NO}_3^-, 2e^-, \text{H}_2\text{O}/\text{NO}_2^- + 2\text{HO}^-$	0.01
$\text{O}_2, e^-/\text{O}_2^{\bullet-}$	-0.18
$\text{FAD}, 2e^-, 2\text{H}^+/\text{FADH}_2$	-0.22
$\text{NADP}^+, 2e^-, \text{H}^+/\text{NADPH}$	-0.32
$\text{NAD}^+, 2e^-, \text{H}^+/\text{NADH}$	-0.32
$\text{O}_2, e^-, \text{H}^+/\text{HOO}^\bullet$	-0.46
$\text{NO}, e^-/\text{NO}^-$	-0.81
$2\text{NO}_3^-, 2e^-, 2\text{H}_2\text{O}/\text{N}_2\text{O}_4 + 4\text{HO}^-$	-0.85
$\text{GSSG}, e^-/\text{GSSG}^{\bullet-}$	-1.5

Adapted from References 89 and 114.

The net equation gave a positive ΔE° value of +0.28 V (Eq. 1.87). For a reaction to occur spontaneously, the ΔG° must be negative. However, according to Equation 1.84, E° must be positive to meet the requirement for spontaneity, and therefore, reaction of H_2O_2 with Fe(II) is considered highly favorable.

1.3.2 Kinetic Considerations

Although free energies are useful entities to predict if a reaction will take place, it does not address the rate by which the process will occur. Thermodynamics only describes the relative stability of the reactants versus products. The rate of reaction is proportional to the molar concentration of a component (Eq. 1.88).

$$-d[\text{reactant}]/dt \text{ or } +d[\text{product}]/dt \quad (1.88)$$

at isothermal and constant volume. As the reaction proceeds, the reactant/s concentrations decrease and this is accompanied by a decrease in the rate of the reaction as they usually tend to slow down overtime. Since rates have variability, a way to quantify the rate of a chemical reaction is through the use of an experimental measure of a reaction rate which is usually referred to as rate constants (k). (Note that by convention, small letter k is referred to as the rate constant and the capitalized K as equilibrium constant). Rate constant is independent of how far the reaction proceeded and its scale. Reactive species in biological systems could exhibit unimolecular, bimolecular or higher order reactions and each of these types of reaction are described by a rate constant.

1.3.2.1 Unimolecular or First-Order Reactions Only one reactant in which the rate of its reaction is solely proportional to its concentration at constant volume where the reaction is described in Equation 1.89,



and where the rate law is described in Equation 1.90:

$$\text{Rate of reaction} = -d[A]/dt = k_1[A] \quad (1.90)$$

Experimentally, one can determine the first-order rate constant (k_1) by monitoring the formation or decay of A as a function of time (Eq. 1.91).

$$\ln\left(\frac{[A]_t}{[A]_0}\right) = -k_1 t \text{ or } \log\left(\frac{[A]_t}{[A]_0}\right) = \frac{-k_1 t}{2.303} \quad (1.91)$$

where $[A]_0$ and $[A]_t$ are concentrations at time = 0 and time = t , respectively. The first-order rate constant has a dimension of time^{-1} and is usually expressed in s^{-1} unit. The half-life ($t_{1/2}$) of a first-order reaction which is the time required for the $[A]$ to decrease by 50% is described as

$$k_1 t_{1/2} = 0.693$$

Therefore, based on this equation, by knowing $t_{1/2}$, one will be able to determine k_1 . Examples of this reaction is the decomposition of $\text{GSSG}^{\bullet-}$ to form GS^- and GS^\bullet , or ONOOH to form NO_2^\bullet and HO^\bullet .

1.3.2.2 Bimolecular or Second-Order Reactions This reaction occurs from two reactants that are the same species (Eq. 1.92). The rate law is described in Equation 1.93.



$$\text{Rate of reaction} = -d[A]/dt = k_2[A]^2 \quad (1.93)$$

where the rate is proportional to the instantaneous concentration of A. The second-order rate constant is usually expressed in M^{-1}/s unit.

Experimentally, one can determine the second-order rate constant (k_2) by monitoring the formation or decay of A as a function of time (Eq. 1.94).

$$\frac{1}{[A]_t} - \frac{1}{[A]_0} = k_2 t \quad (1.94)$$

The half-life for second-order reaction is described by Equation 1.95,

$$k_2 t_{1/2} = 1/[A] \quad (1.95)$$

which indicates that the $t_{1/2}$ of the second-order rate constant is inversely proportional to $[A]$. Examples of this reaction are the bimolecular reaction between two HO^\bullet to form H_2O_2 , or the dismutation of HOO^\bullet to form H_2O_2 and O_2 .

Majority of reactions, however, are between two different species (Eq. 1.96) as described by the rate law (Eq. 1.97):



$$\text{Rate of reaction} = -d[A]/dt = -d[B]/dt = k_2[A][B] \quad (1.97)$$

The integrated rate law for k_2 determination is described by Equation 1.98:

$$\ln\left(\frac{[A]_t}{[B]_t}\right) = ([A]_0 - [B]_0)k_2 t + \ln\left(\frac{[A]_0}{[B]_0}\right) \quad (1.98)$$

To simplify the kinetic measurements, second-order kinetics can be investigated using first-order rate law by making one of the reagents in large excess. For example, if A is in large excess over B, that is, $[A]_0 \gg [B]_0$, then $[A]_t \sim [A]_0$, therefore, Equation 1.98 can be rewritten as $k_2[A]_0 = k_1'$ where k_1' is the pseudo-first-order rate constant that is related to the concentrations of B according to Equation 1.99,

$$\ln\left(\frac{[B]_t}{[B]_0}\right) = -k_1' t \quad (1.99)$$

Using the known initial concentration of the reactant that is in excess, that is $[A]_0$, the second-order rate constant k_2 can be calculated from k_1' .

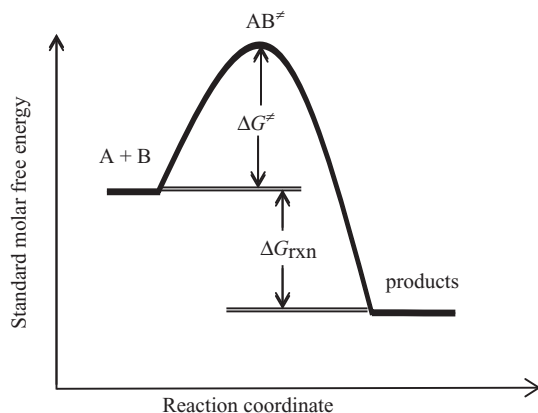


Figure 1.33 Classical reaction coordinate for an exothermic reaction showing the free energies of activation (ΔG^\ddagger) and reaction (ΔG_{rxn}).

1.3.2.3 Transition State Theory, Reaction Coordinates and Activation Energies Transition state theory is the current model used to describe a chemical reaction in terms of physical processes. It assumes that reactions are in equilibrium between the reactants and an activated transition state structure. By determining the reaction rate constants (k_c), the standard Gibbs free energy of activation (ΔG^\ddagger) can be calculated using Equation 1.100,

$$k_c = \frac{k_B T}{h} e^{-\Delta G^\ddagger / RT} \quad (1.100)$$

where $k_B T/h$ is the universal factor composed of Boltzman (k_B) and Planck (h) constants and the absolute temperature (T).

In a simple reaction coordinate composed of reactants ($A + B$), activated complex (AB^\ddagger) and products, the potential energy diagram for an exothermic reaction is shown in Figure 1.33.

The activated complex lie at the saddle point (highest energy of a potential energy surface) and is in “quasi-equilibrium” with the reactant molecules which is later converted into products.

The magnitude of ΔG^\ddagger therefore determines the rate of the reaction; that is, the higher the activation barrier the slower the reaction rate will be. One also has to consider that free energy is temperature dependent and hence the kinetics of a reaction. Several external factors can affect the magnitude of ΔG^\ddagger and the rate of reactions. For example, increased temperature, concentration, and pressure can increase the probability of collision between two particles and therefore, the rate of reaction increases. Catalysts such as enzymes provide lower activation barrier by increasing the collision rate between reactants by arranging the orientation of the

reactants for optimal reactivity; by changing the electronic property of the reactants through increased electrophilicity or nucleophilicity; through changes in intramolecular forces of attraction that can hinder reactants reactivity; or by simply providing alternative pathways for the reaction mechanism.

The range of rates by which reactions in biological system occurs is wide from very slow (<1) to diffusion controlled rate (10^9 – 10^{10}). Table 1.3 shows the various biologically relevant reaction and their experimental rate constants.

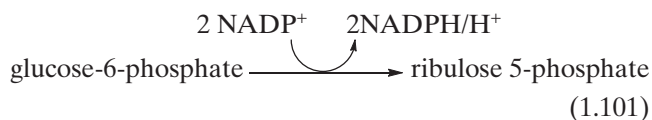
Based on Table 1.3, in general, the fastest reactions (10^9 – 10^{10}) involve either addition reaction or electron transfer reaction between two radicals. Intermediate rate reactions (10^5 – 10^8) are mostly characterized by H-atom abstraction, reaction between radical anions or electron transfer between the pi-radicals such as in the case of NO and O_2 . Slow reactions (10^{-2} – 10^4), are mostly unimolecular decomposition that involves bond breaking of N–O, O–O or N–N bonds and electron transfer between anions and neutral molecules.

1.4 ORIGINS OF REACTIVE SPECIES

1.4.1 Biological Sources

Among the numerous reactive species formed in biological systems, $O_2^{\bullet -}$ and NO are the two major precursors. The enzymatic generation of $O_2^{\bullet -}$ and $\bullet NO$ has been shown to originate from O_2 and arginine, respectively as substrates. These radicals are formed in various subcellular compartments such as membrane, mitochondria, endoplasmic reticulum¹⁷² or golgi apparatus.¹⁷³ Below are the common sources of $O_2^{\bullet -}$ and NO but the mechanistic details will be left in the succeeding chapters and the list below only offers a general overview of the different enzymes responsible for their generation.

1.4.1.1 NADPH Oxidase Superoxide radical anion are generated through stimulated professional phagocytes (e.g., neutrophils, macrophages monocytes, dendritic cells and mast cells).¹⁷⁴ Pentose phosphate pathway generates NADPH during the oxidative phase in which two molecules of $NADP^+$ are reduced to NADPH though the utilization of glucose-6-phosphate into ribulose 5-phosphate according to Equation 1.101,

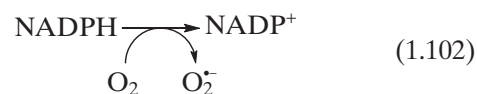


where NADPH subsequently reduce O_2 to $O_2^{\bullet -}$ via the NADPH oxidase pathway (Eq. 1.102). The details of which are discussed in Chapter 2.

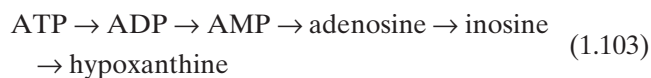
TABLE 1.3 Various Reactions of Reactive Species and their Respective Rate Constants at Normal Conditions

Reaction	Rate Constants
$O_2^{\cdot-} + \cdot NO \rightarrow ONOO^-$	$1.9 \times 10^{10} M^{-1} s^{-1}$
$O_2^{\cdot-} + HO^{\cdot} \rightarrow O_2 + HO^-$	$1.0 \times 10^{10} M^{-1} s^{-1}$
$\cdot NO + HO^{\cdot} \rightarrow HNO_2$	$1.0 \times 10^{10} M^{-1} s^{-1}$
$\cdot NO_2 + HO^{\cdot} \rightarrow \cdot NO_2 + HO^-$	$1.0 \times 10^{10} M^{-1} s^{-1}$
$\cdot NO + R^{\cdot} \rightarrow RNO$	$1.0 \times 10^{10} M^{-1} s^{-1}$
$2O_2^{\cdot-} + 2H^+ \rightarrow O_2 + H_2O_2$ (SOD catalyzed)	$1.0 \times 10^9 M^{-1} s^{-1}$
$O_2^{\cdot-} + \cdot NO_2 \rightarrow O_2NOO^-$	$4.5 \times 10^9 M^{-1} s^{-1}$
$\cdot NO_2 + \cdot NO_2 \rightarrow N_2O_3$	$1.1 \times 10^9 M^{-1} s^{-1}$
$\cdot NO + TyrO^{\cdot} \rightarrow Tyr-ONO$	$1.0 \times 10^9 M^{-1} s^{-1}$
$\cdot NO_2 + TyrO^{\cdot} \rightarrow Tyr-NO_2$	$1.3 \times 10^9 M^{-1} s^{-1}$
$NO_2^{\cdot} + HO^{\cdot} \rightarrow \cdot NO_2 + HO^-$	$5.3 \times 10^9 M^{-1} s^{-1}$
$GSSG^{\cdot-} + O_2 \rightarrow GSSG + O_2^{\cdot-}$	$5 \times 10^9 M^{-1} s^{-1}$
$2GS^{\cdot} \rightarrow GSSG$	$1.5 \times 10^9 M^{-1} s^{-1}$
$\cdot NO + GS^{\cdot} \rightarrow GSNO$	$3 \times 10^9 M^{-1} s^{-1}$
$\cdot NO_2 + GS^{\cdot} \rightarrow GSNO_2$	$3 \times 10^9 M^{-1} s^{-1}$
$GS^{\cdot} + GSNO \rightarrow GSSG + \cdot NO$	$1.7 \times 10^9 M^{-1} s^{-1}$
$GS^{\cdot} + O_2 \rightarrow GSOO^{\cdot}$	$2 \times 10^9 M^{-1} s^{-1}$
$GSOO^{\cdot} + \cdot NO_2 \rightarrow GSOONO_2$	$1 \times 10^9 M^{-1} s^{-1}$
$GSOO^{\cdot} + \cdot NO \rightarrow GSOONO$	$3 \times 10^9 M^{-1} s^{-1}$
$CO_3^{\cdot-} + \cdot NO + HO^- \rightarrow HCO_3^- + NO_2^-$	$3.9 \times 10^9 M^{-1} s^{-1}$
$GSOO^{\cdot} + GSNO \rightarrow GSSG + O_2 + \cdot NO$	$3.8 \times 10^8 M^{-1} s^{-1}$
$CO_3^{\cdot-} + O_2^{\cdot-} + H^+ \rightarrow HCO_3^- + O_2$	$4.0 \times 10^8 M^{-1} s^{-1}$
$N_2O_3 + RH \rightarrow RNO + H^+ + NO_2^-$	$1.8 \times 10^8 M^{-1} s^{-1}$
$CO_3^{\cdot-} + Tyr \rightarrow HCO_3^- + TyrO^{\cdot}$	$4.5 \times 10^7 M^{-1} s^{-1}$
$2TyrO^{\cdot} \rightarrow diTyr$	$8.05 \times 10^7 M^{-1} s^{-1}$
$N_2O_3 + GSH \rightarrow GSNO + H^+ + NO_2^-$	$6.6 \times 10^7 M^{-1} s^{-1}$
$\cdot NO_2 + GSH \rightarrow GS^{\cdot} + H^+ + NO_2^-$	$2 \times 10^7 M^{-1} s^{-1}$
$H_2O_2 + Catalase-Fe(III) \rightarrow \text{Compound 1}$	$k_1 = 1.7 \times 10^7$;
$\text{Compound 1} + H_2O_2 \rightarrow \text{Cat}$	$k_2 = 2.6 \times 10^7$
$Fe(III) + 2H_2O + O_2$	$M^{-1} s^{-1}$
$UH_2^{\cdot-} + \cdot NO_2 \rightarrow NO_2^- + UH^{\cdot-} + H^+$	$1.8 \times 10^7 M^{-1} s^{-1}$
$2\cdot NO + O_2 \rightarrow 2\cdot NO_2$	$2 \times 10^6 M^{-1} s^{-1}$
$4\cdot NO + O_2 + 2H_2O \rightarrow 4HNO_2$	$8.0 \times 10^6 M^{-1} s^{-1}$
$GS^{\cdot} + GS^{\cdot} \rightarrow GSSG^{\cdot-}$	$9.6 \times 10^6 M^{-1} s^{-1}$
$CO_3^{\cdot-} + GSH \rightarrow HCO_3^- + GS^{\cdot}$	$5.3 \times 10^6 M^{-1} s^{-1}$
$LOO^{\cdot} + TOH \rightarrow LOOH + TO^{\cdot}$	$2.5 \times 10^6 M^{-1} s^{-1}$
$UH^{\cdot-} + Asc^- \rightarrow UH_2^- + A^{\cdot-}$	$1 \times 10^6 M^{-1} s^{-1}$
$ROO^{\cdot} + UH_2^- \rightarrow ROO^- + UH^{\cdot-} + H^+$	$3 \times 10^6 M^{-1} s^{-1}$
$CO_3^{\cdot-} + RH \rightarrow HCO_3^- + R^{\cdot}$	$4 \times 10^5 M^{-1} s^{-1}$
$\cdot NO_2 + Tyr \rightarrow NO_2^- + TyrO^{\cdot}$	$3.2 \times 10^5 M^{-1} s^{-1}$
$GSSG^{\cdot-} \rightarrow GS^{\cdot} + GS^{\cdot-}$	$1.6 \times 10^5 s^{-1}$
$GSOO^{\cdot} \rightarrow GS^{\cdot} + O_2$	$6 \times 10^5 s^{-1}$
$\cdot NO_2 + RH \rightarrow NO_2^- + R^{\cdot} + H^+$	$3.2 \times 10^5 M^{-1} s^{-1}$
$GSH + TyrO^{\cdot} \rightarrow GS^{\cdot} + Tyr$	$3.5 \times 10^5 M^{-1} s^{-1}$
$GS^{\cdot} + Tyr \rightarrow GSH + TyrO^{\cdot}$	$3.5 \times 10^5 M^{-1} s^{-1}$
$2O_2^{\cdot-} + 2H^+ \rightarrow O_2 + H_2O_2$	$2.54 \times 10^5 M^{-1} s^{-1}$
$N_2O_3 \rightarrow \cdot NO + \cdot NO_2$	$8.1 \times 10^4 s^{-1}$
$ONOO^- + CO_2 \rightarrow NO_3^- + CO_2$	$2 \times 10^4 M^{-1} s^{-1}$
$ONOO^- + CO_2 \rightarrow \cdot NO_2 + CO_3^{\cdot-}$	$1 \times 10^4 M^{-1} s^{-1}$
$Tyr-ONO \rightarrow \cdot NO + TyrO^{\cdot}$	$1 \times 10^3 s^{-1}$
$Urate + ONOO^- \rightarrow \text{products}$	$4.8 \times 10^2 M^{-1} s^{-1}$
$ONOO^- + GSH \rightarrow NO_2^- + GSOH$	$6.6 \times 10^2 M^{-1} s^{-1}$
$LOO^{\cdot} + LH \rightarrow LOOH + L^{\cdot}$	$10-50 M^{-1} s^{-1}$
$GSOONO_2 \rightarrow GSOO^{\cdot} + \cdot NO_2$	$0.75 s^{-1}$
$ONOO^- + H^+ \rightarrow HNO_3$	0.568
$ONOO^- + H^+ \rightarrow \cdot NO_2 + HO^{\cdot}$	$0.232 s^{-1}$
$UH^{\cdot-} + O_2 \rightarrow \text{no measurable reaction}$	$<10^{-2} M^{-1} s^{-1}$

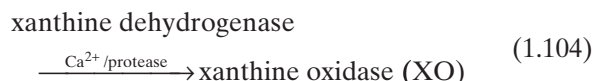
Adapted from References 170, 171 and 277.



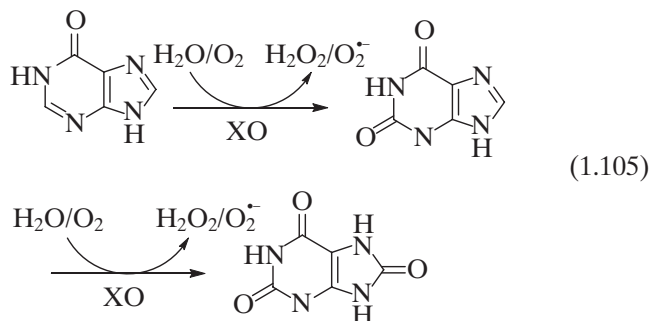
1.4.1.2 Xanthine Oxidoreductase or Oxidase During ischemia, ATP is metabolized to adenosine and through adenosine deaminase, adenosine is converted to inosine which further decomposes to hypoxanthine (Eq. 1.103).¹⁷⁵ Although hypoxanthine can be converted to xanthine by xanthine oxidase (XO) via a reductive half-reaction, xanthine can be independently formed from GMP through purine metabolism. This catalytic purine degradation is also associated with the formation of H_2O_2 and $O_2^{\cdot-}$.



XO belongs to a family of molybdoflavoenzymes and is released by a calcium-triggered protease during hypoxia (Eq. 1.104).



Hypoxanthine or xanthine can undergo reductive half-reaction with XO at the Mo-Co centers. Two electrons are transferred to XO from xanthine, thereby reducing Mo(VI) to Mo(IV). The oxidative half-reaction then takes place at FAD where electron transfer between the reduced Mo-Co occurs with FAD as mediated by Fe_2S_2 centers, thus maintaining Mo to be as Mo(VI) and FAD as $FADH_2$. Transfer of electrons from $FADH_2$ to NAD^+ or O_2 occurs during the reoxidation of fully six electron-reduced XO. The first two processes involve 2-electron reduction of O_2 to form H_2O_2 , then the remaining two electrons are each used to reduced O_2 to $O_2^{\cdot-}$. The total ROS produced is, therefore, two molecules of each H_2O_2 and $O_2^{\cdot-}$ (Eq. 1.105).



1.4.1.3 Mitochondrial Electron Transport Chain (METC) Metabolism of O_2 involves a series of electron transfer between an electron donor (NADH) and

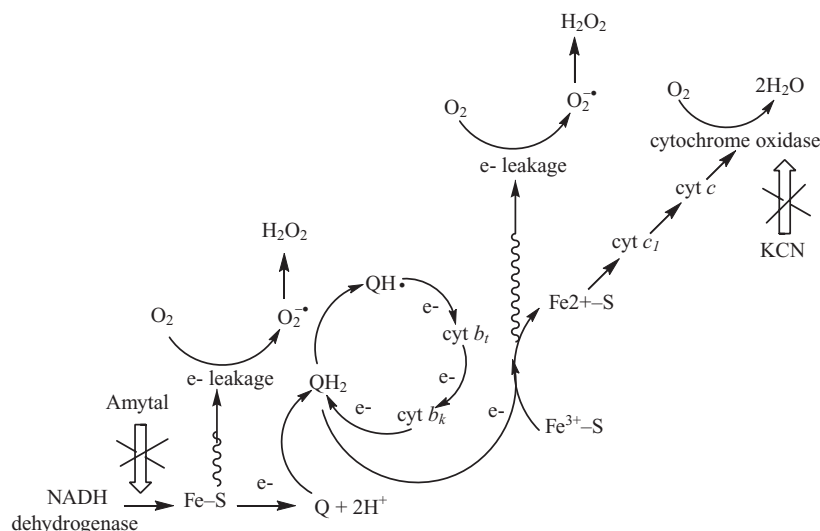


Figure 1.34 The ubiquinone cycle of the mitochondrial electron transport chain showing the formation of reactive oxygen species.

an electron acceptor, O_2 , via the METC, with concomitant transfer of protons from the inner mitochondrial membrane.¹⁷⁶ This process involves transfer of four electrons from cytochrome *c* oxidase to O_2 to form two molecules of water and four molecules of H^+ according to Equation 1.106:



However, partial metabolism of O_2 occurs prior to its full reduction to water by cytochrome *c* oxidase. Although it is estimated that under normal conditions, 1–2% of O_2 consumed by mitochondria are converted to ROS. This phenomenon called *electron leakage* maybe more prevalent in pathophysiological conditions.

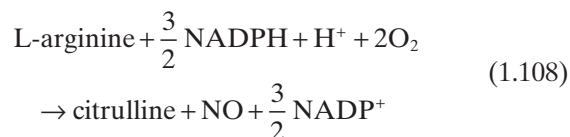
The major sources of radical generation within the mitochondria have been identified to be the NADH dehydrogenase and ubiquinone. Figure 1.34 shows the ubiquinone cycle in which ubiquinone (Q) reduces cytochrome *b* through multiple processes that also leads to the oxidation of NADH dehydrogenase. The cycle is coupled to the electron transfer process that occurs between ubiquinol (QH_2) and cytochrome *c*1 via proteins containing Fe–S clusters. At the site of this electron transfer process, an electron is “leaked” to the O_2 molecule to give $O_2^{\bullet-}$ then subsequently forming H_2O_2 . Studies on heart and nonsynaptic brain mitochondria of mammals and birds show that oxygen radicals are generated at complex I in heart and brain mitochondria in States 4 and 3, while complex III (ubiquinone cytochrome *c* reductase) generates radicals only in heart mitochondria and only in State 4.¹⁷⁷ Other sources of

ROS in the mitochondria are the dehydrogenases, quinone oxidoreductase and monoamine oxidase B.

1.4.1.4 Hemoglobin (Hb) Oxygen binds to the heme Fe(II) on a reversible and stable manner and is the basis of Hb function. However, the Fe(II) heme can undergo auto-oxidation (~3 within 24-hour period) to form Fe(III) and $O_2^{\bullet-}$ (Eq. 1.107) and is a common mechanism of oxidative stress in red blood cells.¹⁷⁸



1.4.1.5 Nitric Oxide Synthases Nitric oxide synthase catalyzes the production of nitric oxide from L-arginine via an electron flow from $NADPH \rightarrow FAD \rightarrow FMN \rightarrow$ heme \rightarrow oxygen based on Equation 1.108.¹⁷⁹



The Fe(III) heme upon reduction by $FMNH_2$ to Fe(II) enables binding to O_2 to form the ferrous-dioxy complex or $Fe(II)O_2^{\bullet-}$ (species 1). Species 1 can presumably further undergo a one-electron reduction by tetrahydrobiopterin (H_4B) to form the iron-peroxo species (species II) and O–O bond cleavage yields water (Fig. 1.35) and iron-oxo species which is thought to hydroxylate the guanidino nitrogen of the L-arginine and ultimately leading to the generation of NO (Fig. 1.36).

Under oxidative conditions such as in the presence of ONOO^- , the oxidation state for H_4B is altered such that conversion of species 1 to 2 is hampered. The peroxy group of species 1 then decomposes to $\text{O}_2^{\bullet-}$ and Fe(III) .

1.4.1.6 Cytochrome P450 (CYP) CYP is one of the most important class of enzymes responsible for the oxidation of organic substances using lipids and steroids as well as xenobiotics as substrates.^{180,181} The catalytic action of CYP mirrors that of NOS enzymes where the formation of oxo-ferryl ($\text{Fe}^{\text{IV}}=\text{O}$), species II (shown in Fig. 1.35) is the oxidizing form of the heme. Like in NOS, non-reduction of Fe(III)O_2^- results in the production of $\text{O}_2^{\bullet-}$.

1.4.1.7 Cyclooxygenase (COX) and Lipoxygenase (LPO) Arachidonic metabolism can mediate several important cellular events such as inflammation, chemotaxis, and regulation of muscle tone. However, the formation of metabolites such as prostaglandins, thromboxane and leukotriene generates ROS.¹⁸² The formation of GG_2 and HpETEs hydroperoxides has been

shown to be mediated by COX and LPO. These unstable peroxides can yield HO^\bullet and RO^\bullet via O–O bond cleavage.

1.4.1.8 Endoplasmic Reticulum (ER) ER is an organelle responsible for protein folding and maturation. Along with Golgi complex, it is involved in the transport of new proteins, lipids and other small molecules to their proper destination. Recently, ER has been implicated in hypoxia- and diabetes-mediated oxidative stress.¹⁷² During accumulation of newly synthesized unfolded proteins, the unfolded protein response (UPR) is activated and causes a variety of inflammatory and stress signaling responses. The mechanism of radical production from ER was proposed to originate from an enzyme Ero1p, a flavin-containing oxidase, due to its ability to reduce molecular O_2 to yield H_2O_2 when acting on thiol substrates according to Equation 1.109 and Equation 1.110.¹⁸³



Ero1p is an enzyme responsible for the disulfide bond formation in eukaryotic cells under aerobic and anaerobic conditions. The ability of Ero1p to transfer electron to other small molecules and macromolecular electron acceptor has also been demonstrated.

1.4.2 Nonbiochemical Sources

1.4.2.1 Photolysis Shown in Equation 1.111 and Equation 1.112 is the generation of $\text{O}_2^{\bullet-}$ during ionizing radiation of air-saturated sodium formate using stopped-flow radiolysis apparatus on line with a Van de Graaff electron generator at 2-MeV.¹⁸⁴

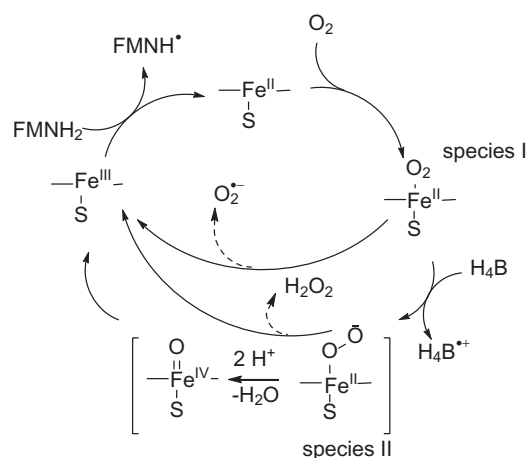
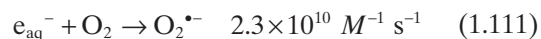
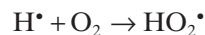


Figure 1.35 Production of superoxide radical anion from nitric oxide synthase. (Adapted with permission from *Chem. Rev.*, **2003**, 103(6), 2365–2384. Copyright 2003 American Chemical Society.)

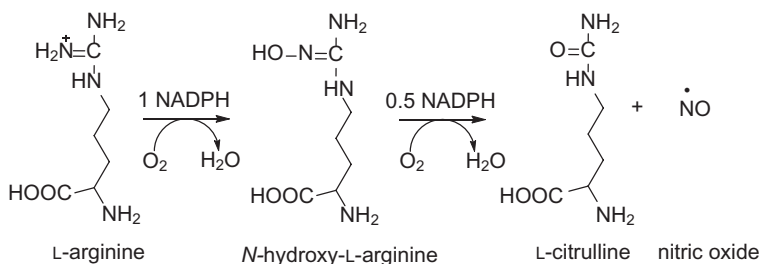


Figure 1.36 Production of nitric oxide from L-arginine, NADPH, and O_2 .

combination of KO_2 and Me_4NOH with high purity.¹⁹⁹ Also, Me_4NO_2 can be prepared from NH_3 treatment of KO_2 with Me_4NF or reaction of $\text{Me}_4\text{NOH} \cdot 5\text{H}_2\text{O}$ with excess KO_2 .²⁰⁰

Quinones are active sites of mitochondrial *bc* complex (III) or as active moieties of xenobiotics.²⁰¹ One electron reduction of quinone leads to the formation of semiquinone. In general, reduction of quinone to hydroquinone can be accomplished nonenzymatically via two-electron reduction with the reducing equivalents of NADPH, or by one-electron reduction to semiquinone with mitochondrial or mitochondrial enzymes (Fig. 1.38). Semiquinone can reduce O_2 to form $\text{O}_2^{\bullet-}$ and the original quinone. The process is repeated until ROS production is at its maximum and semiquinone begins to accumulate, at which time the system becomes depleted

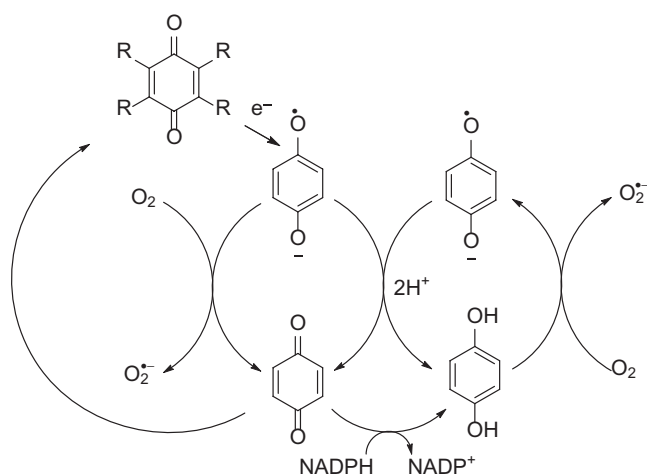


Figure 1.38 NADPH-mediated redox cycling of ROS by quinones.

with O_2 . This process is usually referred to as redox cycling. The diagram below shows the redox cycling of ROS by quinone as mediated by an electron donor, NADPH. Redox cycling has also been observed in ortho-bezoquinones.

Nitric oxide can be generated from chemical sources directly or indirectly by enzymatic or nonenzymatic systems. Nitric oxide can be photochemically or thermally generated from metal-NO complexes, *N*-nitrosamines, *N*-hydroxyl nitrosamines, nitrosoimines, nitrosothiols, C-nitrosothiols, and diazotine dioxides. NO can also be generated indirectly through enzymatic metabolism of organic nitrates/nitrites, guanidines, hydroxyureas, oximes, oxatriazole-5-imines, or furoxans.²⁰²

Stable ONOO^- solution can be generated directly from ozone and sodium azide,²⁰³ nitrite and H_2O_2 ,⁴³ or organic nitrite and H_2O_2 .²⁰⁴ Since 3-*N*-morpholinoyd-nonimine (SIN-1) comes in solid form, the use of SIN-1 is the most common form of ONOO^- delivery due to its ease of handling. Figure 1.39 shows the proposed decomposition pathway for SIN-1, which involves electron transfer reaction with O_2 to form $\text{O}_2^{\bullet-}$. The oxidized SIN-1 intermediate decomposes to form NO. Combination of the generated NO and $\text{O}_2^{\bullet-}$ in solution then yields ONOO^- .²⁰⁵

1.5 METHODS OF DETECTION

Reactive species in *in vitro* and in *in vivo* systems can be directly or indirectly detected. Due to the instability and short half-lives of the common radicals, reagents are needed for their detection. By exploiting the chemistry of radical addition or electron transfer reactions to some reagents, one can use this process as an analytical tool to detect ROS production. In particular, the detection

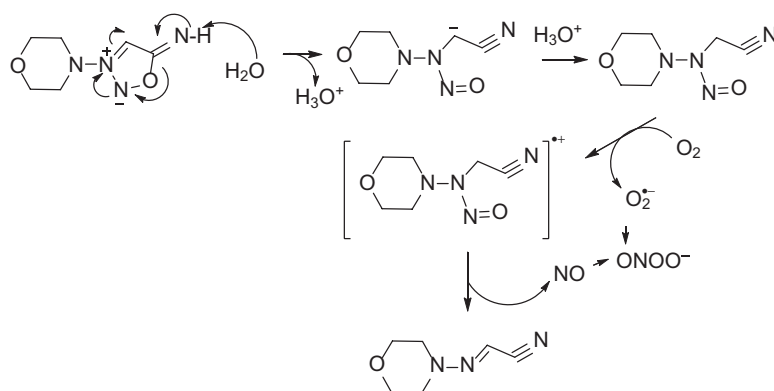


Figure 1.39 Proposed mechanism for the generation of peroxynitrite from SIN-1.²⁰⁵

of $O_2^{\bullet-}$ is the most relevant since it is the major precursor of most reactive species and it signals the first sign of oxidative burst in biological systems. However, in *in vitro* and *in vivo* systems where the flux of $O_2^{\bullet-}$ can be below the detection limit of the commonly used analytical techniques, secondary products such as the formation of other ROS, RNS, RSS as well as the formation of biomolecular radicals such as protein or nucleotide radicals can be directly or indirectly detected. Analysis of the primary or secondary addition products of radicals to substrates can be analyzed using various methods such as by chromatography, electrochemistry, mass spectrometry, spectrophotometry or by magnetic resonance spectroscopy.

1.5.1 In Vitro

1.5.1.1 Fluorescence and Chemiluminescence Fluorescence (FL) occurs when light is absorbed by a fluorophore (excitation) with subsequent emission of light, while chemiluminescence (CL) occurs with the emission of light as a result of a chemical reaction; the latter is more sensitive than the former by 2 orders of magnitude.²⁰⁶ Although FL and CL are among the most sensitive techniques for radical detection *in vitro* (i.e., >1 nM), caution is needed for their application. FL and CL probes are capable of detecting various ROS/RNS via two-electron oxidation, and therefore, suffer from selectivity and may compete with endogenous intracellular antioxidants such as ascorbate, urate and thiols. Moreover, these probes can generate $O_2^{\bullet-}$ via formation of an active intermediate after reaction with ROS/RNS. Due to the lack of selectivity to a particular reactive species, FL and CL are more appropriately called redox probes to indicate their general reactivity to various reactive species. Some of the most common FL probes are

dichlorodihydrofluorescein (DCFH₂), rhodamine (RhH₂) and ethidine (DHE) (Fig. 1.40). DCFH₂ and RhH₂ react with $O_2^{\bullet-}$ or H_2O_2 poorly, and fluorescence arising from this reaction could be catalyzed by metal ion impurities, and therefore are not suitable probes for ROS. Carbonate radical anion and $\cdot NO_2$ are better detected using DCFH₂ due to their higher reactivity and higher fluorescence yield, however, this is not true for $HO\cdot$ and $HOCl$. RhH₂ gives fluorescence with all of the reactive species. Unlike DCFH₂ and RhH₂, DHE is highly reactive to $O_2^{\bullet-}$ but yields two fluorescent products: (1) specific to $O_2^{\bullet-}$ (i.e., 2-hydroxyethidium, 2-OH- E^+); and (2) nonspecific to $O_2^{\bullet-}$ that can be formed photochemically (E^+). To differentiate between 2-OH- E^+ and E^+ , the use of HPLC/FL assay has been suggested and provides unequivocal differentiation of the two products.²⁰⁷ In spite of this complication, DHE is currently perhaps the most specific FL probe for $O_2^{\bullet-}$.

Lucigenin (LC) is the most commonly used CL probe for $O_2^{\bullet-}$ but like DCFH₂, it can also generate $O_2^{\bullet-}$ and is not specific for $O_2^{\bullet-}$ because it also gives luminescence in the presence of nucleophiles and reducing agents to form $LC^{\bullet+}$. Addition of $O_2^{\bullet-}$ to $LC^{\bullet+}$ (formed from its enzymatic reduction) forms a dioxetane intermediate that cleaves to form the excited state *N*-methylacridone which later can emit light (Fig. 1.41). Other reductants that can generate $LC^{\bullet+}$ are H_2O_2 , flavoproteins, eNOS, NADPH reductases and cyt P450.²⁰⁶

Boronates have been shown to react with $ONOO^-$, $HOCl$, and H_2O_2 imparting fluorescence but with varying rates of reaction.^{208,209} The second-order rate constants show $ONOO^-$ to be the most reactive ($\sim 10^5$ – $10^6 M^{-1} s^{-1}$) followed by $HOCl$ ($\sim 10^3$ – $10^4 M^{-1} s^{-1}$) and by H_2O_2 ($\sim 2 M^{-1} s^{-1}$).²⁰⁹ The mechanism of oxidant reaction to boronates involves nucleophilic addition of the oxidant to the boron atom followed by the heterolytic

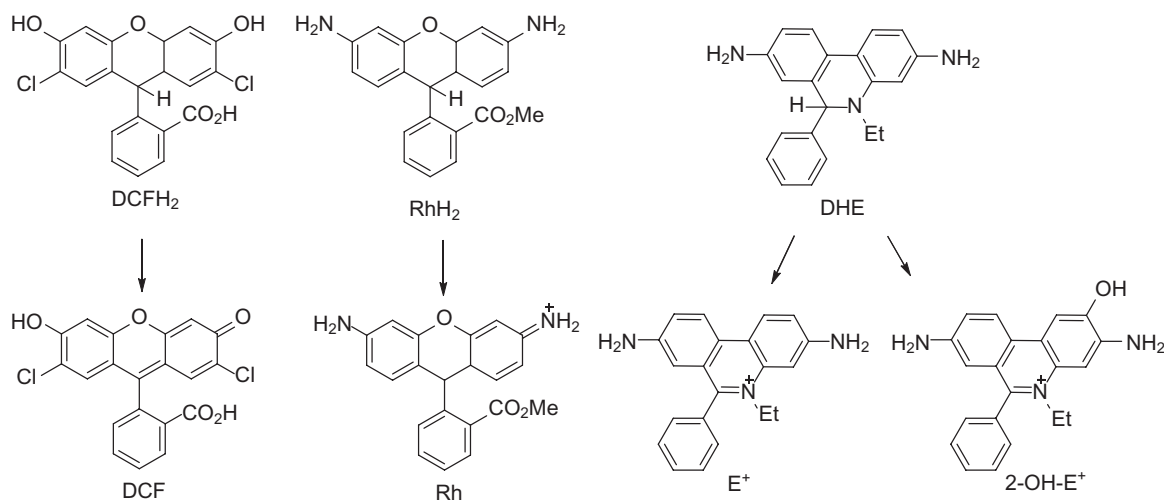


Figure 1.40 Fluorescence probes for ROS and their various products.

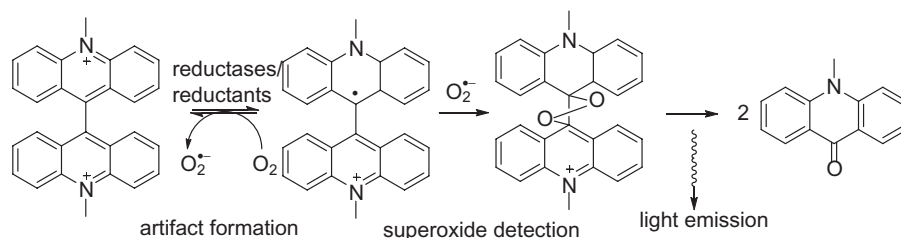
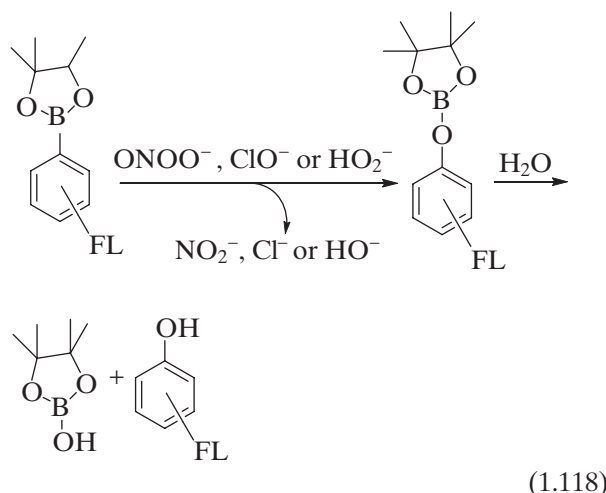
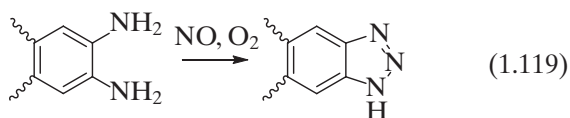


Figure 1.41 Formation of superoxide radical anion from lucigenin^{•+} and its reaction with superoxide resulting in chemiluminescence.

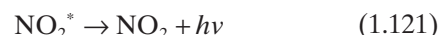
cleavage of the X-O bond to form the respective ion. Intramolecular rearrangement of the B-O yields the final fluorescent phenolic products (Eq. 1.118).



For NO detection, fluorescence probes have been employed such as those containing the vicinal diamines (e.g., fluorescein based, DAF-2; rhodamine-based, DAR-4M; BODIPY-based, DAMBO; and cyanine-based, DACs). Reaction of NO with diamine proceeds in the presence of oxygen to form the highly fluorescent *N*-nitrosated product (Eq. 1.119).²¹⁰



The reaction of NO with ozone imparts chemiluminescence and has been exploited to detect NO formation. This ozone-based detection of NO in the gas phase involves light emission along with the formation of $\cdot NO_2$ (Eq. 1.120 and Eq. 1.121).²¹¹ This technique, although very sensitive, requires the use of an NO analyzer equipped with ozone generator and sensitive photomultiplier tube and purging of NO from the sample is required.



1.5.1.2 UV-Vis Spectrophotometry and HPLC

Several assays for $O_2^{\cdot-}$ based on 1-electron transfer reaction have been employed due to the high rate constants observed for this type of reaction. Cytochrome (cyt) c^{3+} can be reduced to cyt c^{2+} by $O_2^{\cdot-}$ and can be detected spectrophotometrically. Due to the relatively low rate constant of this reaction ($\sim 10^5 M^{-1} s^{-1}$), the amount of $O_2^{\cdot-}$ generated can be underestimated. Another popular spectrophotometric technique for $O_2^{\cdot-}$ detection is through the use of p-nitrotriazolium blue (NBT) which forms a colored monoformazan anion. However, the use of cyt c and NBT have limitations such that their reduction is not specific to $O_2^{\cdot-}$ and cannot be applied in *in vivo* systems.²¹²

Nitric oxide can be measured by using reduced hemoglobin according to Equation 1.122. Oxidation of hemoglobin to methemoglobin can be detected spectrophotometrically with a detection threshold of 1 nmol.



Also, by using thioproline, NO can be trapped and the adduct formed can be detected using mass spectroscopy.²¹³ Nitrite as an oxidation end product of NO can also be detected spectrophotometrically using Griess assay. Nitrite is detected as red pink coloration produced from the reaction of sulphanilic acid with NO_2^- where the product formed reacts further with an azo dye (alpha-naphthylamine) giving a colored product. In systems where NO_3^- are present, prior reduction of NO_3^- to NO_2^- is required to obtain the total NO_2^-/NO_3^- content by treatment of the sample with sodium formate and nitrate reductase.²¹⁴

Hypochlorous acid can be trapped by taurine forming taurine chloramine. Taurine chloramine can then be spectrophotometrically assayed using 5-thio-2-nitrobenzoic acid (TNB)²¹⁵ but has some limitations

such as the need to predetermine the chloramine concentration for accurate measurements, poor selectivity as other oxidants can bleach TNB, and the light sensitivity of TNB. Iodide was proposed to be an alternative to TNB and by using 3,3',5,5'-tetramethylbenzidine (TMB) as chromophore due to its ability to be oxidized by hypiodous acid with a sensitivity of 1 μM of taurine chloramine. Dihydrorhodamine was also used as chromophore giving 10-fold greater sensitivity than TMB.²¹⁶

Other radicals such as HO^\bullet , NO_2^\bullet or HO_2^\bullet have been shown to form adducts with various substrates such as amino acids, DNA bases or lipids via hydroxylation, nitration and hydroperoxide formation, respectively, which can be detected using a variety of analytical methods such as HPLC, electrochemical, spectrophotometric or by MS. Hydroxyl radical for example adds to 8-hydroxyguanine of the DNA to yield the 8-hydroxy-2-deoxyguanosine (8-OHdG) which can be isolated and analyzed using HPLC/electrochemical methods.²¹⁷ Recently, more improved methods using HPLC/electrochemical detection for hydroxylation was proposed using 4-hydroxybenzoic acid and terephthalate assays which do not have the drawbacks associated with the use of salicylate or phenylalanine.²¹⁸ Using tandem mass spectroscopic techniques, nitration of amino acid residues in peptides²¹⁹ have been demonstrated while proteomic approach have been successful in identifying nitration in proteins.^{220,221}

Ferrous oxidation-xylenol orange (FOX) assay has been used as a conventional technique for hydroperoxide formation in lipids,^{222,223} and peptide/protein systems.^{27,224,225} FOX assay technique uses the Fenton chemistry to generate the HO^\bullet from the O-O homolytic cleavage from the ROOH which decolorizes the xylenol orange dye. RNS adduct of lipids have been characterized using HPLC coupled with UV and MS detection.²²⁶ MDA, being one of the end products of lipid hydroperoxide formation, can be measured using TBARS assay with thiobarbituric acid (TBA) as a reagent. Caution is required in interpreting TBARS data since MDA participates in other reactions other than TBA and is not exclusively formed from lipid peroxidation. Moreover, MDA is only formed from a particular lipid peroxidation process out of a myriad of several lipid peroxidation decomposition reactions.²²⁷ Analysis of F_2 -isoprostanes (F_2 -IPs) are more reliable marker of lipid peroxidation which possesses a 1,3-dihydroxycyclopentane ring with the OH groups in the *syn* position and are mainly formed from the arachidonic acid oxidation. Analysis of F_2 -IPs can be carried *ex vivo* using LC/MS/MS or GC/MS.^{48,228}

1.5.1.3 Immunochemical Formation of macromolecular radical systems such as protein and DNA radi-

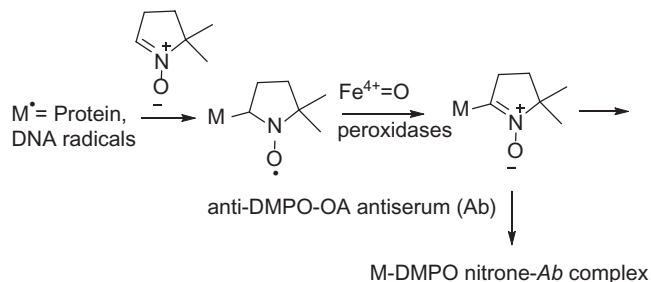


Figure 1.42 Immuno-spin trapping of macromolecular radicals using DMPO and anti-DMPO octanoic acid antiserum.

cals are relevant intermediates for the initiation of oxidative stress in biological systems. Nitronium spin traps, for example 5,5-dimethyl pyrroline *N*-oxide (DMPO) adds to protein radicals to form a longer-lived protein spin adduct. This radical adduct can later form the diamagnetic analogue, nitronium-protein adduct (formed via a variety of oxidative pathways mostly mediated by heme iron centers) which can be detected at 1 μM sensitivity using polyclonal antibodies against DMPO coupled to octanoic acid antiserum. This immune-spin trapping (ISP)²²⁹ approach combines the specificity of spin trapping to free radical formation and antigen-antibody interactions (Fig. 1.42). Coupled with MS/MS technique, one would be able to also identify the specific site/s of radical formation. Immunochemical detection using ISP has been employed in various radical systems formed from hemoglobin-tyrosyl,²³⁰ myoglobin-tyrosyl,²³¹ Cu,Zn-SOD,²³² thyroid peroxidase,²³³ catalase-peroxidase,²³⁴ and DNA.²³⁵⁻²³⁷

1.5.1.4 Electron Paramagnetic Resonance (EPR) Spectroscopy EPR spectroscopy exploits the magnetic moment of an electron through absorption of microwave radiation in the presence of external magnetic field. As shown in Figure 1.43, there are three major approaches for the detection of $\text{O}_2^{\bullet-}$ using EPR and various probes, that is, (1) spin-quenching (or spin-loss) using trityl; (2) spin-formation using hydroxylamine; (3) spin trapping using nitrones where the former involves loss of signal and the latter two involve signal formation. Due to the inherent stability of trityl radicals, they have been employed as probes for the detection of $\text{O}_2^{\bullet-}$. The most common are the triarylmethyl (trityl)-based radicals²³⁸⁻²⁴⁰ which can undergo electron transfer reaction with $\text{O}_2^{\bullet-}$ to yield O_2 and the EPR silent trityl anion. The synthetic trityl radicals, TAM OX063 and perchlorotriphenylmethyl (PCM-TC), have been shown to give high reactivity to $\text{O}_2^{\bullet-}$ with second-order rate constants of $3.1 \times 10^3 \text{ M}^{-1} \text{ s}^{-1}$ and $8.3 \times 10^8 \text{ M}^{-1} \text{ s}^{-1}$, respectively.^{238,239} Trityl radicals show inertness toward a majority of the

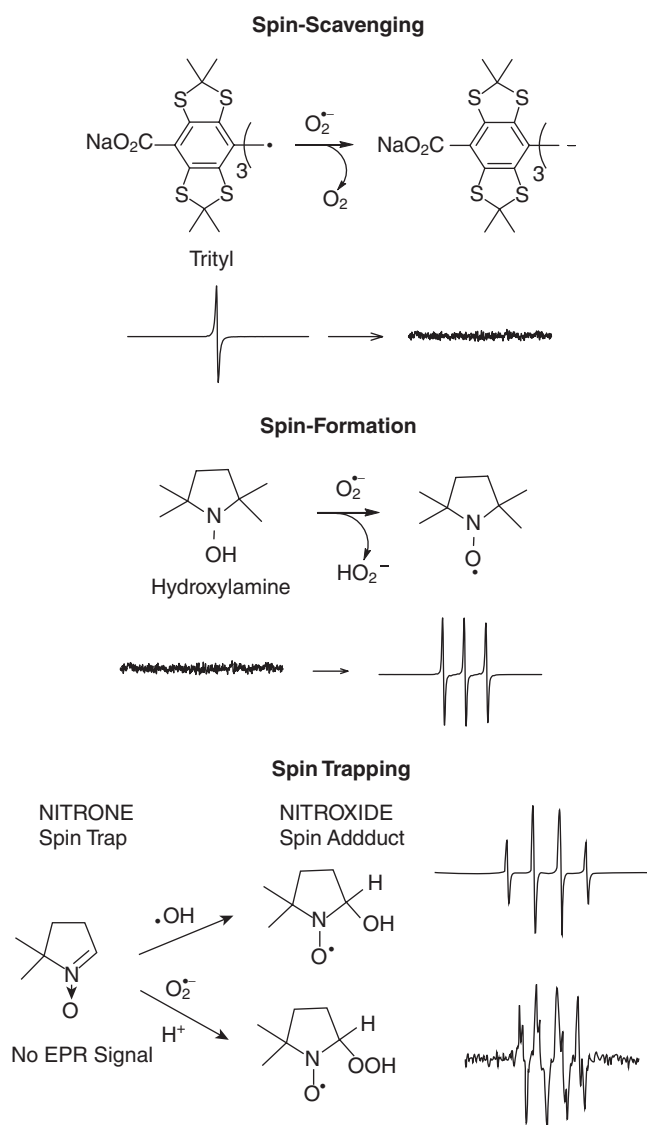


Figure 1.43 Radical detection using EPR spectroscopy and various radical probes.

common oxido-reductant species, however, they exhibit reactivity with other radical species, such as HO_2^\bullet , RO_2^\bullet and HO^\bullet .²³⁹

Although trityls offer some degree of specificity to $\text{O}_2^{\bullet-}$, the loss of signal also brings concern about other unknown factors that can result in the loss of signal, and therefore, other non-EPR technique is recommended to confirm the results from using trityl as reagent. A spin-generating system uses diamagnetic probes such as hydroxylamines and nitron spin traps which involves electron transfer or addition reactions with $\text{O}_2^{\bullet-}$, respectively, forming an EPR-detectable paramagnetic aminoxyl (or commonly called nitroxides) species. Hydroxylamines are oxidized by $\text{O}_2^{\bullet-}$ via a

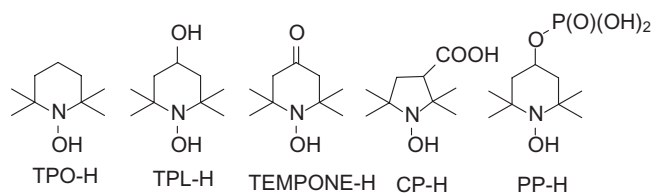
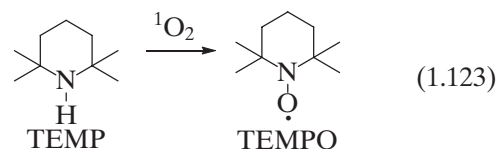


Figure 1.44 Various *N*-hydroxy-pyrrole or piperidine derivatives used as probes for superoxide.

simple electron transfer mechanism to yield a paramagnetic aminoxyl species and H_2O_2 . Figure 1.44 shows the commonly used hydroxylamines, TPO-H, TPL-H, TEMPONE-H,²⁴¹ CP-H,²⁴² and PP-H²⁴³ which are *N*-hydroxy-pyrrole or piperidine derivatives able to react with $\text{O}_2^{\bullet-}$. Rate constants for hydroxylamine probe reaction with $\text{O}_2^{\bullet-}$ are dependent on the structure of the probe. In the case of the negatively charged probe, PP-H, its rate of reaction to $\text{O}_2^{\bullet-}$ was found to be slower with $k = 840 \pm 60 \text{ M}^{-1} \text{ s}^{-1}$ due mostly to repulsive effect, while the neutral probes, TPO-H and TPL-H have higher rate constants in the range of $1\text{--}2 \times 10^3 \text{ M}^{-1} \text{ s}^{-1}$.¹⁰⁷ The redox reaction of $\text{O}_2^{\bullet-}$ with the hydroxylamine produces H_2O_2 and can be considered an artifactual source of other ROS. Since other ROS/RNS species as well as metal ions and O_2 can also give the exact same EPR triplet signal, caution should be practiced in data interpretation using hydroxylamine probes.

Detection of $^1\text{O}_2$ can be accomplished using the amine 2,2,6,6-tetramethyl-4-piperidone (TEMP). Reaction of $^1\text{O}_2$ with TEMP leads to the formation of the nitroxide 2,2,6,6-tetramethyl-4-piperidone-*N*-oxyl (TEMPO) which can be detected using EPR as shown in Equation 1.123.²⁴⁴



Spin traps are nitron-based molecules. Although hydroxylamines exhibit 10- to 1000-fold higher reactivity to $\text{O}_2^{\bullet-}$ than the nitrones, the paramagnetic species generated from hydroxylamine does not allow discrimination between the different radicals generated.²⁴³ Spin traps, however, add to a free radical at its α -carbon (C-2) position to form an aminoxyl adduct (or spin adduct), except that the signal is more complex than the ones observed from hydroxylamines (Fig. 1.43).²⁴⁵ The complex spectrum of the spin adduct is due to the presence of a β -H and the nature of the radical moiety, and is the basis for their popularity not only in

free radical detection but also in their identification. Shown in Figure 1.45 are the commonly used spin traps, and are divided into two major classes, the cyclic nitrones, 5,5-dimethyl-1-pyrroline *N*-oxide (DMPO), 5-(ethoxycarbonyl)-5-methyl-1-pyrroline *N*-oxide (EMPO), and 5-(diethoxyphosphoryl)-5-methyl-1-pyrroline *N*-oxide (DEPMPO), and the linear, *N*-*tert*-butyl- α -phenylnitrone (PBN).

Aside from $O_2^{\bullet-}$, other radicals that can also be identified using spin trapping are HO^{\bullet} , RO^{\bullet} , RS^{\bullet} , $\bullet NO_2$, $CO_3^{\bullet-}$, $CO_2^{\bullet-}$, $N_3^{\bullet-}$ and so on. The half-lives of the spin adducts vary significantly which range from seconds to hours depending on the type of the radical and nitron used. The least stable are the $O_2^{\bullet-}$ adducts of DMPO and PBN with a half-life of <1 minute in aqueous solution. However, C-5 derivatized spin traps such as EMPO and DEPMPO exhibit longer $O_2^{\bullet-}$ adduct half-lives of ~8 and ~14 minutes, respectively. One major disadvantage of this technique, in spite of the improved $O_2^{\bullet-}$ adduct half-lives, is the slow reactivity of these spin traps with $O_2^{\bullet-}$ with rate constants ranging from $<1\text{--}10\text{ M}^{-1}\text{ s}^{-1}$ which requires the use of high concentrations (typically 10–100 mM) of these reagents in solution for $O_2^{\bullet-}$ detection. However, other radicals exhibit significantly fast reactivity and long adduct half-lives with spin traps.

Spin trapping has been employed to detect $O_2^{\bullet-}$ from xanthine oxidase,^{238,246} the mitochondrial ETC,^{247,248} and NADPH oxidase.²⁴⁹ Nitrones have also been success-

fully used to detect $O_2^{\bullet-}$ generation in human epithelial cells,²⁵⁰ human neutrophils,²⁵¹ reperfused cardiac tissue,²⁵² and small animals using *ex vivo* techniques.^{253,254} *Ex vivo* spin trapping was also demonstrated in ischemia-reperfusion studies where the spin trap was administered to the animals before the onset of ischemia. Reperfusates were then collected and radical adduct generation was detected by EPR spectroscopy.^{252,255}

Nitric oxide does not add to nitron spin traps but they undergo redox reaction with nitronyl nitroxides (NN) and addition reaction with iron-thiocarbamate complexes with fast rates of reaction whose products are detectable by EPR. Oxidation of NO by NN as opposed to reduction of O_2 by hydroxylamine occurs. There are two commonly used NN's, the 2-phenyl-4,4,5,5-tetramethylimidazoline-1-oxyl 3-oxide (PTIO) and its water soluble analogue 2-(4-carboxyphenyl)-4,4,5,5-tetramethylimidazoline-1-oxyl 3-oxide (C-PTIO) (Fig. 1.46).

Nitric oxide reacts with NN via addition reaction to the nitroxyl-O and subsequent liberation of $\bullet NO_2$ to form the imino nitroxide (IN) as shown in Figure 1.46. The detection of NO through the use of NN shows clear distinction between the spectral profile imparted by the NN versus the IN product formed (Fig. 1.47). By virtue of symmetry, the spectral profile of NN is characterized by two equivalent N hyperfine splitting constants with $a_{N1,3} = 8.2\text{ G}$, while the IN gives asymmetrical product with the two nitrogens giving two different hfsc's of $a_{N1} = 9.8\text{ G}$ and $a_{N3} = 4.4\text{ G}$. The rate constant for the reaction of NO with NN is in the order of $\sim 10^3\text{ M}^{-1}\text{ s}^{-1}$ which is fast enough to compete with O_2 but not with $O_2^{\bullet-}$. Moreover, nitroxyl (HNO) also reacts with NN to form the similar IN product and that the $\bullet NO_2$ formed can participate with other reactions involving NN and therefore requires careful consideration in the interpretation of the signal formed.^{256,257} One main disadvantage of NN as probes for NO is their ability to be reduced to

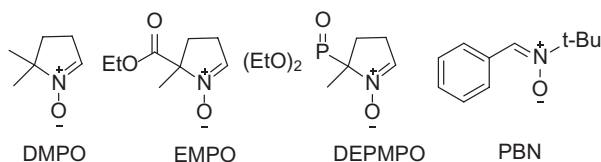


Figure 1.45 Commonly used spin traps for radical detection and identification.

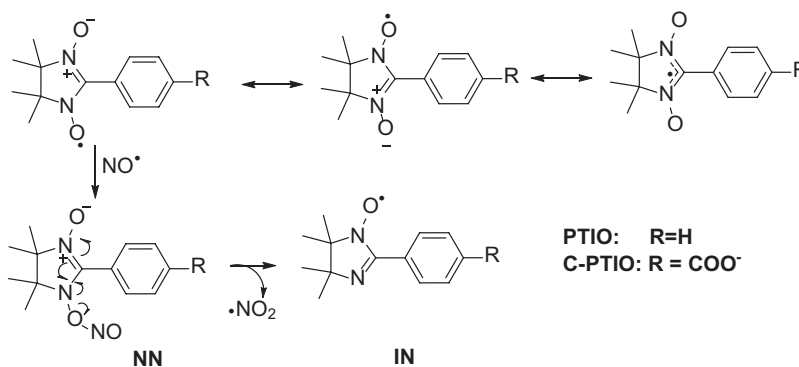


Figure 1.46 Reaction of nitric oxide with nitronyl nitroxides (NN), PTIO, and C-PTIO, to form the imino nitroxide (IN).

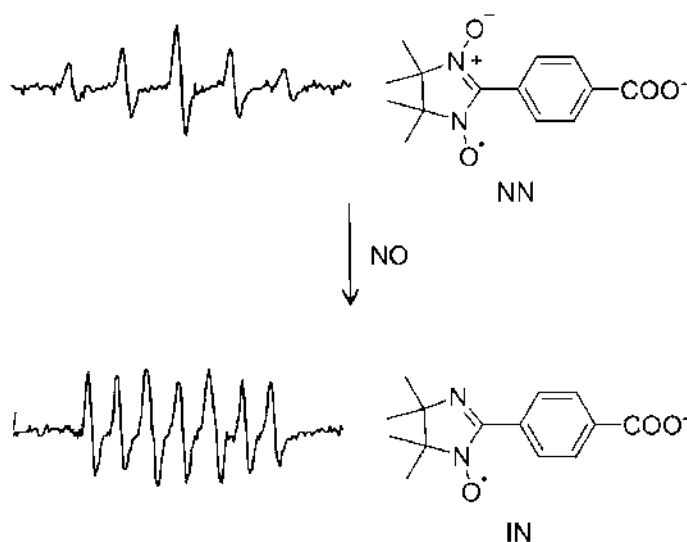


Figure 1.47 EPR spectra of nitronyl nitroxides (NN) and imino nitroxide (IN) after reaction with NO. (Adapted with permission from *J. Am. Chem. Soc.* **2010**, *132*(24), 8428–8432. Copyright 2010 American Chemical Society.)

EPR-silent hydroxylamine by reductants such as ascorbate or metal ions.

Several NO traps such as Fe^{2+} -dithiocarbamate complexes have been developed that allows NO detection using EPR (Fig. 1.48). This technique was first introduced by Vanin et al.^{258–260} *In vivo* EPR experiments using mice showed that NO trapping by the hydrophobic Fe^{2+} -DETC is more efficient than by the hydrophilic Fe^{2+} -MGD due to the higher stability of the latter in animal tissues.²⁶¹ The redox state of Fe-dithiocarbamates plays a critical role in the detection of NO. Under aerobic condition, Fe^{2+} complex can be readily oxidized to form Fe^{3+} -dithiocarbamate. Reaction of ferric complex with NO forms the EPR-silent NO- Fe^{3+} -MGD complex but can be converted to an EPR detectable NO- Fe^{2+} -MGD by NO itself with 50% yield and by reductants such as ascorbate, hydroquinone, or cysteine with conversion efficiency of up to 99.9%. The use of iron carbamate complexes involves premixing of the FeSO_4 with excess dithiocarbamate co-ligand. Water insoluble $\text{Fe}(\text{DETC})_2$ can be introduced as suspension with serum albumin²⁶² and has been reported to measure NO in porcine aorta with high sensitivity of 10 pmol/mL. Detection of NO in blood vessels as well as human umbilical endothelial cells has been successfully demonstrated using colloidal Fe^{2+} -DETC prepared by mixing DETC and Fe^{2+} in concentrated Krebs-HEPES solution.^{263,264} Compared when using NN as probe for NO, Fe dithiocarbamate complexes are better probes for the detection of NO due to the stability of the adducts formed. Cautions should be observed however since iron complexes also have been shown to detect HNO , nitrite and *S*-nitrosothiols. Dithiocarbamates have

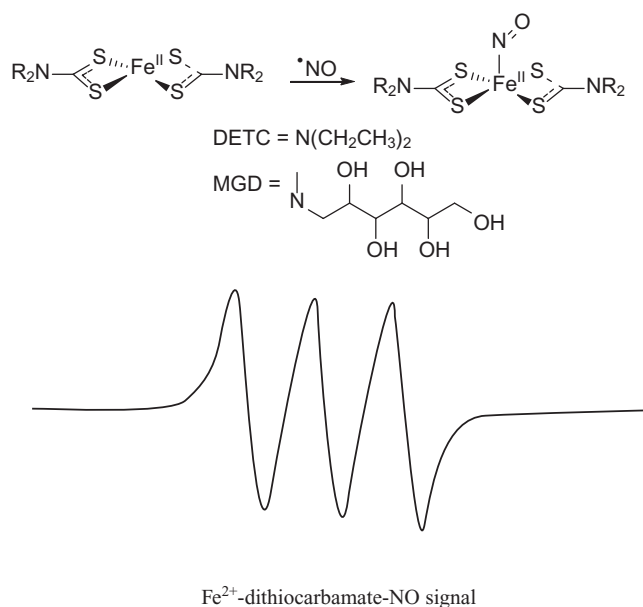


Figure 1.48 Complexation of nitric oxide with iron (II) dithiocarbamates, Fe-DETC, and Fe-MGD, giving a triplet EPR signal.

potential to chelate metals and may act as enzyme inhibitors. Through the use of NOS inhibitors, the triplet signal can be integrated to represent NOS-derived NO.²⁶⁵ Nitric oxide can be trapped by hemoglobin/myoglobin (Hb) as well and can be detected using EPR but with the disadvantage of cooling the sample to ~100 K to allow observation of the signal thus making Hb impractical for real time monitoring of NO production

but proved useful in determining NO production in tissues. However, deoxygenated ferrous haem forms HbNO and is detectable by EPR at normal conditions and the complex formed is very stable.²⁶⁵

1.5.2 *In Vivo*

Formation of reactive species *in vivo* are conventionally determined through analysis of biomarkers by using various methods such as histochemical, immunocytochemical, or EPR imaging. It should be noted that samples taken *in vivo* can be analyzed using the same techniques mentioned above employed for the formation of reactive species in *in vitro*.

1.5.2.1 Histochemical Protein carbonyls are biomarkers of protein oxidation and their detection can be accomplished by their derivatization using dinitrophenylhydrazine to form the protein-bound hydrazone and by using the anti-2,4-dinitrophenyl antibody. Another approach is through the use of biotin-hydrazide in which the protein-bound acyl hydrazone is detected by the enzyme-linked avidin or streptavidin.²⁶⁶

1.5.2.2 Immunocytochemical Methods Nitrotyrosine, lipid peroxidation end products, and DNA damage can be visualized in tissues using monoclonal or polyclonal antibodies for nitrotyrosine, HNE and 8-OHG, respectively.^{266,267} Nitrated tyrosine has been considered as biochemical marker of ONOO-induced damage to proteins and lipids. By employing two dimensional polyacrylamide gel electrophoresis (2DE) and western blotting, coupled with mass spectroscopy, targets of protein nitration and HNE modification have been determined in protein systems.²²⁰

1.5.2.3 Low Frequency EPR Imaging The availability of low frequency EPR instrumentation could limit the application of radical imaging to many investigators, however, provides direct visualization of probe response to ROS formation or O₂ concentrations in whole animals.^{268,269} The method involves the use of low frequency, highly sensitive spectrometers, operating between 200 MHz and 1.5 GHz and paramagnetic probes. As mentioned earlier, probes such as nitroxides²⁵² and trityls react with ROS and show characteristic spectral behavior, that is, signal formation or its disappearance, respectively. Since ROS production has direct correlation with O₂ consumption, probes that respond to the pO₂ are very desirable such as trityl,²⁷⁰ charcoal²⁷¹ and phthalocyanines,^{272,273} the latter two are stable enough from being metabolized. Significant advancements have already been achieved in the development of highly sensitive detectors, data acquisition

and analysis modalities. *In vivo* imaging of NO have also been achieved using commonly use iron-dithiocarbamate spin traps.²⁷⁴

1.5.2.4 In Vivo EPR Spin Tapping-Ex Vivo Measurement *In vivo* spin trapping of radical metabolites have been extensively employed using the commonly used spin traps, DMPO, PBN or POBN. However, due to the susceptibility of the radical adducts to be reduced to diamagnetic hydroxylamine species, post-treatment of the samples are needed to re-oxidize the hydroxylamine back to the EPR-detectable nitroxide using mild oxidants such as potassium ferricyanide or bubbling with O₂. Carbon- or S-centered radicals have been detected from blood or bile samples after systemic injection of the xenobiotics. Spin traps have been extensively employed for the detection of transient radicals in animals.^{253,275,276}

REFERENCES

1. Lelieveld, J. Atmospheric chemistry: A missing sink for radicals. *Nature* **2010**, 466, 925–926.
2. Baumgarten, M., Muellen, K. Radical ions: Where organic chemistry meets materials sciences. *Top. Curr. Chem.* **1994**, 169, 1–103.
3. Halliwell, B., Gutteridge, J.M.C. *Free Radicals in Biology and Medicine*, 4th ed. Oxford University Press, New York, 2007.
4. Gomberg, M. An instance of trivalent carbon: Triphenylmethyl. *J. Am. Chem. Soc.* **1900**, 22, 757–771.
5. Adam, F.C., Weissman, S.I. Electron spin resonance and electronic structure of triphenylmethyl. *J. Am. Chem. Soc.* **1958**, 80, 2057–2059.
6. Kazzaz, J.A., Xu, J., Palaia, T.A., Mantell, L., Fein, A.M., Horowitz, S. Cellular oxygen toxicity. Oxidant injury without apoptosis. *J. Biol. Chem.* **1996**, 271, 15182–15186.
7. Song, Y., Wagner, B.A., Lehmler, H.J., Buettner, G.R. Semiquinone radicals from oxygenated polychlorinated biphenyls: Electron paramagnetic resonance studies. *Chem. Res. Toxicol.* **2008**, 21(7), 1359–1367.
8. Fu, H., Zhou, Y.-H., Chen, W.-L., Deqing, Z.-G., Tong, M.-L., Ji, L.-N., Mao, Z.-W. Complexation, structure, and superoxide dismutase activity of the imidazolate-bridged dinuclear copper moiety with beta-cyclodextrin and its guanidinium-containing derivative. *J. Am. Chem. Soc.* **2006**, 128(15), 4924–4925.
9. Valgimigli, L., Amorati, R., Fumo, M.G., DiLabio, G.A., Pedulli, G.F., Ingold, K.U., Pratt, D.A. The unusual reaction of semiquinone radicals with molecular oxygen. *J. Org. Chem.* **2008**, 73(5), 1830–1841.
10. Sawyer, D.T., Valentine, J.S. How super is superoxide? *Acc. Chem. Res.* **1981**, 14(12), 393–400.

11. Evans, M.G., Uri, N. Dissociation constant of hydrogen peroxide and the electron affinity of the HO₂ radical. *J. Chem. Soc. Faraday Trans.* **1949**, 45, 224–230.
12. Liu, G.-F., Filipovic, M., Ivanovic-Burmazovic, I., Beuerle, F., Witte, P., Hirsch, A. High catalytic activity of dendritic C60 monoadducts in metal-free superoxide dismutation. *Angew. Chem. Int. Ed Engl.* **2008**, 47(21), 3991–3994.
13. Ali, S.S., Hardt, J.I., Quick, K.L., Sook Kim-Han, J., Erlanger, B.F., Huang, T.-T., Epstein, C.J., Dugan, L.L. A biologically effective fullerene (C60) derivative with superoxide dismutase mimetic properties. *Free Radic. Biol. Med.* **2004**, 37(8), 1191–1202.
14. Osuna, S., Swart, M., Sola, M. On the mechanism of action of fullerene derivatives in superoxide dismutation. *Chem. Eur. J.* **2010**, 16(10), 3207–3214, S3207/1–S3207/33.
15. Tietze, D., Tischler, M., Voigt, S., Imhof, D., Ohlenschlaeger, O., Goerlach, M., Buntkowsky, G. Development of a functional cis-prolyl bond biomimetic and mechanistic implications for nickel superoxide dismutase. *Chem. Eur. J.* **2010**, 16(25), 7572–7578.
16. Batinic-Haberle, I., Spasojevic, I., Stevens, R.D., Hambright, P., Neta, P., Okado-Matsumoto, A., Fridovich, I. New class of potent catalysts of O₂.bul.-dismutation. Mn(III) ortho-methoxyethylpyridyl- and di-ortho-methoxyethylimidazolylporphyrins. *Dalton Trans.* **2004**, 11, 1696–1702.
17. Riley, D.P., Weiss, R.H. Manganese macrocyclic ligand complexes as mimics of superoxide dismutase. *J. Am. Chem. Soc.* **1994**, 116(1), 387–388.
18. Nagano, T., Hirano, T., Hirobe, M. Superoxide dismutase mimics based on iron *in vivo*. *J. Biol. Chem.* **1989**, 264(16), 9243–9249.
19. Ivanovic-Burmazovic, I., Eldik, R.V. Metal complex-assisted activation of small molecules. From NO to superoxide and peroxides. *Dalton Trans.* **2008**, 39, 5259–5275.
20. Spasojevic, I., Batinic-Haberle, I., Reboucas, J.S., Idemori, Y.M., Fridovich, I. Electrostatic contribution in the catalysis of O₂.bul.-dismutation by superoxide dismutase mimics. MnIIITE-2-PyP⁵⁺ versus MnIIIBr8T-2-PyP. *J. Biol. Chem.* **2003**, 278(9), 6831–6837.
21. Krishna, M.C., Grahame, D.A., Samuni, A., Mitchell, J.B., Russo, A. Oxoammonium cation intermediate in the nitroxide-catalyzed dismutation of superoxide. *Proc. Natl. Acad. Sci. U.S.A.* **1992**, 89(12), 5537–5541.
22. Krishna, M.C., Russo, A., Mitchell, J.B., Goldstein, S., Dafni, H., Samuni, A. Do nitroxide antioxidants act as scavengers of superoxide radical or as SOD mimics? *J. Biol. Chem.* **1996**, 271(42), 26026–26031.
23. Chern, C.-I., DiCosimo, R., De Jesus, R., San Filippo, J., Jr. A study of superoxide reactivity. Reaction of potassium superoxide with alkyl halides and tosylates. *J. Am. Chem. Soc.* **1978**, 100(23), 7317–7327.
24. Davico, G.E., Bierbaum, V.M. Reactivity and secondary kinetic isotope effects in the SN₂ reaction mechanism: Dioxygen radical anion and related nucleophiles. *J. Am. Chem. Soc.* **2000**, 122(8), 1740–1748.
25. Das, A.B., Nagy, P., Abbott, H.F., Winterbourn, C.C., Kettle, A.J. Reactions of superoxide with the myoglobin tyrosyl radical. *Free Radic. Biol. Med.* **2004**, 48(11), 1540–1547.
26. Winterbourn, C.C., Parsons-Mair, H.N., Gebicki, S., Gebicki, J.M., Davies, M.J. Requirements for superoxide-dependent tyrosine hydroperoxide formation in peptides. *Biochem. J.* **2004**, 381(Pt 1), 241–248.
27. Field, S.M., Villamena, F.A. Theoretical and experimental studies of tyrosyl hydroperoxide formation in the presence of H-bond donors. *Chem. Res. Toxicol.* **2008**, 21(10), 1923–1932.
28. Sawyer, D.T., Stamp, J.J., Menton, K.A. Reactivity of superoxide ion with ethyl pyruvate, α -diketones, and benzil in dimethylformamide. *J. Org. Chem.* **1983**, 48, 3733–3736.
29. Rene, A., Abasq, M.-L., Hauchard, D., Hapiot, P. How do phenolic compounds react toward superoxide ion? A simple electrochemical method for evaluating antioxidant capacity. *Anal. Chem.* **2010**, 82, 8703–8710.
30. Salazar, R., Navarrete-Encina, P.A., Squella, J.A., Camargo, C., Nunez-Vergara, L.J. Reactivity of C4-indolyl substituted 1,4-dihydropyridines toward superoxide anion (O₂⁻) in dimethylsulfoxide. *J. Phys. Org. Chem.* **2009**, 22, 569–577.
31. Winterbourn, C.C., Metodiewa, D. Reactivity of biologically important thiol compounds with superoxide and hydrogen peroxide. *Free Radic. Biol. Med.* **1999**, 27(3/4), 322–328.
32. Cardey, B., Foley, S., Enescu, M. Mechanism of thiol oxidation by the superoxide radical. *J. Phys. Chem. A* **2007**, 111(50), 13046–13052.
33. Sutton, V.R., Stubna, A., Patschkowski, T., Munck, E., Beinert, H., Kiley, P.J. Superoxide destroys the [2Fe-2S]₂⁺ cluster of FNR from *Escherichia coli*. *Biochemistry* **2004**, 43(3), 791–798.
34. Flint, D.H., Tuminello, J.F., Emptage, M.H. The inactivation of Fe-S cluster containing hydro-lyases by superoxide. *J. Biol. Chem.* **1993**, 268(30), 22369–22376.
35. Sawyer, D.T. The chemistry of dioxygen species (oxygen, super oxide radical anion, peroxide radical and hydrogen peroxide) and their activation by transition metals. *Int. Rev. Exp. Pathol.* **1990**, 31, 109–131.
36. Cheng, Z., Li, Y. What is responsible for the initiating chemistry of iron-mediated lipid peroxidation: An update. *Chem. Rev.* **2007**, 107(3), 748–766.
37. Czapski, G., Bielski, B.H.J. The formation and decay of H₂O₃ and HO₂ in electronirradiated aqueous solutions. *J. Phys. Chem.* **1963**, 67(10), 2180–2184.
38. Haber, F., Weiss, J. The catalytic decomposition of hydrogen peroxide by iron salts. *Proc. R. Soc. London, Ser. A* **1934**, 147, 332.
39. Perez-Benito, J.F. Iron(III)-hydrogen peroxide reaction: Kinetic evidence of a hydroxyl-mediated chain mechanism. *J. Phys. Chem. A* **2004**, 108, 4853–4858.
40. Furtmuller, P.G., Obinger, C., Hsuanyu, Y., Dunford, H.B. Mechanism of reaction of myeloperoxidase with hydrogen

- peroxide and chloride ion. *Eur. J. Biochem.* **2000**, 267(19), 5858–5864.
41. Kettle, A.J., Winterbourn, C.C. A kinetic analysis of the catalase activity of myeloperoxidase. *Biochemistry* **2001**, 40(34), 10204–10212.
 42. Silanikove, N., Shapiro, F., Silanikove, M., Merin, U., Leitner, G. Hydrogen peroxide-dependent conversion of nitrite to nitrate as a crucial feature of bovine milk catalase. *J. Agric. Food Chem.* **2009**, 57(17), 8018–8025.
 43. Robinson, K.M., Beckman, J.S. Synthesis of peroxynitrite from nitrite and hydrogen peroxide. *Methods Enzymol.* **2005**, 396, 207–214.
 44. Oury, T.D., Tatro, L., Ghio, A.J., Piantadosi, C.A. Nitration of tyrosine by hydrogen peroxide and nitrite. *Free Radic. Res.* **1995**, 23, 537–547.
 45. Adimora, N.J., Jones, D.P., Kemp, M.L. A model of redox kinetics implicates the thiol proteome in cellular hydrogen peroxide responses. *Antioxid. Redox Signal.* **2010**, 13(6), 731–743.
 46. Scrivens, G., Gilbert, B.C., Lee, T.C.P. EPR studies of the copper-catalysed oxidation of thiols with peroxides. *J. Chem. Soc. Perkin Trans. 2* **1995**, 5, 955–963.
 47. Koppenol, W.H., Liebman, J.F. The oxidizing nature of the hydroxyl Radical. A comparison with the ferryl ion (FeO_2^+). *J. Phys. Chem.* **1984**, 88, 99–101.
 48. Li, H., Lawson, J.A., Reilly, M., Adiyaman, M., Hwang, S.W., Rokach, J., FitzGerald, G.A. Quantitative high performance liquid chromatography/tandem mass spectrometric analysis of the four classes of F(2)-isoprostanes in human urine. *Proc. Natl. Acad. Sci. U.S.A.* **1999**, 96(23), 13381–13386.
 49. Song, Y., Buettner, G.R., Parkin, S., Wagner, B.A., Robertson, L.W., Lehmler, H.J. Chlorination increases the persistence of semiquinone free radicals derived from polychlorinated biphenyl hydroquinones and quinones. *J. Org. Chem.* **2008**, 73(21), 8296–8304.
 50. Buxton, G.V., Greenstock, C.L., Helman, W.P., Ross, A.B. Critical review of rate constants for reactions of hydrated electrons, hydrogen atoms and hydroxyl radicals (OH/O) in aqueous solution. *J. Phys. Chem. Ref. Data* **1988**, 17, 513–886.
 51. Adhikari, S., Sprinz, H., Brede, O. Thiol radical induced isomerization of unsaturated fatty acids: Determination of equilibrium constants. *Res. Chem. Intermed.* **2001**, 27, 549–559.
 52. Alam, M.S., Rao, B.S.M., Janata, E. $\bullet\text{OH}$ reactions with aliphatic alcohols: Evaluation of kinetics by direct optical absorption measurement. A pulse radiolysis study. *Radiat. Phys. Chem.* **2003**, 67, 723–728.
 53. Galano, A., Alvarez-Idaboy, J.R., Bravo-Pérez, G., Ruiz-Santoyo, M.E. Gas phase reactions of C1–C4 alcohols with the OH radical: A quantum mechanical approach. *Phys. Chem. Chem. Phys.* **2002**, 4, 4648–4662.
 54. Rachmilovich-Calis, S., Meyerstein, N., Meyerstein, D. A mechanistic study of the effects of antioxidants on the formation of malondialdehyde-like products in the reaction of hydroxyl radicals with deoxyribose. *Chem. Eur. J.* **2009**, 15(31), 7717–7723.
 55. Esterbauer, H., Schaur, R.J., Zollner, H. Chemistry and biochemistry of 4-hydroxynonenal, malonaldehyde and related aldehydes. *Free Radic. Biol. Med.* **1991**, 11(1), 81–128.
 56. Onyango, A.N., Baba, N. New hypotheses on the pathways of formation of malondialdehyde and isofurans. *Free Radic. Biol. Med.* **2010**, 49(10), 1594–1600.
 57. Bucknall, T., Edwards, H.E., Kemsley, K.G., Moore, J.S., Phillips, G.O. The formation of malonaldehyde in irradiated carbohydrates. *Carbohydr. Res.* **1978**, 62, 49–59.
 58. Gligorovski, S., Herrmann, H. Kinetics of reactions of OH with organic carbonyl compounds in aqueous solution. *Phys. Chem. Chem. Phys.* **2004**, 6, 4118–4126.
 59. Alvarez-Idaboy, J.R., Cruz-Torres, A., Galano, A., Ruiz-Santoyo, M.E. Structure-reactivity relationship in ketones + OH reactions: A quantum mechanical and TST. *J. Phys. Chem. A* **2004**, 108, 2740–2749.
 60. Alvarez-Idaboy, J.R., Mora-Diez, N., Boyd, R.J., Vivier-Bunge, A. On the importance of prereactive complexes in molecule-radical reactions: Hydrogen abstraction from aldehydes by OH. *J. Am. Chem. Soc.* **2001**, 123, 2018–2024.
 61. Ervens, B., Gligorovski, S., Herrmann, H. Temperature-dependent rate constants for hydroxyl radical reactions with organic compounds in aqueous solutions. *Phys. Chem. Chem. Phys.* **2003**, 5, 1811–1824.
 62. Morris, E.D., Niki, H. Reactivity of hydroxyl radicals with olefins. *J. Phys. Chem.* **1971**, 75, 3640–3641.
 63. Atkinson, R. Kinetics and mechanisms of the gas-phase reactions of the hydroxyl radical with organic compounds under atmospheric conditions. *Chem. Rev.* **1985**, 85, 69–201.
 64. Poole, J.S., Shi, X., Hadad, C.M., Platz, M.S. Reaction of hydroxyl radical with aromatic hydrocarbons in non-aqueous solutions: A laser flash photolysis study in acetonitrile. *J. Phys. Chem. A* **2005**, 109, 2547–2551.
 65. DeMatteo, M.P., Poole, J.S., Shi, X., Sachdeva, R., Hatcher, P.G., Hadad, C.M., Platz, M.S. On the electrophilicity of hydroxyl radical: A laser flash photolysis and computational study. *J. Am. Chem. Soc.* **2005**, 127(19), 7094–7109.
 66. Geeta, S., Rao, B.S.M., Mohan, H., Mittal, J.P. Radiation-induced oxidation of substituted benzaldehydes: A pulse radiolysis study. *J. Phys. Org. Chem.* **2004**, 17, 194–198.
 67. Enescu, M., Cardey, B. Mechanism of cysteine oxidation by a hydroxyl radical: A theoretical study. *ChemPhysChem* **2006**, 7(4), 912–919.
 68. Cruz-Torres, A., Galano, A. On the mechanism of gas-phase reaction of C1–C3 aliphatic thiols + OH radicals. *J. Phys. Chem. A* **2007**, 111(8), 1523–1529.
 69. Karoui, H., Hogg, N., Frejaville, C., Tordo, P., Kalyanaram, B. Characterization of sulfur-centered radical intermediates formed during the oxidation of thiols and sulfite by peroxynitrite. ESR-spin trapping and oxygen uptake studies. *J. Biol. Chem.* **1996**, 271(11), 6000–6009.

70. DeRosa, M.C., Crutchley, R.J. Photosensitized singlet oxygen and its applications. *Coord. Chem. Rev.* **2002**, 233–234, 351–371.
71. Wilkinson, F., Helman, W.P., Ross, A.B. Rate constants for the decay and reactions of the lowest electronically excited singlet state of molecular oxygen in solution. An expanded and revised compilation. *J. Phys. Chem. Ref. Data* **1995**, 24, 663–1021.
72. Greer, A. Christopher Foote's discovery of the role of singlet oxygen [$^1\text{O}_2$ ($^1\Delta_g$)] in photosensitized oxidation reactions. *Acc. Chem. Res.* **2006**, 39(11), 797–804.
73. Sun, S., Bao, Z., Ma, H., Zhang, D., Zheng, X. Singlet oxygen generation from the decomposition of α -linolenic acid hydroperoxide by cytochrome c and lactoperoxidase. *Biochemistry* **2007**, 46(22), 6668–6673.
74. Escobar, J.A., Vasquez-Vivar, J., Cilento, G. Free radicals and excited species in the metabolism of indole-3-acetic acid and its ethyl ester by horseradish peroxidase and by neutrophils. *Photochem. Photobiol.* **1992**, 55(6), 895–902.
75. King, M.M., Lai, E.K., McCay, P.B. Singlet oxygen production associated with enzyme-catalyzed lipid peroxidation in liver microsomes. *J. Biol. Chem.* **1975**, 250(16), 6496–6502.
76. Kiryu, C., Makiuchi, M., Miyazaki, J., Fujinaga, T., Kakinuma, K. Physiological production of singlet molecular oxygen in the myeloperoxidase- H_2O_2 -chloride system. *FEBS Lett.* **1999**, 443(2), 154–158.
77. Medeiros, M.H., Wefers, H., Sies, H. Generation of excited species catalyzed by horseradish peroxidase or hemin in the presence of reduced glutathione and H_2O_2 . *Free Radic. Biol. Med.* **1987**, 3(2), 107–110.
78. Zacharia, I.G., Deen, W.M. Diffusivity and solubility of nitric oxide in water and saline. *Ann. Biomed. Eng.* **2005**, 33, 214–222.
79. Zhao, Y.L., Bartberger, M.D., Goto, K., Shimada, K., Kawashima, T., Houk, K.N. Theoretical evidence for enhanced NO dimerization in aromatic hosts: Implications for the role of the electrophile (NO)(2) in nitric oxide chemistry. *J. Am. Chem. Soc.* **2005**, 127(22), 7964–7965.
80. Lewis, R.S., Deen, W.M. Kinetics of the reaction of nitric oxide with oxygen in aqueous solutions. *Chem. Res. Toxicol.* **1994**, 7, 568–574.
81. Goldstein, S., Czapski, G. Kinetics of nitric oxide autoxidation in aqueous solution in the absence and presence of various reductants. The nature of the oxidizing intermediates. *J. Am. Chem. Soc.* **1995**, 117, 12078–12084.
82. Czapski, G., Holman, J., Bielski, B.H.J. Reactivity of nitric oxide with simple short-lived radicals in aqueous solutions. *J. Am. Chem. Soc.* **1994**, 116, 11465–11469.
83. Batt, L., Rattray, G.N. The reaction of methoxy radicals with nitric oxide and nitrogen dioxide. *Int. J. Chem. Kinet.* **1979**, 11, 1183–1196.
84. Goldstein, S., Lind, J., Merenyi, G. Reaction of organic peroxy radicals with NO_2 and NO in aqueous solution: Intermediacy of organic peroxyxynitrate and peroxyxynitrite species. *J. Phys. Chem. A* **2004**, 108, 1719–1725.
85. Ford, P.C., Lorkovic, I.M. Mechanistic aspects of the reactions of nitric oxide with transition-metal complexes. *Chem. Rev.* **2002**, 102(4), 993–1018.
86. Scheidt, W.R., Lee, Y.J., Hatano, K. Preparation and structural characterization of nitrosyl complexes of ferric porphyrinates. Molecular structure of aquonitrosyl (meso-tetraphenylporphinato)iron(III) perchlorate and nitrosyl(octaethylporphinato)iron(III) perchlorate. *J. Am. Chem. Soc.* **1984**, 106, 3191–3198.
87. Enami, S., Hoffmann, M.R., Colussi, A.J. Absorption of inhaled $\text{NO}(2)$. *J. Phys. Chem. B* **2009**, 113(23), 7977–7981.
88. Huie, R.E. The reaction kinetics of NO_2 . *Toxicology* **1994**, 89, 193–216.
89. Dutton, A.S., Fukuto, J.M., Houk, K.N. Theoretical reduction potentials for nitrogen oxides from CBS-QB3 energetics and (C)PCM solvation calculations. *Inorg. Chem.* **2005**, 44(11), 4024–4028.
90. Napolitano, A., Camera, E., Picardo, M., d'Ischia, M. Acid-promoted reactions of ethyl linoleate with nitrite ions: Formation and structural characterization of isomeric nitroalkene, nitrohydroxy, and novel 3-nitro-1,5-hexadiene and 1,5-dinitro-1, 3-pentadiene products. *J. Org. Chem.* **2000**, 65(16), 4853–4860.
91. d'Ischia, M., Napolitano, A., Manini, P., Panzella, L. Secondary targets of nitrite-derived reactive nitrogen species: Nitrosation/nitration pathways, antioxidant defense mechanisms and toxicological implications. *Chem. Res. Toxicol.* **2011**, 24(12), 2071–2092.
92. Solar, S., Solar, W., Getoff, N. Reactivity of hydroxyl with tyrosine in aqueous solution studied by pulse radiolysis. *J. Phys. Chem.* **1984**, 88, 2091–2095.
93. Prütz, W.A., Mönig, H., Butler, J., Land, E.J. Reactions of nitrogen dioxide in aqueous model systems: Oxidation of tyrosine units in peptides and proteins. *Arch. Biochem. Biophys.* **1985**, 243, 125–134.
94. Deeb, R.S., Resnick, M.J., Mittar, D., McCaffrey, T., Hajjar, D.P., Upmacis, R.K. Tyrosine nitration in prostaglandin $\text{H}(2)$ synthase. *J. Lipid Res.* **2002**, 43(10), 1718–1726.
95. Surmeli, N.B., Litterman, N.K., Miller, A.F., Groves, J.T. Peroxynitrite mediates active site tyrosine nitration in manganese superoxide dismutase. Evidence of a role for the carbonate radical anion. *J. Am. Chem. Soc.* **2010**, 132(48), 17174–17185.
96. Abriata, L.A., Cassina, A., Tortora, V., Marin, M., Souza, J.M., Castro, L., Vila, A.J., Radi, R. Nitration of solvent-exposed tyrosine 74 on cytochrome c triggers heme iron-methionine 80 bond disruption. Nuclear magnetic resonance and optical spectroscopy studies. *J. Biol. Chem.* **2009**, 284(1), 17–26.
97. Jourdain, D., Jourdain, F.L., Feelisch, M. Oxidation and nitrosation of thiols at low micromolar exposure to nitric oxide. Evidence for a free radical mechanism. *J. Biol. Chem.* **2003**, 278(18), 15720–15726.

98. Hofstetter, D., Nauser, T., Koppenol, W.H. The glutathione thiyl radical does not react with nitrogen monoxide. *Biochem. Biophys. Res. Commun.* **2007**, 360(1), 146–148.
99. Goldstein, S., Lind, J., Merenyi, G. Chemistry of peroxynitrites as compared to peroxynitrates. *Chem. Rev.* **2005**, 105(6), 2457–2470.
100. Merenyi, G., Lind, J., Eriksen, T.E. The reactivity of superoxide (O₂⁻) and its ability to induce chemiluminescence with luminol. *Photochem. Photobiol.* **1985**, 41(2), 203–208.
101. Szabo, C., Ischiropoulos, H., Radi, R. Peroxynitrite: Biochemistry, pathophysiology and development of therapeutics. *Nat. Rev. Drug Discov.* **2007**, 6(8), 662–680.
102. Pearce, L.L., Martinez-Bosch, S., Manzano, E.L., Winnica, D.E., Epperly, M.W., Peterson, J. The resistance of electron-transport chain Fe-S clusters to oxidative damage during the reaction of peroxynitrite with mitochondrial complex II and rat-heart pericardium. *Nitric Oxide* **2009**, 20(3), 135–142.
103. Rubbo, H., Denicola, A., Radi, R. Peroxynitrite inactivates thiol-containing enzymes of *Trypanosoma cruzi* energetic metabolism and inhibits cell respiration. *Arch. Biochem. Biophys.* **1994**, 308(1), 96–102.
104. Mere'nyi, G.b., Lind, J., Czapski, G., Goldstein, S. Direct determination of the Gibbs' energy of formation of peroxynitrous acid. *Inorg. Chem.* **2003**, 42, 3796–3800.
105. Lyman, S.V., Hurst, J.K. Rapid reaction between peroxynitrite ion and carbon dioxide: Implications for biological activity. *J. Am. Chem. Soc.* **1995**, 117, 8867–8868.
106. Bonini, M.G., Siraki, A.G., Atanassov, B.S., Mason, R.P. Immunolocalization of hypochlorite-induced, catalase-bound free radical formation in mouse hepatocytes. *Free Radic. Biol. Med.* **2007**, 42(4), 530–540.
107. Zhang, R., Goldstein, S., Samuni, A. Kinetics of superoxide-induced exchange among nitroxide antioxidants and their oxidized and reduced forms. *Free Radic. Biol. Med.* **1999**, 26, 1245–1252.
108. Massari, J., Tokikawa, R., Zanolli, L., Tavares, M.F.M., Assuncao, N.A., Bechara, E.J.H. Acetyl radical production by the methylglyoxal-peroxynitrite system: A possible route for L-lysine acetylation. *Chem. Res. Toxicol.* **2010**, 23(11), 1762–1770.
109. Royer, L.O., Knudsen, F.S., De Oliveira, M.A., Tavares, M.F.M., Bechara, E.J.H. Peroxynitrite-initiated oxidation of acetoacetate and 2-methylacetoacetate esters by oxygen: Potential sources of reactive intermediates in keto acidoses. *Chem. Res. Toxicol.* **2004**, 17(12), 1725–1732.
110. Imaram, W., Gersch, C., Kim, K.M., Johnson, R.J., Henderson, G.N., Angerhofer, A. Radicals in the reaction between peroxynitrite and uric acid identified by electron spin resonance spectroscopy and liquid chromatography mass spectrometry. *Free Radic. Biol. Med.* **2010**, 49(2), 275–281.
111. Imaram, W., Johnson, R.J., Angerhofer, A. ESR spin trapping of the reaction between urate and peroxynitrite: The hydrogen adduct. *Appl. Magn. Reson.* **2009**, 37(1–4), 463–472.
112. Olson, L.P., Bartberger, M.D., Houk, K.N. Peroxynitrate and peroxynitrite: A complete basis set investigation of similarities and differences between these NO_x species. *J. Am. Chem. Soc.* **2003**, 125(13), 3999–4006.
113. Goldstein, S., Saha, A., Lyman, S.V., Czapski, G. Oxidation of peroxynitrite by inorganic radicals: A pulse radiolysis study. *J. Am. Chem. Soc.* **1998**, 120, 5549–5554.
114. Koppenol, W.H. Thermodynamics of reactions involving nitrogen-oxygen compounds. *Methods Enzymol.* **1996**, 268, 7–12.
115. Trujillo, M., Radi, R. Peroxynitrite reaction with the reduced and the oxidized forms of lipoic acid: New insights into the reaction of peroxynitrite with thiols. *Arch. Biochem. Biophys.* **2002**, 397(1), 91–98.
116. Radi, R., Beckman, J.S., Bush, K.M., Freeman, B.A. Peroxynitrite oxidation of sulfhydryls. The cytotoxic potential of superoxide and nitric oxide. *J. Biol. Chem.* **1991**, 266, 4244–4250.
117. Dubuisson, M., Vander Stricht, D., Clippe, A., Etienne, F., Nauser, T., Kissner, R., Koppenol, W.H., Rees, J.F., Knoop, B. Human peroxiredoxin 5 is a peroxynitrite reductase. *FEBS Lett.* **2004**, 571, 161–165.
118. Alvarez, B., Ferrer-Sueta, G., Freeman, B.A., Radi, R. Kinetics of peroxynitrite reaction with amino acids and human serum albumin. *J. Biol. Chem.* **1999**, 274(2), 842–848.
119. Jursic, B.S. Reliability of hybrid density theory-semiempirical approach for evaluation of bond dissociation energies. *J. Chem. Soc. Perkin Trans. 2* **1999**, 2, 369–372.
120. Hoffman, M.Z., Hayon, E. Pulse radiolysis study of sulfhydryl compounds in aqueous solution. *J. Phys. Chem. Ref. Data* **1973**, 77, 990–996.
121. Folkes, L.K., Trujillo, M., Bartsaghi, S., Radi, R., Wardman, P. Kinetics of reduction of tyrosine phenoxyl radicals by glutathione. *Arch. Biochem. Biophys.* **2011**, 506, 242–249.
122. Ferreri, C., Kratzsch, S., Landic, L., Bredeb, O. Thiyl radicals in biosystems: Effects on lipid structures and metabolisms. *Cell. Mol. Life Sci.* **2005**, 62, 834–847.
123. Chatgililoglu, C., Altieri, A., Fischer, H. The kinetics of thiyl radical-induced reactions of monounsaturated fatty acid esters. *J. Am. Chem. Soc.* **2002**, 124(43), 12816–12823.
124. Schöneich, C., Dillinger, U., Bruchhausen, F.v., Asmus, K.-D. Oxidation of polyunsaturated fatty acids and lipids through thiyl and sulfonyl radicals: Reaction kinetics, and influence of oxygen and structure of thiyl radicals. *Arch. Biochem. Biophys.* **1992**, 292, 456–467.
125. Schoneich, C., Asmus, K.-D., Bonifacic, M. Determination of absolute rate constants for the reversible hydrogen-atom transfer between thiyl radicals and alcohols or ethers. *J. Chem. Soc. Faraday Trans.* **1995**, 91, 1923–193.

126. Nauser, T., Schoneich, C. Thiyl radicals abstract hydrogen atoms from the $^{\circ}\text{C-H}$ bonds in model peptides: Absolute rate constants and effect of amino acid structure. *J. Am. Chem. Soc.* **2003**, *125*, 2042–2043.
127. Schoneich, C. Cysteine residues as catalysts for covalent peptide and protein modification: A role for thiyl radicals? *Biochem. Soc. Trans.* **2011**, *39*(5), 1254–1259.
128. Hofstetter, D., Nauser, T., Koppenol, W.H. Hydrogen exchange equilibria in glutathione radicals: Rate constants. *Chem. Res. Toxicol.* **2010**, *23*(10), 1596–1600.
129. Pogocki, D., Schoneich, C. Thiyl radicals abstract hydrogen atoms from carbohydrates: Reactivity and selectivity. *Free Radic. Biol. Med.* **2001**, *31*(1), 98–107.
130. Madej, E., Folkes, L.K., Wardman, P., Czapski, G., Goldstein, S. Thiyl radicals react with nitric oxide to form S-nitrosothiols with rate constants near the diffusion-controlled limit. *Free Radic. Biol. Med.* **2008**, *44*, 2013–2018.
131. Sevilla, M.D., Becker, D., Swarts, S., Herrington, J. Sulfinyl radical formation from the reaction of cysteine and glutathione thiyl radicals with molecular oxygen. *Biochem. Biophys. Res. Commun.* **1987**, *144*, 1037–1042.
132. Mönig, J., Asmus, K.D., Forni, L.G., Willson, R.L. On the reaction of molecular oxygen with thiyl radicals: A re-examination. *Int. J. Radiat. Biol. Relat. Stud. Phys. Chem. Med.* **1987**, *52*, 589–602.
133. Tamba, M., Simone, G., Quintiliani, M. Interactions of thiyl free radicals with oxygen: A pulse radiolysis study. *Int. J. Radiat. Biol.* **1986**, *50*, 595–600.
134. Zhao, R., Lind, J., Merbnyi, G., Eriksen, T.E. Kinetics of one-electron oxidation of thiols and abstraction by thiyl radicals from α -amino C-H bonds. *J. Am. Chem. Soc.* **1994**, *116*, 12010–12015.
135. Hayon*, M.Z.H.a.E. One-electron reduction of the disulfide linkage in aqueous solution. Formation, protonation, and decay kinetics of the RSSR anion radical. *J. Am. Chem. Soc.* **1972**, *94*, 7950–7957.
136. Quintiliani, M., Badiello, R., Tamba, M., Esfandi, A., Gorin, G. Radiolysis of glutathione in oxygen-containing solutions of pH 7. *Int. J. Radiat. Biol.* **1977**, *32*, 195–202.
137. Voronkov, M.G., Deryagin, E.N. Thermal reactions of thiyl radicals. *Russ. Chem. Rev.* **1990**, *59*, 778–791.
138. Guo, W., Pleasants, J., Rabenstein, D.L. Nuclear magnetic resonance studies of thiol/disulfide chemistry. 2. Kinetics of symmetrical thiol/disulfide interchange reactions. *J. Org. Chem.* **1990**, *55*, 373–376.
139. Trivedi, M.V., Laurence, J.S., Siahaan, T.J. The role of thiols and disulfides on protein stability. *Curr. Protein Pept. Sci.* **2009**, *10*(6), 614–625.
140. Giles, G.I., Tasker, K.M., Jacob, C. Hypothesis: The role of reactive sulfur species in oxidative stress. *Free Radic. Biol. Med.* **2001**, *31*(10), 1279–1283.
141. Racker, E. Glutathione reductase from baker's yeast and beef liver. *J. Biol. Chem.* **1955**, *217*, 855–866.
142. Collet, J.F., Messens, J. Structure, function, and mechanism of thioredoxin proteins. *Antioxid. Redox Signal.* **2010**, *13*(8), 1205–1216.
143. Singh, R., Lamoureux, G.V., Lees, W.J., Whitesides, G.M. Reagents for rapid reduction of disulfide bonds. *Methods Enzymol.* **1995**, *251*, 167–173.
144. Pattison, D.I., Davies, M.J. Reactions of myeloperoxidase-derived oxidants with biological substrates: Gaining chemical insight into human inflammatory diseases. *Curr. Med. Chem.* **2006**, *13*(27), 3271–3290.
145. Khan, A.U., Kasha, M. Chemiluminescence arising from simultaneous transitions in pairs of singlet oxygen molecules. *J. Am. Chem. Soc.* **1970**, *92*, 3293–3300.
146. Long, C.A., Bielski, B.H.J. Rate of reaction of superoxide radical with chloride-containing species. *J. Phys. Chem.* **1980**, *84*, 555–557.
147. Zuo, Z., Katsumura, Y., Ueda, K., Ishigur, K. Reactions between some inorganic radicals and oxychlorides studied by pulse radiolysis and laser photolysis. *J. Chem. Soc. Faraday Trans.* **1997**, *93*, 1885–1891.
148. Miyamoto, S., Martinez, G.R., Rettori, D., Augusto, O., Medeiros, M.H., Di Mascio, P. Linoleic acid hydroperoxide reacts with hypochlorous acid, generating peroxy radical intermediates and singlet molecular oxygen. *Proc. Natl. Acad. Sci. U.S.A.* **2006**, *103*(2), 293–298.
149. Eiserich, J.P., Cross, C.E., Jones, A.D., Halliwell, B., van der Vliet, A. Formation of nitrating and chlorinating species by reaction of nitrite with hypochlorous acid. A novel mechanism for nitric oxide-mediated protein modification. *J. Biol. Chem.* **1996**, *271*(32), 19199–19208.
150. Eiserich, J.P., Hristova, M., Cross, C.E., Jones, A.D., Freeman, B.A., Halliwell, B., van der Vliet, A. Formation of nitric oxide-derived inflammatory oxidants by myeloperoxidase in neutrophils. *Nature* **1998**, *391*(6665), 393–397.
151. Fogelman, K.D., Walker, D.M., Margerum, D.W. Non-metal redox kinetics: Hypochlorite and hypochlorous acid reactions with sulfite. *Inorg. Chem.* **1989**, *28*, 986–993.
152. Chesney, J.A., Mahoney, J.R.J., Eaton, J.W. A spectrophotometric assay for chlorine-containing compounds. *Anal. Biochem.* **1991**, *196*, 262–266.
153. Folkes, L.K., Candeias, L.P., Wardman, P. Kinetics and mechanisms of hypochlorous acid reactions. *Arch. Biochem. Biophys.* **1995**, *323*, 120–126.
154. Hawkins, C.L., Davies, M.J. Reaction of HOCl with amino acids and peptides: EPR evidence for rapid rearrangement and fragmentation reactions of nitrogen-centred radicals. *J. Chem. Soc. Perkin Trans. 2* **1998**, *9*, 1937–1945.
155. Peskin, A.V., Winterbourn, C.C. Kinetics of the reactions of hypochlorous acid and amino acid chloramines with thiols, methionine, and ascorbate. *Free Radic. Biol. Med.* **2001**, *30*(5), 572–579.
156. Carr, A.C., Winterbourn, C.C. Oxidation of neutrophil glutathione and protein thiols by myeloperoxidase-derived hypochlorous acid. *Biochem. J.* **1997**, *327*, 275–281.
157. Peskin, A.V., Turner, R., Maghzal, G.J., Winterbourn, C.C., Kettle, A.J. Oxidation of methionine to dehydromethionine

- by reactive halogen species generated by neutrophils. *Biochemistry* **2009**, 48(42), 10175–10182.
158. Fu, S., Wang, H., Davies, M., Dean, R. Reactions of hypochlorous acid with tyrosine and peptidyl-tyrosyl residues give dichlorinated and aldehydic products in addition to 3-chlorotyrosine. *J. Biol. Chem.* **2000**, 275(15), 10851–10858.
 159. Prutz, W.A., Kissner, R., Nauser, T., Koppenol, W.H. On the oxidation of cytochrome c by hypohalous acids. *Arch. Biochem. Biophys.* **2001**, 389(1), 110–122.
 160. Winterbourn, C.C., Berg, J.J.M.v.D., Roitman, E., Kuypers, F.A. Chlorohydrin formation from unsaturated fatty acids reacted with hypochlorous acid. *Arch. Biochem. Biophys.* **1992**, 296, 547–555.
 161. Hawkins, C.L., Davies, M.J. Hypochlorite-induced damage to nucleosides: Formation of chloramines and nitrogen-centered radicals. *Chem. Res. Toxicol.* **2001**, 14(8), 1071–1081.
 162. Stanley, N.R., Pattison, D.I., Hawkins, C.L. Ability of hypochlorous acid and N-chloramines to chlorinate DNA and its constituents. *Chem. Res. Toxicol.* **2010**, 23(7), 1293–1302.
 163. Whiteman, M., Jenner, A., Halliwell, B. Hypochlorous acid-induced base modifications in isolated calf thymus DNA. *Chem. Res. Toxicol.* **1997**, 10(11), 1240–1246.
 164. Prutz, W.A., Kissner, R., Koppenol, W.H., Ruegger, H. On the irreversible destruction of reduced nicotinamide nucleotides by hypohalous acids. *Arch. Biochem. Biophys.* **2000**, 380(1), 181–191.
 165. Koppenol, W.H., Stanbury, D.M., Bounds, P.L. Electrode potentials of partially reduced oxygen species, from dioxygen to water. *Free Radic. Biol. Med.* **2010**, 49(3), 317–322.
 166. Koppenol, W.H., Butler, J. Energetics of interconversion reactions of oxyradicals. *Adv. Free Radic. Biol. Med.* **1985**, 1, 91–131.
 167. Pfeiffer, S., Mayer, B., Janoschek, R. Gibbs energies of reactive species involved in peroxyxynitrite chemistry calculated by density functional theory. *J. Mol. Struct.* **2003**, 623, 95–103.
 168. Lagager, T., Sehested, K. Formation and decay of peroxyxynitrous acid: A pulse radiolysis study. *J. Phys. Chem.* **1993**, 97, 6664–6669.
 169. Buettner, G.R. The pecking order of free radicals and antioxidants: Lipid peroxidation, α -tocopherol, and ascorbate. *Arch. Biochem. Biophys.* **1993**, 300, 535–543.
 170. Simic, M.G., Jovanovi, S.V. Antioxidation mechanisms of uric acid? *J. Am. Chem. Soc.* **1989**, 111, 5718–5718.
 171. Lancaster, J.R., Jr. Nitroxidative, nitrosative, and nitrative stress: Kinetic predictions of reactive nitrogen species chemistry under biological conditions. *Chem. Res. Toxicol.* **2006**, 19(9), 1160–1174.
 172. Hotamisligil, G.S. Endoplasmic reticulum stress and the inflammatory basis of metabolic disease. *Cell* **2010**, 140(6), 900–917.
 173. Jiang, Z., Hu, Z., Zeng, L., Lu, W., Zhang, H., Li, T., Xiao, H. The role of the Golgi apparatus in oxidative stress: Is this organelle less significant than mitochondria? *Free Radic. Biol. Med.* **2011**, 50, 907–917.
 174. Quinn, M.T., Gauss, K.A. Structure and regulation of the neutrophil respiratory burst oxidase: Comparison with non-phagocyte oxidases. *J. Leukoc. Biol.* **2004**, 76, 760–781.
 175. Berry, C.E., Hare, J.M. Xanthine oxidoreductase and cardiovascular disease: Molecular mechanisms and pathophysiological implications. *J. Physiol.* **2004**, 555(Pt 3), 589–606.
 176. Cadenas, E., Davies, K.J.A. Mitochondrial free radical generation, oxidative stress, and aging. *Free Radic. Biol. Med.* **2000**, 29, 222–230.
 177. Barja, G. Mitochondrial oxygen radical generation and leak: Sites of production in states 4 and 3, organ specificity, and relation to aging and longevity. *J. Bioenerg. Biomembr.* **1999**, 31(4), 347–366.
 178. Rifkind, J.M., Ramasamy, S., Manoharan, P.T., Nagababu, E., Mohanty, J.G. Redox reactions of hemoglobin. *Antioxid. Redox Signal.* **2004**, 6, 657–666.
 179. Wei, C.-C., Crane, B.R., Stuehr, D.J. Tetrahydrobiopterin radical enzymology. *Chem. Rev.* **2003**, 103, 2365–2384.
 180. Surawatanawong, P., Tye, J.W., Hall, M.B. Density functional theory applied to a difference in pathways taken by the enzymes cytochrome P450 and superoxide reductase: Spin states of ferric hydroperoxo intermediates and hydrogen bonds from water. *Inorg. Chem.* **2010**, 49, 188–198.
 181. Kuthan, H., Tsuji, H., Graf, H., Ullrich, V., Werrigloer, J., Estabrook, R.W. Generation of superoxide anion as a source of hydrogen peroxide in a reconstituted monooxygenase system. *FEBS Lett.* **1978**, 91, 343–345.
 182. Roy, P., Roy, S.K., Mitra, A., Kulkarni, A.P. Superoxide generation by lipoxygenase in the presence of NADH and NADPH. *Biochem. Biophys. Acta, Lipids Lipid Metab.* **1994**, 1214, 171–179.
 183. Gross, E., Sevier, C.S., Heldman, N., Vitu, E., Bentzur, M., Kaiser, C.A., Thorpe, C., Fass, D. Generating disulfides enzymatically: Reaction products and electron acceptors of the endoplasmic reticulum thiol oxidase Ero1p. *Proc. Natl. Acad. Sci. U.S.A.* **2006**, 103(2), 299–304.
 184. Richter, B.H.J.B.a.H.W. A study of the superoxide radical chemistry by stopped-flow radiolysis and radiation induced oxygen consumption. *J. Am. Chem. Soc.* **1977**, 99, 3019–3023.
 185. Holroyd, R.A., Bielski, B.H.J. Photochemical generation of superoxide radicals in aqueous solutions. *J. Am. Chem. Soc.* **1978**, 100, 5796–5800.
 186. Hohanadel, C.J. Photolysis of dilute H_2O_2 solution in the presence of dissolved H_2 and O_2 . Evidence relating to the nature of the OH radical and the H atom produced in the radiolysis of H_2O . *Radiat. Res.* **1962**, 17, 286–301.
 187. Joshi, A., Yang, G.C. Spin trapping of radicals generated in the UV photolysis of alkyl disulfides. *J. Org. Chem.* **1981**, 46, 3736–3738.
 188. Misik, V., Miyoshi, N., Riesz, P. EPR spin-trapping study of the sonolysis of $\text{H}_2\text{O}/\text{D}_2\text{O}$ mixtures: Probing the tem-

- peratures of cavitation regions. *J. Phys. Chem.* **1995**, *99*, 3605–3611.
189. Makino, K., Mossoba, M.M., Riesz, P. Chemical effects of ultrasound on aqueous solutions. Formation of hydroxyl radicals and hydrogen atoms. *J. Phys. Chem.* **1983**, *87*, 1369–1377.
 190. Misik, V., Riesz, P. Free radical intermediates in sonodynamic therapy. *Ann. N. Y. Acad. Sci.* **2000**, *899*, 335–348.
 191. Draper, W.M., Crosby, D.G. Photochemical generation of superoxide radical anion in water. *J. Agric. Food Chem.* **1983**, *31*, 734–737.
 192. Maurette, M.-T., Oliveros, E., Infelta, P.P., Ramsteiner, K., Braun, A.M. Singlet oxygen and superoxide: Experimental differentiation and analysis. *Helv. Chim. Acta* **1983**, *66*, 722–732.
 193. Yamakoshi, Y., Sueyoshi, S., Fukuhara, K., Miyata, N. OH and O₂ generation in aqueous C60 and C70 solutions by photoirradiation: An EPR study. *J. Am. Chem. Soc.* **1998**, *120*, 12363–12364.
 194. Garg, S., Rose, A.L., Waite, T.D. Production of reactive oxygen species on photolysis of dilute aqueous quinone solutions. *Photochem. Photobiol.* **2007**, *83*(4), 904–913.
 195. Matsumoto, F., Okajima, T., Uesugi, S., Koura, N., Ohsaka, T. Electrogenation of superoxide ion and its mechanism at thiol-modified Au electrodes in alkaline aqueous solution. *Electrochemistry* **2003**, *71*, 266–273.
 196. Merritt, M.V., Sawyer, D.T. Electrochemical studies of the reactivity of superoxide ion with several alkyl halides in dimethyl sulfoxide. *J. Org. Chem.* **1970**, *35*, 2157–2159.
 197. Maricle, D.L., Hodgson, W.G. Reduction of oxygen to superoxide in aprotic solvents. *Anal. Chem.* **1965**, *37*, 1562–1565.
 198. Martiz, B., Keyrouz, R., Gmouh, S., Vaultier, M., Jouikov, V. Superoxide-stable ionic liquids: New and efficient media for electrosynthesis of functional siloxanes. *Chem. Commun.* **2004**, *6*, 674–675.
 199. Bohle, D.S., Sagan, E.S., Koppenol, W.H., Kissner, R. Tetramethylammonium salts of superoxide and peroxy-nitrite. *Inorg. Synth.* **2004**, *34*, 36–42.
 200. McElroy, A.D., Hashman, J.S. Synthesis of tetramethylammonium superoxide. *Inorg. Chem.* **1964**, *3*, 1798–1799.
 201. Bolton, J.L., Trush, M.A., Penning, T.M., Dryhurst, G., Monks, T.J. Role of quinones in toxicology. *Chem. Res. Toxicol.* **2000**, *13*, 135–160.
 202. Wang, P.G., Xian, M., Tang, X., Wu, X., Wen, Z., Cai, T., Janczuk, A.J. Nitric oxide donors: Chemical activities and biological applications. *Chem. Rev.* **2002**, *102*(4), 1091–1134.
 203. Pryor, W.A., Cueto, R., Jin, X., Koppenol, W.H., Ngu-Schwemlein, M., Squadrito, G.L., Uppu, P.L., Uppu, R.M. A practical method for preparing peroxy-nitrite solutions of low ionic strength and free of hydrogen peroxide. *Free Radic. Biol. Med.* **1995**, *18*(1), 75–83.
 204. Uppu, R.M. Synthesis of peroxy-nitrite using isoamyl nitrite and hydrogen peroxide in a homogeneous solvent system. *Anal. Biochem.* **2006**, *354*(2), 165–168.
 205. Wahl, R.U.R. Decomposition mechanism of 3-N-morpholinolinosynonimine (SIN-1)—a density functional study on intrinsic structures and reactivities. *J. Mol. Model.* **2004**, *10*, 121–129.
 206. Wardman, P. Fluorescent and luminescent probes for measurement of oxidative and nitrosative species in cells and tissues: Progress, pitfalls, and prospects. *Free Radic. Biol. Med.* **2007**, *43*(7), 995–1022.
 207. Zhao, H., Joseph, J., Fales, H.M., Sokoloski, E.A., Levine, R.L., Vasquez-Vivar, J., Kalyanaram, B. Detection and characterization of the product of hydroethidine and intracellular superoxide by HPLC and limitations of fluorescence. *Proc. Natl. Acad. Sci. U.S.A.* **2005**, *102*(16), 5727–5732.
 208. Miller, E.W., Chang, C.J. Fluorescent probes for nitric oxide and hydrogen peroxide in cell signaling. *Curr. Opin. Chem. Biol.* **2007**, *11*(6), 620–625.
 209. Sikora, A., Zielonka, J., Lopez, M., Joseph, J., Kalyanaram, B. Direct oxidation of boronates by peroxy-nitrite: Mechanism and implications in fluorescence imaging of peroxy-nitrite. *Free Radic. Biol. Med.* **2009**, *47*(10), 1401–1407.
 210. Nagano, T. Bioimaging probes for reactive oxygen species and reactive nitrogen species. *J. Clin. Biochem. Nutr.* **2009**, *45*(2), 111–124.
 211. Fontijn, A., Sabadell, A.J., Ronco, R.J. Homogeneous chemiluminescent measurement of nitric oxide with ozone: Implications for continuous selective monitoring of gaseous air pollutants. *Anal. Chem.* **1970**, *42*, 575–579.
 212. Afanasev, I. Detection of superoxide in cells, tissues and whole organisms. *Front. Biosci.* **2009**, *E1*, 153–160.
 213. Archer, S. Measurement of nitric oxide in biological models. *FASEB J.* **1993**, *7*, 349–360.
 214. Kleinbongard, P., Rassaf, T., Dejam, A., Kerber, S., Kelm, M. Griess method for nitrite measurement of aqueous and protein-containing samples. *Methods Enzymol.* **2002**, *359*, 158–168.
 215. Thomas, E.L., Grisham, M.B., Jefferson, M.M. Preparation and characterization of chloramines. *Methods Enzymol.* **1986**, *132*, 569–585.
 216. Dypbukt, J.M., Bishop, C., Brooks, W.M., Thong, B., Eriksson, H., Kettle, A.J. A sensitive and selective assay for chloramine production by myeloperoxidase. *Free Radic. Biol. Med.* **2005**, *39*(11), 1468–1477.
 217. Floyd, R.A., West, M.S., Eneff, K.L., Hogsett, W.E., Tingey, D.T. Hydroxyl free radical mediated formation of 8-hydroxyguanine in isolated DNA. *Arch. Biochem. Biophys.* **1988**, *262*(1), 266–272.
 218. Freinbichler, W., Bianchi, L., Colivicchi, M.A., Ballini, C., Tipton, K.F., Linert, W., Corte, L.D. The detection of hydroxyl radicals *in vivo*. *J. Inorg. Biochem.* **2008**, *102*(5–6), 1329–1333.
 219. Rebrin, I., Bregere, C., Gallaher, T.K., Sohal, R.S. Detection and characterization of peroxy-nitrite-induced modifications of tyrosine, tryptophan, and methionine residues

- by tandem mass spectrometry. *Methods Enzymol.* **2008**, *441*, 283–294.
220. Sultana, R., Reed, T., Butterfield, D.A. Detection of 4-hydroxy-2-nonenal- and 3-nitrotyrosine-modified proteins using a proteomics approach. *Methods Mol. Biol.* **2009**, *519*, 351–361.
 221. Butt, Y.K., Lo, S.C. Detecting nitrated proteins by proteomic technologies. *Methods Enzymol.* **2008**, *440*, 17–31.
 222. Nourooz-Zadeh, J., Tajaddini-Sarmadi, J., Ling, K.L., Wolff, S.P. Low-density lipoprotein is the major carrier of lipid hydroperoxides in plasma. Relevance to determination of total plasma lipid hydroperoxide concentrations. *Biochem. J.* **1996**, *313*(Pt 3), 781–786.
 223. Fukuzawa, K., Fujisaki, A., Akai, K., Tokumura, A., Terao, J., Gebicki, J.M. Measurement of phosphatidylcholine hydroperoxides in solution and in intact membranes by the ferric-xylenol orange assay. *Anal. Biochem.* **2006**, *359*(1), 18–25.
 224. Gieseg, S.P., Pearson, J., Firth, C.A. Protein hydroperoxides are a major product of low density lipoprotein oxidation during copper, peroxy radical and macrophage-mediated oxidation. *Free Radic. Res.* **2003**, *37*(9), 983–991.
 225. Winterbourn, C.C., Pichorner, H., Kettle, A.J. Myeloperoxidase-dependent generation of a tyrosine peroxide by neutrophils. *Arch. Biochem. Biophys.* **1997**, *338*(1), 15–21.
 226. O'Donnell, V.B., Eiserich, J.P., Chumley, P.H., Jablonsky, M.J., Krishna, N.R., Kirk, M., Barnes, S., Darley-Usmar, V.M., Freeman, B.A. Nitration of unsaturated fatty acids by nitric oxide-derived reactive nitrogen species peroxynitrite, nitrous acid, nitrogen dioxide, and nitronium ion. *Chem. Res. Toxicol.* **1999**, *12*(1), 83–92.
 227. Janero, D.R. Malondialdehyde and thiobarbituric acid-reactivity as diagnostic indices of lipid peroxidation and peroxidative tissue injury. *Free Radic. Biol. Med.* **1990**, *9*(6), 515–540.
 228. Lawson, J.A., Rokach, J., FitzGerald, G.A. Isoprostanes: Formation, analysis and use as indices of lipid peroxidation *in vivo*. *J. Biol. Chem.* **1999**, *274*(35), 24441–24444.
 229. Mason, R.P. Using anti-5,5-dimethyl-1-pyrroline N-oxide (anti-DMPO) to detect protein radicals in time and space with immuno-spin trapping. *Free Radic. Biol. Med.* **2004**, *36*(10), 1214–1223.
 230. Ramirez, D.C., Chen, Y.R., Mason, R.P. Immunochemical detection of hemoglobin-derived radicals formed by reaction with hydrogen peroxide: Involvement of a protein-tyrosyl radical. *Free Radic. Biol. Med.* **2003**, *34*(7), 830–839.
 231. Detweiler, C.D., Lardinois, O.M., Deterding, L.J., de Montellano, P.R., Tomer, K.B., Mason, R.P. Identification of the myoglobin tyrosyl radical by immuno-spin trapping and its dimerization. *Free Radic. Biol. Med.* **2005**, *38*(7), 969–976.
 232. Ramirez, D.C., Gomez Mejiba, S.E., Mason, R.P. Mechanism of hydrogen peroxide-induced Cu,Zn-superoxide dismutase-centered radical formation as explored by immuno-spin trapping: The role of copper- and carbonate radical anion-mediated oxidations. *Free Radic. Biol. Med.* **2005**, *38*(2), 201–214.
 233. Ehrenshaft, M., Mason, R.P. Protein radical formation on thyroid peroxidase during turnover as detected by immuno-spin trapping. *Free Radic. Biol. Med.* **2006**, *41*(3), 422–430.
 234. Rangelova, K., Suarez, J., Magliozzo, R.S., Mason, R.P. Spin trapping investigation of peroxide- and isoniazid-induced radicals in *Mycobacterium tuberculosis* catalase-peroxidase. *Biochemistry* **2008**, *47*(43), 11377–11385.
 235. Ramirez, D.C., Mejiba, S.E., Mason, R.P. Immuno-spin trapping of DNA radicals. *Nat. Methods* **2006**, *3*(2), 123–127.
 236. Ramirez, D.C., Gomez-Mejiba, S.E., Mason, R.P. Immuno-spin trapping analyses of DNA radicals. *Nat. Protoc.* **2007**, *2*(3), 512–522.
 237. Gomez-Mejiba, S.E., Zhai, Z., Akram, H., Deterding, L.J., Hensley, K., Smith, N., Towner, R.A., Tomer, K.B., Mason, R.P., Ramirez, D.C. Immuno-spin trapping of protein and DNA radicals: “Tagging” free radicals to locate and understand the redox process. *Free Radic. Biol. Med.* **2009**, *46*(7), 853–865.
 238. Kutala, V.K., Villamena, F.A., Ilangoan, G., MasPOCH, D., Roques, N., Veciana, J., Rovira, C., Kuppusamy, P. Reactivity of superoxide anion radical with a perchlorotriphenylmethyl (trityl) radical. *J. Phys. Chem. B* **2008**, *112*(1), 158–167.
 239. Rizzi, C., Samouilov, A., Kutala, V.K., Parinandi, N.L., Zweier, J.L., Kuppusamy, P. Application of a trityl-based radical probe for measuring superoxide. *Free Radic. Biol. Med.* **2003**, *35*(12), 1608–1618.
 240. Ballester, M., Riera-Figueras, J., Castaner, J., Badfa, C., Monso, J.M. Inert carbon free radicals. I. Perchlorodiphenylmethyl and perchlorotriphenylmethyl radical series. *J. Am. Chem. Soc.* **1971**, *93*(9), 2215–2225.
 241. Dikalov, S., Skatchkov, M., Bassenge, E. Quantification of peroxynitrite, superoxide, and peroxy radicals by a new spin trap hydroxylamine 1-hydroxy-2,2,6,6-tetramethyl-4-oxo-piperidine. *Biochem. Biophys. Res. Commun.* **1997**, *230*(1), 54–57.
 242. Saito, K., Takeshita, K., Anzai, K., Ozawa, T. Pharmacokinetic study of acyl-protected hydroxylamine probe, 1-acetoxy-3-carbamoyl-2,2,5,5-tetramethylpyrrolidine, for *in vivo* measurements of reactive oxygen species. *Free Radic. Biol. Med.* **2004**, *36*(4), 517–525.
 243. Dikalov, S., Grigor'ev, I.A., Voinov, M., Bassenge, E. Detection of superoxide radicals and peroxynitrite by 1-hydroxy-4-phosphonooxy-2,2,6,6-tetramethylpiperidine: Quantification of extracellular superoxide radicals formation. *Biochem. Biophys. Res. Commun.* **1998**, *248*(2), 211–215.
 244. Zang, L.Y., Misra, B.R., van Kuijk, F.J., Misra, H.P. EPR studies on the kinetics of quenching singlet oxygen. *Biochem. Mol. Biol. Int.* **1995**, *37*(6), 1187–1195.

245. Villamena, F.A., Das, A., Nash, K.M. Potential implication of the chemical properties and bioactivity of nitron spin traps for therapeutics. *Future Med. Chem.* **2012**, 4(9), 1171–1207.
246. Britigan, B.E., Pou, S., Rosen, G.M., Lilleg, D.M., Buettner, G.R. Hydroxyl radical is not a product of the reaction of xanthine oxidase and xanthine. The confounding problem of adventitious iron bound to xanthine oxidase. *J. Biol. Chem.* **1990**, 265(29), 17533–17538.
247. Du, G., Mouithys-Mickalad, A., Sluse, F.E. Generation of superoxide anion by mitochondria and impairment of their functions during anoxia and reoxygenation *in vitro*. *Free Radic. Biol. Med.* **1998**, 25(9), 1066–1074.
248. Nohl, H., Jordan, W., Hegner, D. Identification of free hydroxyl radicals in respiring rat heart mitochondria by spin trapping with the nitron DMPO. *FEBS Lett.* **1981**, 123(2), 241–244.
249. Bannister, J.V., Bellavite, P., Serra, M.C., Thornalley, P.J., Rossi, F. An EPR study of the production of superoxide radicals by neutrophil NADPH oxidase. *FEBS Lett.* **1982**, 145(2), 323–326.
250. Shi, H., Timmins, G., Monske, M., Burdick, A., Kalyanaraman, B., Liu, Y., Clement, J.-L., Burchiel, S., Liu, K.J. Evaluation of spin trapping agents and trapping conditions for detection of cell-generated reactive oxygen species. *Arch. Biochem. Biophys.* **2005**, 437(1), 59–68.
251. Britigan, B.E., Cohen, M.S., Rosen, G.M. Detection of the production of oxygen-centered free radicals by human neutrophils using spin trapping techniques: A critical perspective. *J. Leukoc. Biol.* **1987**, 41(4), 349–362.
252. Hirata, H., He, G., Deng, Y., Salikhov, I., Petryakov, S., Zweier, J.L. A loop resonator for slice-selective *in vivo* EPR imaging in rats. *J. Magn. Reson.* **2008**, 190(1), 124–134.
253. Jiang, J.J., Liu, K.J., Jordan, S.J., Swartz, H.M., Mason, R.P. Detection of free radical metabolite formation using *in vivo* EPR spectroscopy: Evidence of rat hemoglobin thiyl radical formation following administration of phenylhydrazine. *Arch. Biochem. Biophys.* **1996**, 330(2), 266–270.
254. Kadiiska, M.B., Burkitt, M.J., Xiang, Q.H., Mason, R.P. Iron supplementation generates hydroxyl radical *in vivo*. An ESR spin-trapping investigation. *J. Clin. Invest.* **1995**, 96(3), 1653–1657.
255. Bolli, R., Jeroudi, M.O., Patel, B.S., DuBose, C.M., Lai, E.K., Roberts, R., McCay, P.B. Direct evidence that oxygen-derived free radicals contribute to postischemic myocardial dysfunction in the intact dog. *Proc. Natl. Acad. Sci. U.S.A.* **1989**, 86(12), 4695–4699.
256. Goldstein, S., Russo, A., Samuni, A. Reactions of PTIO and carboxy-PTIO with .bul.NO, .bul.NO₂, and O₂-.bul. *J. Biol. Chem.* **2003**, 278(51), 50949–50955.
257. Samuni, U., Samuni, Y., Goldstein, S. On the distinction between nitroxyl and nitric oxide using nitronyl nitroxides. *J. Am. Chem. Soc.* **2010**, 132(24), 8428–8432.
258. Mordvintsev, P., Mulsch, A., Busse, R., Vanin, A.F. On-line detection of nitric oxide formation in liquid aqueous phase by EPR. *Anal. Biochem.* **1991**, 199, 142.
259. Vanin, A.F., Huisman, A., Van Faassen, E.E. Iron dithiocarbamate as spin trap for nitric oxide detection: Pitfalls and successes. *Methods Enzymol.* **2002**, 359 (Nitric Oxide-Part D), 27–42.
260. Vanin, A.F. Iron diethyldithiocarbamate as spin trap for nitric oxide detection. *Methods Enzymol.* **1999**, 301, 269–279.
261. Mikoyan, V.D., Kubrina, L.N., Serezhnikov, V.A., Stukan, R.A., Vanin, A.F. Complexes of Fe(II) with diethyldithiocarbamate or N-methyl-D-glucamine dithiocarbamate as traps of nitric oxide in animal tissues: Comparative investigations. *Biochim. Biophys. Acta* **1997**, 1336, 225–234.
262. Tsuchiya, K., Takasugi, M., Minakuchi, K., Fukuzawa, K. Sensitive quantification of nitric oxide by EPR spectroscopy. *Free Radic. Biol. Med.* **1996**, 21, 733–737.
263. Kleschyov, A.L., Munzel, T. Advanced spin trapping of vascular nitric oxide using colloid iron dithiocarbamate. *Methods Enzymol.* **2002**, 359, 43–51.
264. Kleschyov, A.L., Hanke Mollnau, H., Oelze, M., Meinerz, T., Huang, Y., Harrison, D.G., Munzel, T. Spin trapping of vascular nitric oxide using colloidal Fe(II)-diethyldithiocarbamate. *Biochim. Biophys. Res. Commun.* **2000**, 275, 672–677.
265. Hogg, N. Detection of nitric oxide by electron paramagnetic resonance spectroscopy. *Free Radic. Biol. Med.* **2010**, 49(2), 122–129.
266. Moreira, P.I., Sayre, L.M., Zhu, X., Nunomura, A., Smith, M.A., Perry, G. Detection and localization of markers of oxidative stress by *in situ* methods: Application in the study of Alzheimer disease. *Methods Mol. Biol.* **2010**, 610, 419–434.
267. Celes, M.R., Torres-Duenas, D., Prado, C.M., Campos, E.C., Moreira, J.E., Cunha, F.Q., Rossi, M.A. Increased sarcolemmal permeability as an early event in experimental septic cardiomyopathy: A potential role for oxidative damage to lipids and proteins. *Shock* **2010**, 33(3), 322–331.
268. Kuppusamy, P., Zweier, J.L. Cardiac applications of EPR imaging. *NMR Biomed.* **2004**, 17(5), 226–239.
269. Jackson, S.K., Thomas, M.P., Smith, S., Madhani, M., Rogers, S.C., James, P.E. *In vivo* EPR spectroscopy: Biomedical and potential diagnostic applications. *Faraday Discuss.* **2004**, 126, 103–117; discussion 169–183.
270. Liu, Y., Villamena, F.A., Sun, J., Wang, T.Y., Zweier, J.L. Esterified trityl radicals as intracellular oxygen probes. *Free Radic. Biol. Med.* **2009**, 46(7), 876–883.
271. He, G., Shankar, R.A., Chzhan, M., Samouilov, A., Kuppusamy, P., Zweier, J.L. Noninvasive measurement of anatomic structure and intraluminal oxygenation in the gastrointestinal tract of living mice with spatial and spectral EPR imaging. *Proc. Natl. Acad. Sci. U.S.A.* **1999**, 96(8), 4586–4591.
272. Pandian, R.P., Chacko, S.M., Kuppusamy, M.L., Rivera, B.K., Kuppusamy, P. Evaluation of lithium naphthalocyanine (LiNc) microcrystals for biological EPR oximetry. *Adv. Exp. Med. Biol.* **2011**, 701, 29–36.

273. Khan, N., Williams, B.B., Hou, H., Li, H., Swartz, H.M. Repetitive tissue pO₂ measurements by electron paramagnetic resonance oximetry: Current status and future potential for experimental and clinical studies. *Antioxid. Redox Signal.* **2007**, 9(8), 1169–1182.
274. Berliner, L.J., Fujii, H. *In vivo* spin trapping of nitric oxide. *Antioxid. Redox Signal.* **2004**, 6(3), 649–656.
275. Sentjurs, M., Mason, R.P. Inhibition of radical adduct reduction and reoxidation of the corresponding hydroxylamines in *in vivo* spin trapping of carbon tetrachloride-derived radicals. *Free Radic. Biol. Med.* **1992**, 13(2), 151–160.
276. Chamulitrat, W., Jordan, S.J., Mason, R.P. Fatty acid radical formation in rats administered oxidized fatty acids: *In vivo* spin trapping investigation. *Arch. Biochem. Biophys.* **1992**, 299(2), 361–367.
277. Kirsch, M., Lehnig, M., Korth, H.-G., Sustmann, R., de Groot, H. Inhibition of peroxynitrite-induced nitration of tyrosine by glutathione in the presence of carbon dioxide through both radical repair and peroxynitrate formation. *Chem. Eur. J.* **2001**, 7(15), 3313–3320.